Status and selected results from the SBS nucleon form factor program

Andrew Puckett
University of Connecticut
Hall A/C Summer Meeting
June 17, 2026

UCONN

Acknowledgements

- Support from US DOE Office of Science, Medium-Energy NP program, award DE-SC0021200
- SBS spokespeople and collaboration, including, especially, the 28 SBS Ph.D. students (including 13 already graduated) and the many current and former postdocs and JLab staff involved
- People whose materials I borrowed from heavily for this talk, including: Provakar Datta, Anu Rathnayake, Vimukthi Gamage, Eric Fuchey, Bhashitha Dharmasena, Kip Hunt, Gordon Cates, Hunter Presley, Jack Jackson, Jacob Koenemann, Don Jones, Faraz Chahili, Zeke Wertz, Vimukthi Gamage, Kate Evans, and many others

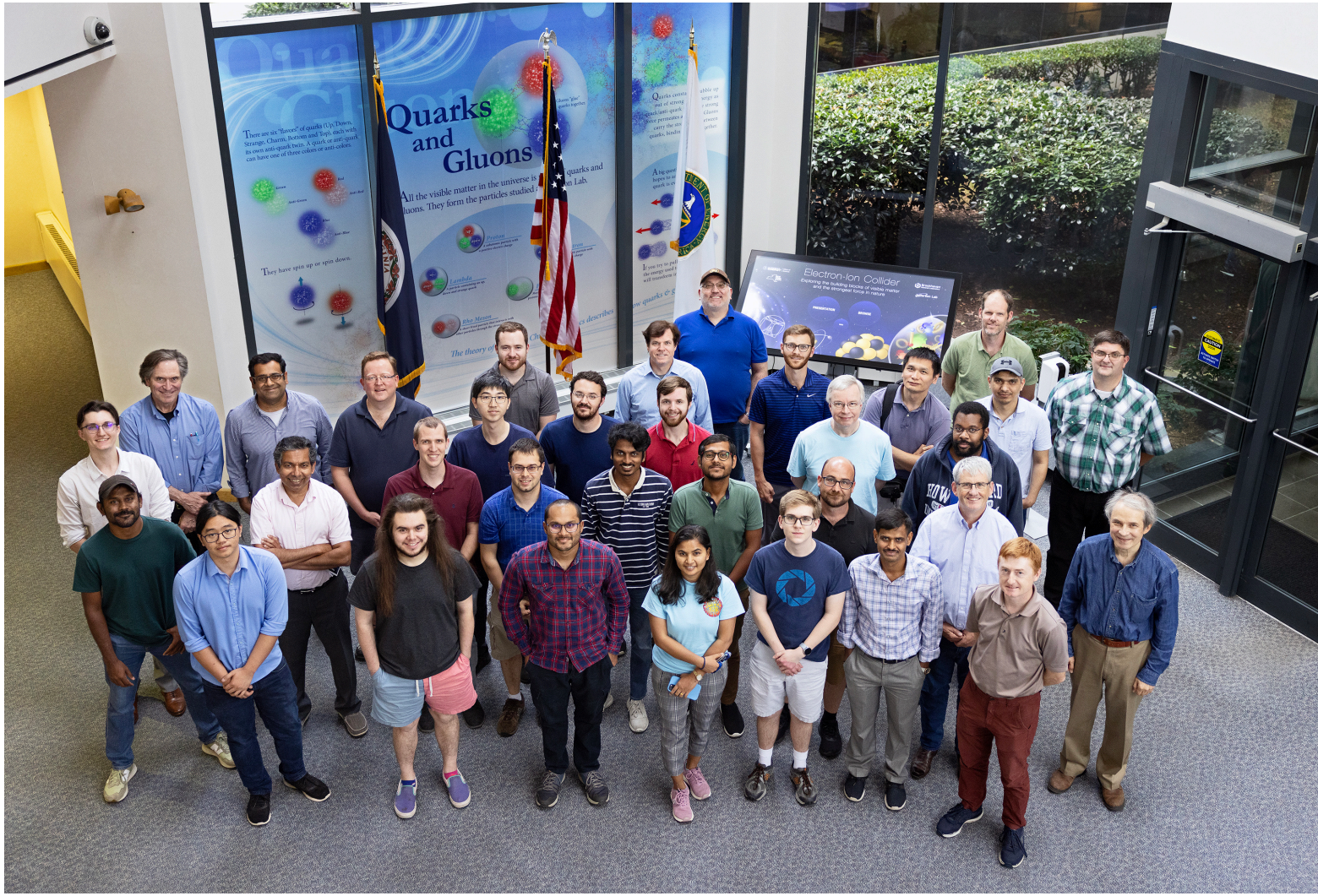

SBS Collaboration Meeting 2023

Elastic Electron-Nucleon Scattering and Form Factors

- The Dirac (F_1) and Pauli (F_2) form factors describe the most general form of the virtual photon-nucleon vertex function consistent with the symmetries of QED; namely, Lorentz invariance, parity conservation and gauge invariance/current conservation
- They are real-valued functions of the (space-like) squared four-momentum transfer $q^2 = (k - k')^2 < 0$.
- Experimental observables sensitive to form factors include differential cross sections and double-spin asymmetries involving polarized e^- beams and/or targets

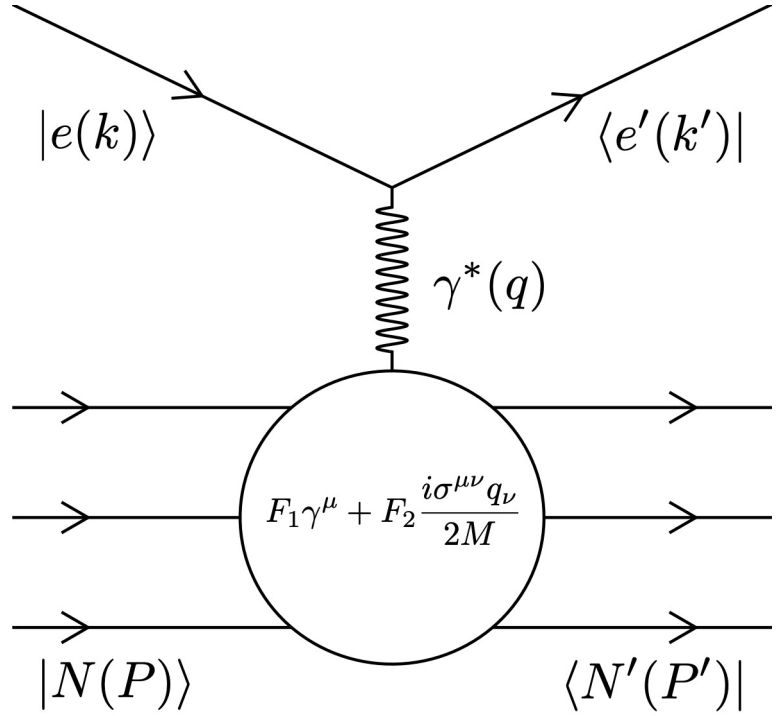

Feynman Diagram for elastic $eN \to eN$ scattering in OPE approximation

$$\text{Invariant amplitude: } \mathcal{M} = 4\pi\alpha\bar{u}(k')\gamma^\mu u(k)\left(\frac{g_{\mu\nu}}{q^2}\right)\bar{u}(P')\Gamma^\nu u(P)$$

$$\gamma^* N \text{ vertex function: } \Gamma^\mu = F_1(q^2)\gamma^\mu + \frac{i\sigma^{\mu\nu}q_\nu}{2M}F_2(q^2)$$

$$\text{Sachs FF: } G_E = F_1 - \tau F_2$$

$$G_M = F_1 + F_2$$

$$\text{Rosenbluth Formula: } \frac{d\sigma}{d\Omega_e} = \left(\frac{d\sigma}{d\Omega_e}\right)_{\text{Mott}} \frac{\epsilon G_E^2 + \tau G_M^2}{\epsilon(1+\tau)}$$

$$\tau \equiv \frac{Q^2}{4M^2}$$

$$\epsilon \equiv \left[1 + 2(1+\tau)\tan^2\left(\frac{\theta_e}{2}\right)\right]^{-1}$$

Theoretical Interpretation of High-Q^2 Nucleon Elastic Form Factors

- Density interpretations: 3D (low Q^2 limit only) or model-independent transverse density (any Q^2)
- Perturbative QCD: for asymptotically large Q^2, form factor behavior is predicted by simple constituent counting rules; $F_1 \propto Q^{-4}, F_2 \propto Q^{-6}$, assuming dominance of multiple hard-gluon exchange mechanism
- Constituent Quark Models—define quarks as effective degrees of freedom, solve bound-state Hamiltonian with confining quark-quark interaction, use wavefunction to predict FFs.
- Lattice QCD—Experiment far ahead of theory in precision/accuracy, but data help to benchmark/improve the calculations
- Dyson-Schwinger Equations: approximate solutions of continuum non-perturbative QCD
- Connection to Generalized Parton Distributions from sum rules; relevant to Ji sum rule for proton spin decomposition.
- Some recent reviews of the subject:
  - PPNP 59, 694 (2007): https://doi.org/10.1016/j.ppnp.2007.05.001
  - EPJ A 51, 79 (2015): https://doi.org/10.1140/epja/i2015-15079-x
  - PPNP 116, 103835 (2021): https://doi.org/10.1016/j.ppnp.2020.103835
  - EPJ C, 83:1125 (2023) (section 10.1 and others): https://doi.org/10.1140/epjc/s10052-023-11949-2

“Measuring” Elastic Form Factors: Rosenbluth Separation

- The structure-dependent part of the cross section factorizes from the “point-like” part.
- The “reduced cross section” σ_R depends linearly on ϵ for a given Q^2, with slope G_E^2 and intercept τG_M^2.
- Experimentally, one measures $d\sigma/d\Omega$ while varying the beam energy and scattering angle to change ϵ while holding Q^2 constant

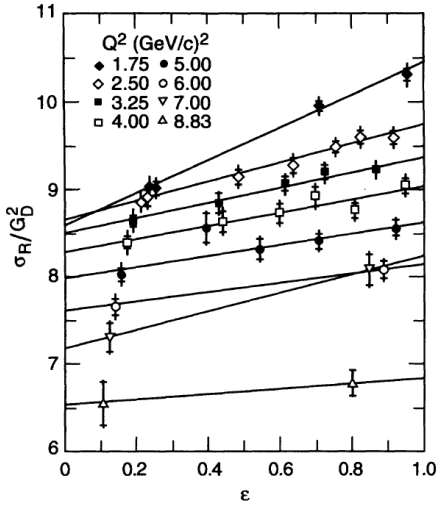

FIG. 22. Reduced cross sections divided by the square of the dipole fit plotted versus ϵ for each value of Q^2. The 1.6 GeV data points correspond to the leftmost point on each line, and the E136 data point is the rightmost point on the $Q^2 = 8.83$ (GeV/c)^2 line. The inner error bars show the statistical error, while the outer error bars show the total point-to-point uncertainty, given by the quadrature sum of the statistical and point-to-point systematic errors. An overall normalization uncertainty of ±1.77% has not been included.

Andivahis *et al.*, **Phys. Rev. D** 50, 5491 (1994)

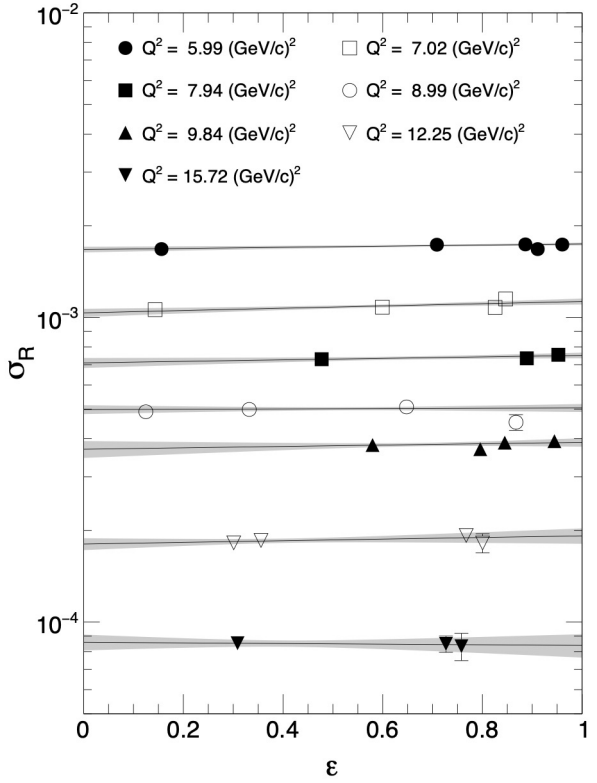

Christy *et al.*, **Phys. Rev. Lett.** 128, 102002 (2022)

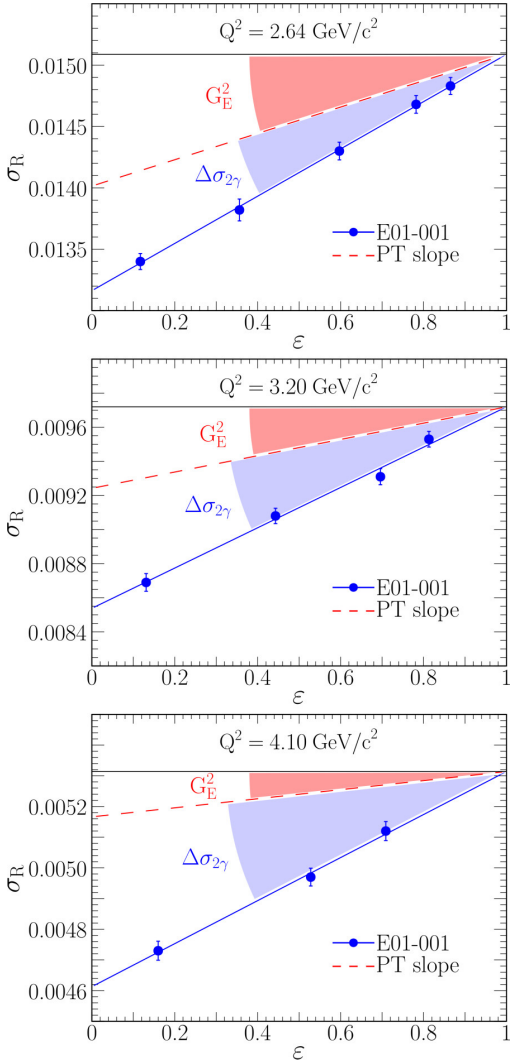

Qattan *et al.*, **Phys. Rev. C** 112 (2025) 3, 035205

$$\tau \equiv \frac{Q^2}{4M_p^2} \qquad \sigma_R = \epsilon G_E^2 + \tau G_M^2$$

$$\epsilon \equiv \left[1 + 2(1+\tau)\tan^2\left(\frac{\theta_e}{2}\right)\right]^{-1}$$

$$\frac{d\sigma}{d\Omega_e} = \left(\frac{d\sigma}{d\Omega_e}\right)_{Mott} \frac{\epsilon G_E^2 + \tau G_M^2}{\epsilon(1+\tau)}$$

$$\left(\frac{d\sigma}{d\Omega_e}\right)_{Mott} = \frac{\alpha^2 \cos^2\left(\frac{\theta_e}{2}\right)}{4E_e^2 \sin^4\left(\frac{\theta_e}{2}\right)} \frac{E_e'}{E_e}$$

”Measuring” Elastic Form Factors—Polarization Observables

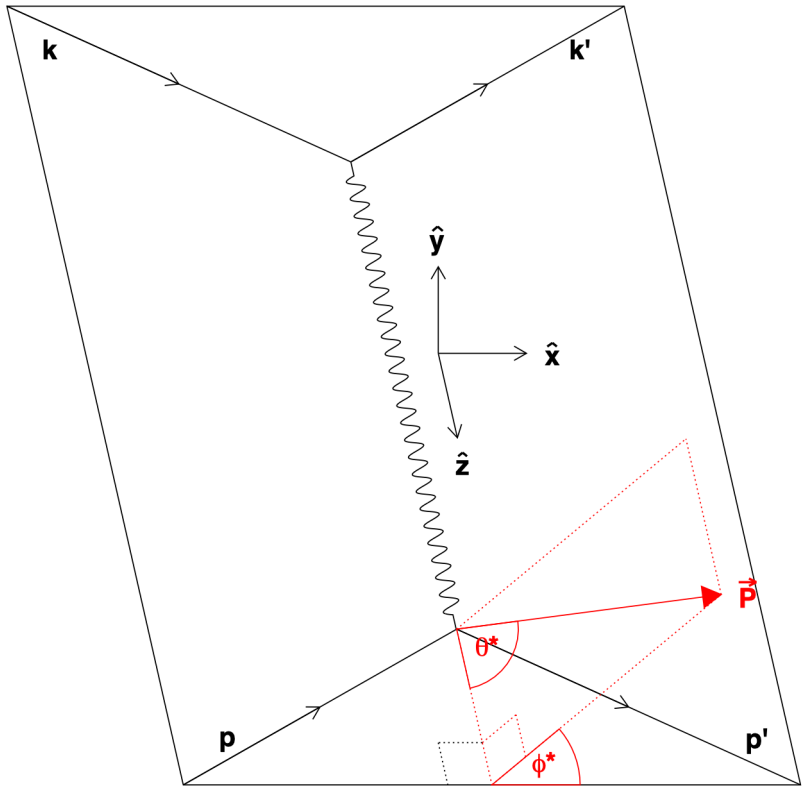

Standard coordinate system and angle definitions for nucleon polarization components in $eN \to eN$

$$
\begin{aligned}
A_{eN} &\equiv \frac{\sigma_+ - \sigma_-}{\sigma_+ + \sigma_-} = P_{\text{beam}} P_{\text{targ}} \left[A_t \sin\theta^* \cos\phi^* + A_\ell \cos\theta^* \right] \\
A_t &= -\sqrt{\frac{2\epsilon(1-\epsilon)}{\tau}} \frac{r}{1 + \frac{\epsilon}{\tau} r^2} \\
A_\ell &= -\frac{\sqrt{1-\epsilon^2}}{1 + \frac{\epsilon}{\tau} r^2} \\
r &\equiv \frac{G_E}{G_M} \\
P_t &= P_{beam} A_t \\
P_\ell &= -P_{beam} A_\ell \\
\frac{G_E}{G_M} &= -\frac{P_t}{P_\ell} \sqrt{\frac{\tau(1+\epsilon)}{2\epsilon}} = -\frac{P_t}{P_\ell} \frac{E_e + E'_e}{2M} \tan\left(\frac{\theta_e}{2}\right)
\end{aligned}
$$

- Polarized beam-polarized target double-spin asymmetry or polarization transfer observables in OPE are sensitive to the electric/magnetic form factor *ratio*, giving enhanced sensitivity to $G_E (G_M)$ for large (small) values of Q^2, as compared to the Rosenbluth method

The APS Bonner Prize in Nuclear Physics, 2017

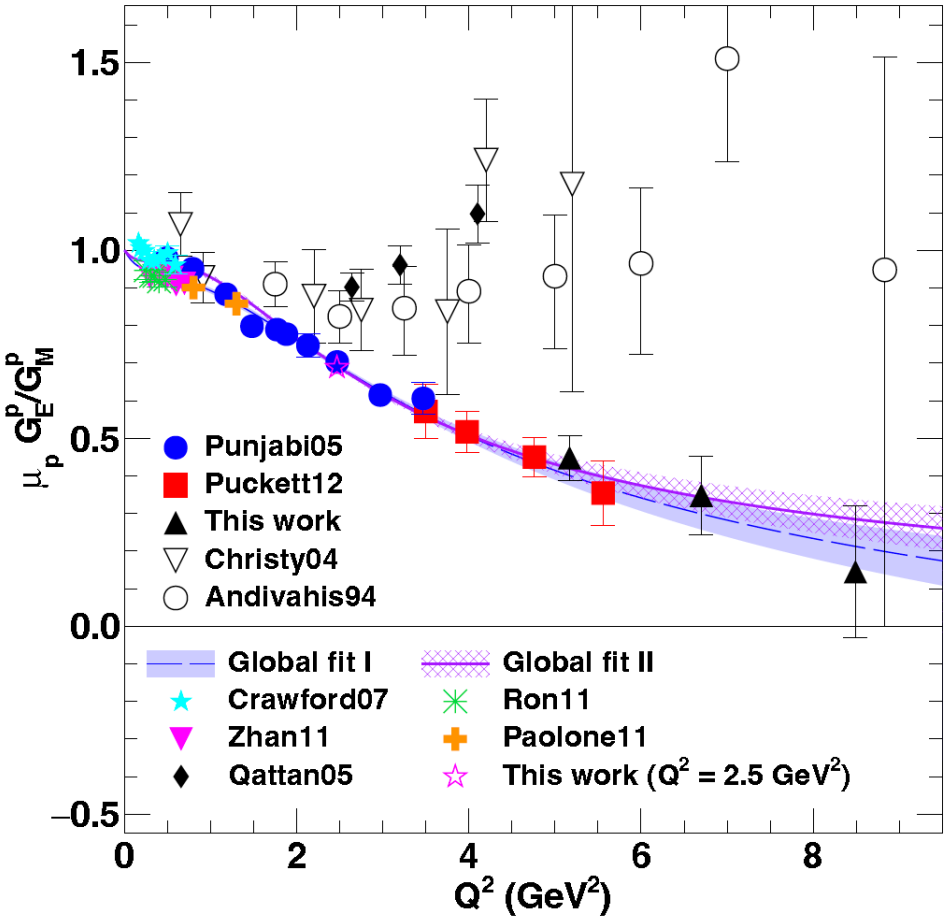

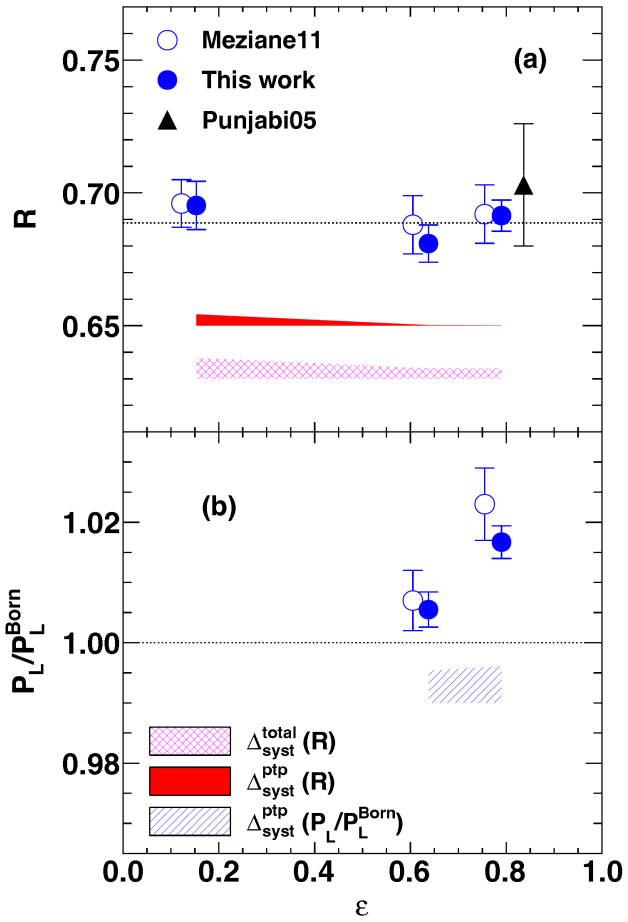

Puckett *et al.*, PRC 96, 055203 (2017)

APS physics

2017 Tom W. Bonner Prize in Nuclear Physics Recipient

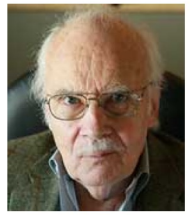

Charles F. Perdrisat
College of William and Mary

Citation:

"*For groundbreaking measurements of nucleon structure, and discovering the unexpected behavior of the magnetic and electric nucleon form factors with changing momentum transfer.*"

Background:

Charles F. Perdrisat, Ph.D., was a professor at the College of William and Mary (Williamsburg, Va.) for the last 50 years having retired earlier this year. Throughout his career, Dr. Perdrisat's research focus included nuclear reactions with proton and deuteron beams, both polarized and unpolarized. He conducted research at SATURNE in Saclay, France, TRIUMF in Vancouver, B.C., LAMPF in Los Alamos, New Mexico, Brookhaven National Laboratory in Upton, N.Y., and JINR in Dubna, Russia. During the last half of his career, he was committed to the investigation of the structure of the proton at Jefferson Laboratory, concentrating in obtaining polarization transfer data in the scattering of polarized electrons on unpolarized protons. These data, from 3 distinct experiments organized in close collaboration with Vina Punjabi, Ph.D., Mark K. Jones, Ph.D., Edward J. Brash, Ph.D., and Lubomir Pentchev, Ph.D., have resulted in a significant change of paradigm in the understanding of the structure of the nucleon. After completing his undergraduate training in physics and mathematics at the University of Geneva in 1956, Dr. Perdrisat became an assistant in the physics department at the Swiss Federal Institute of Technology in Zurich) in Switzerland, under Prof. Paul Scherrer; he received his Ph.D. in 1962. He completed a three-year postdoctoral fellowship at the University of Illinois Urbana-Champaign, before heading to William and Mary in 1966.

Selection Committee:

2017 Selection Committee Members: Rocco Schiavilla (Chair), D. Hertzog, P. Jacobs, Kate Jones, I-Y. Lee

Importance of Combined Proton and Neutron Measurements—Flavor Decomposition

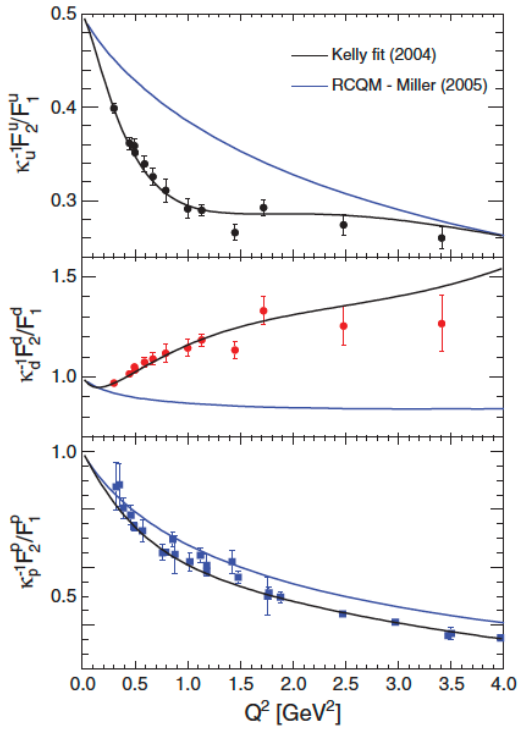

FIG. 2 (color). The ratios $\kappa_d^{-1}F_2^d/F_1^d$, $\kappa_u^{-1}F_2^u/F_1^u$, and $\kappa_p^{-1}F_2^p/F_1^p$ vs momentum transfer Q^2. The data and curves are described in the text.

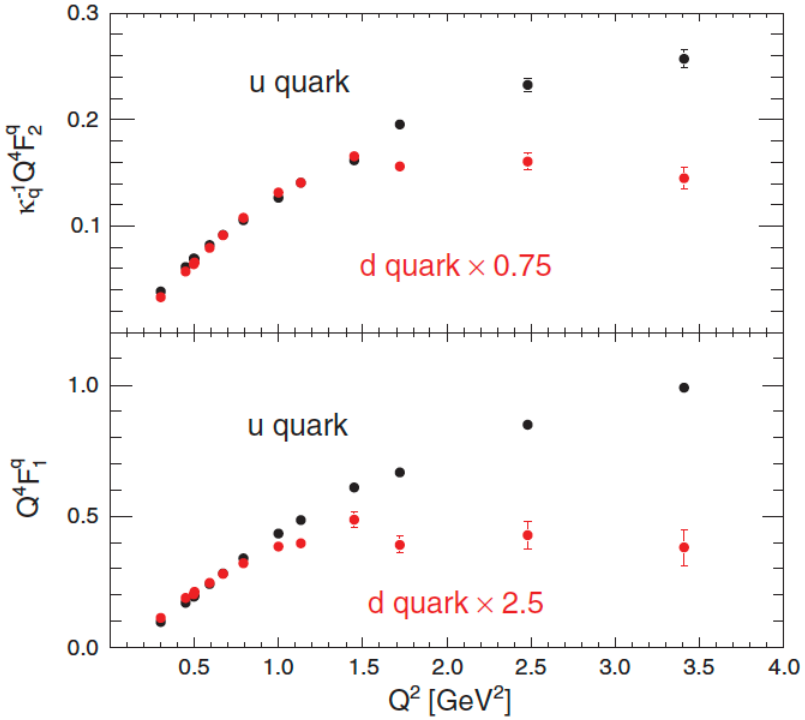

FIG. 3 (color). The Q^2 dependence for the u and d contributions to the proton form factors (multiplied by Q^4). The data points are explained in the text.

Progress in Particle and Nuclear Physics 116 (2021) 103835

Contents lists available at ScienceDirect

Progress in Particle and Nuclear Physics

journal homepage: www.elsevier.com/locate/ppnp

Review

Diquark correlations in hadron physics: Origin, impact and evidence

M.Yu. Barabanov [1], M.A. Bedolla [2], W.K. Brooks [3], G.D. Cates [4], C. Chen [5], Y. Chen [6,7], E. Cisbani [8], M. Ding [9], G. Eichmann [10,11], R. Ent [12], J. Ferretti [13], R.W. Gothe [14], T. Horn [15,12], S. Liuti [4], C. Mezrag [16], A. Pilloni [9], A.J.R. Puckett [17], C.D. Roberts [18,19,*], P. Rossi [12,20], G. Salmé [21], E. Santopinto [22], J. Segovia [23,19], S.N. Syritsyn [24,25], M. Takizawa [26,27,28], E. Tomasi-Gustafsson [16], P. Wein [29], B.B. Wojtsekhowski [12]

[1] Joint Institute for Nuclear Research, Dubna, 141980, Russia

Cates *et al.*, PRL 106, 252003 (2011): Extracted quark flavor FFs F_1^q, F_2^q from proton and neutron Sachs FF data assuming isospin symmetry, valence quark dominance

→ Flavor FFs are a key experimental signature of diquark correlations in nucleon structure (Trento workshop 2019)

Neutron Form Factors Before SBS—Figures from P. Datta Thesis

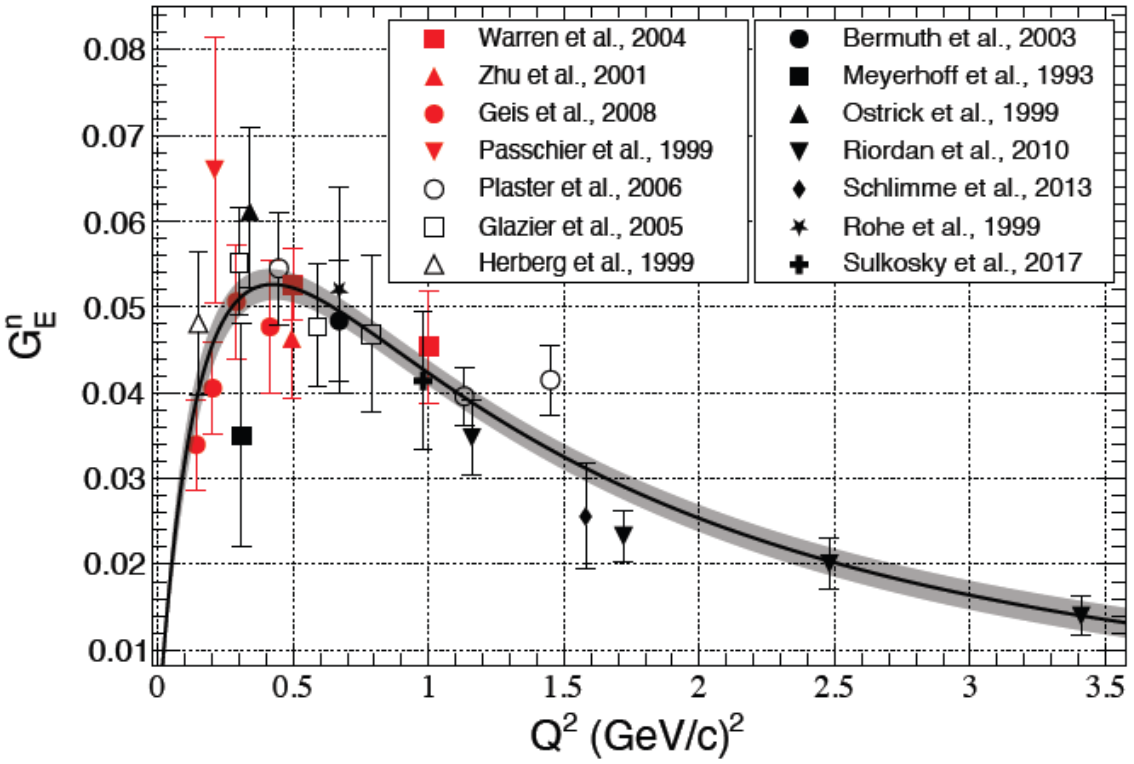

Figure 2.4: World data for the neutron electric form factor G_E^n. Black filled shapes represent beam-target double-spin asymmetry measurement data using a polarized ^{3}He target [64–68]. Red filled shapes denote beam-target double-spin asymmetry data with a polarized deuteron target [69–72], while open shapes represent measurements obtained via recoil neutron polarization [73–75]. The global fit is sourced from [51]. See the text for more details.

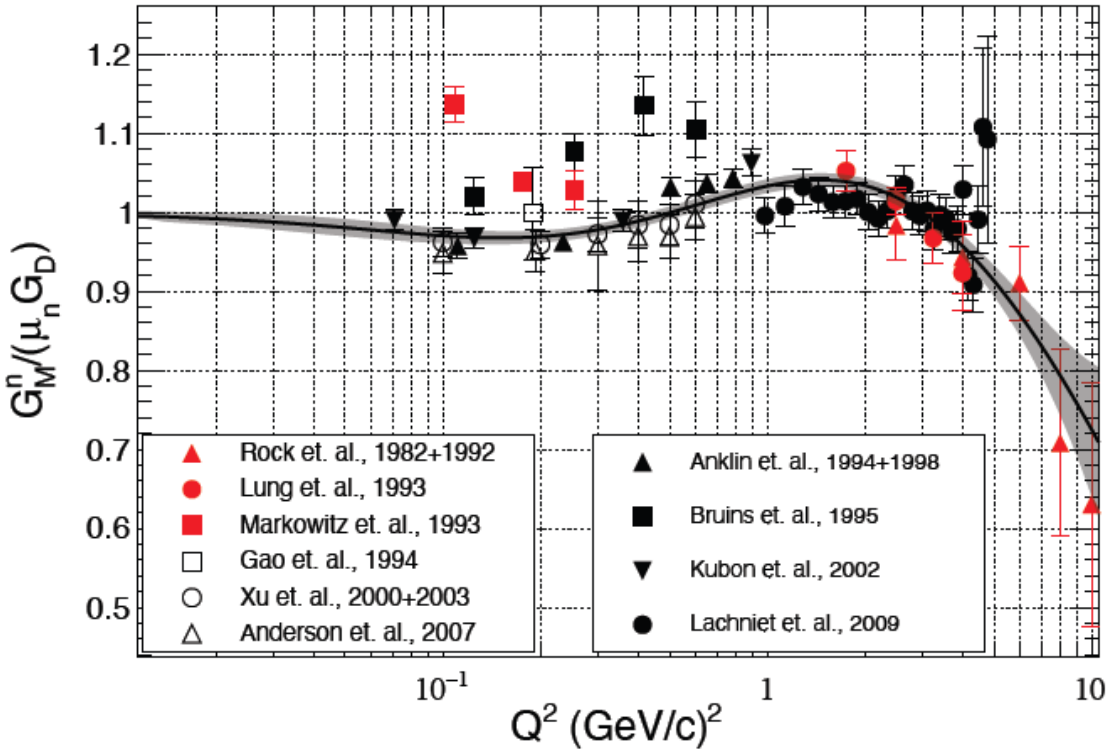

Figure 2.5: World data for the neutron magnetic form factor $G_M^n/(\mu_n G_D)$. Black filled shapes represent measurements obtained using the ratio (or Durand's) method [84–88], while red filled shapes denote absolute cross-section measurements [89–91]. Black open shapes indicate beam-target double-spin asymmetry measurements [92–95]. The global fit is sourced from [51]. See the text for further details.

Proton Form Factors Before SBS: G_E^p and G_M^p

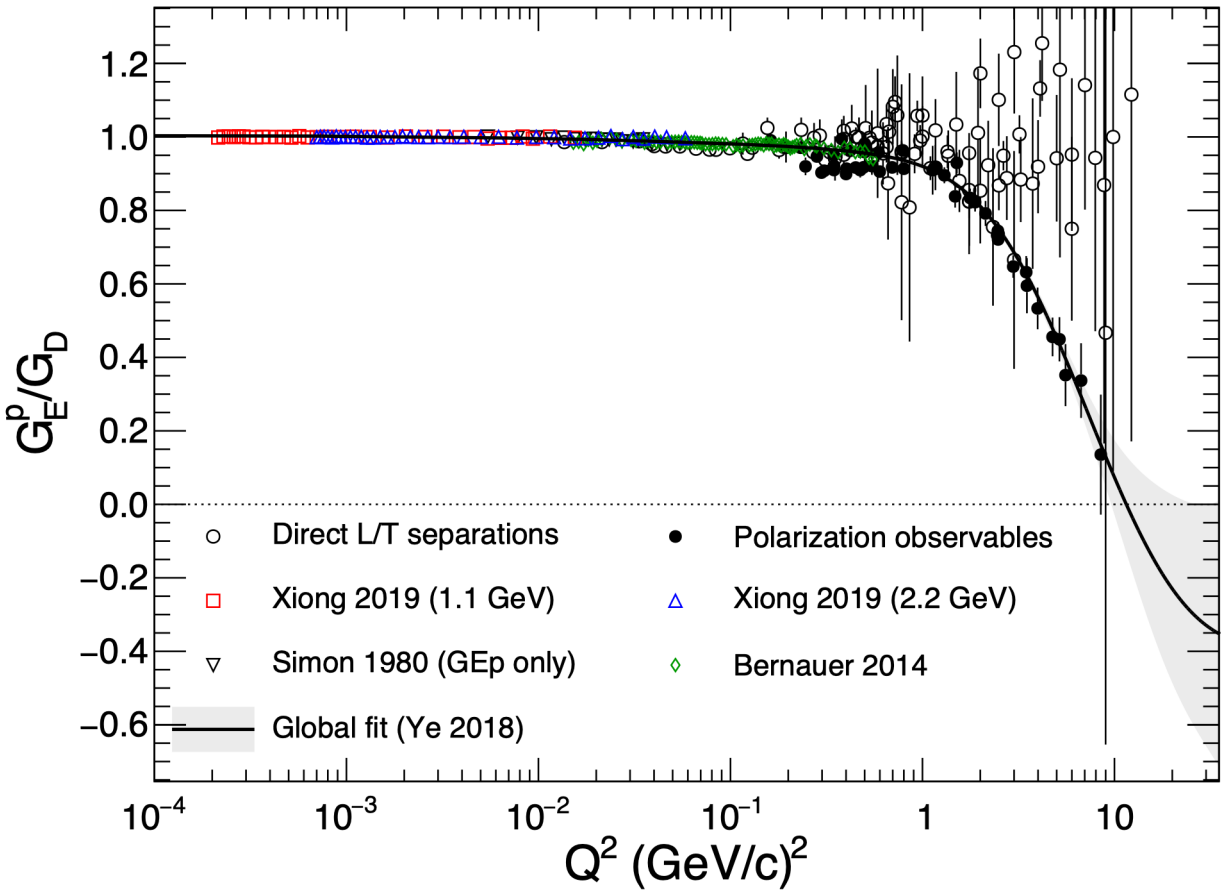

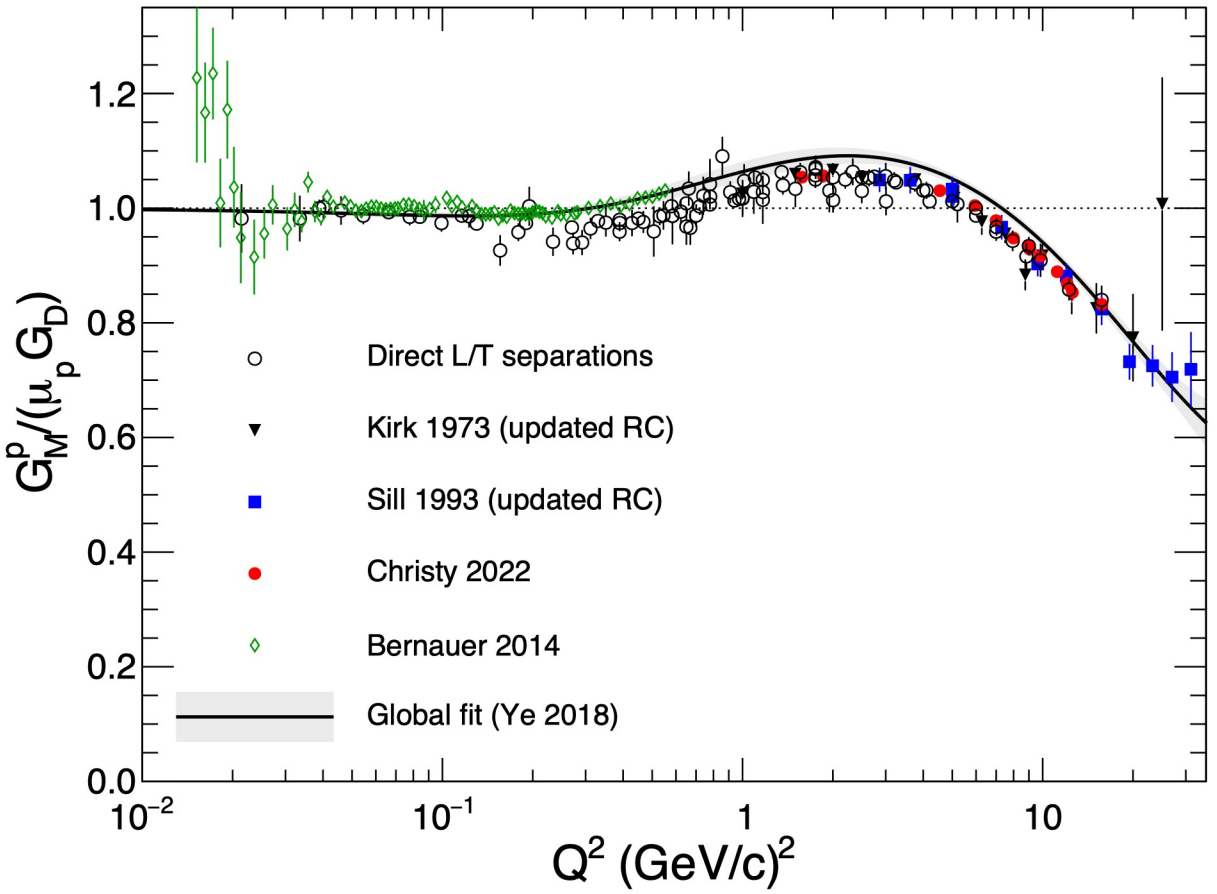

- Left: $\frac{G_E^p}{G_M^p}$. Right: $\frac{G_M^p}{\mu_p G_D}$. Figures, references, explanations from section 10.1 of "50 years of QCD": https://inspirehep.net/literature/2617065 (Eur.Phys.J.C 83 (2023) 1125)

The SBS high-Q^2 Form Factor Program (status as of 2023)

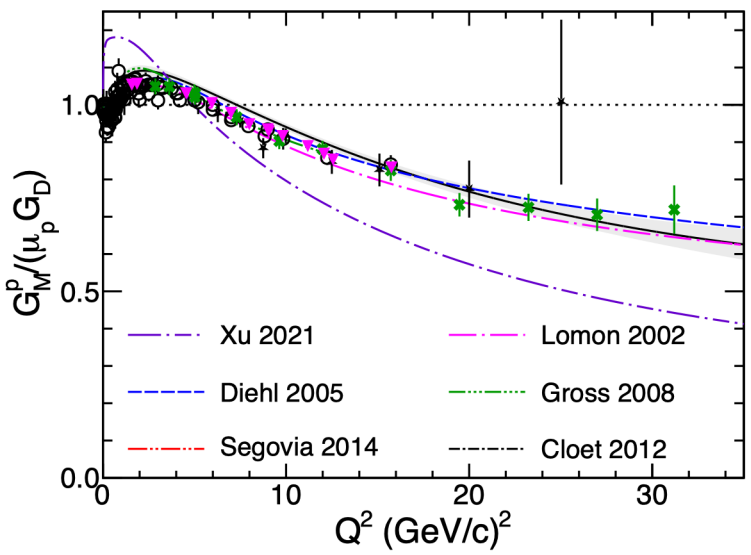

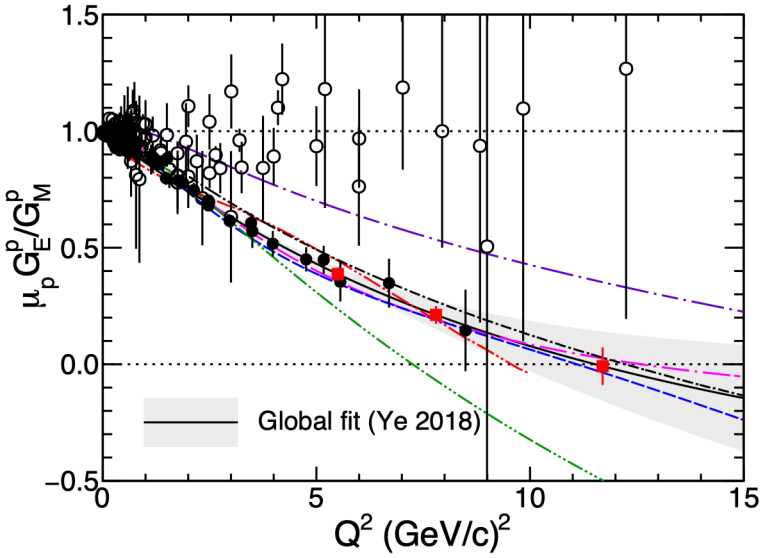

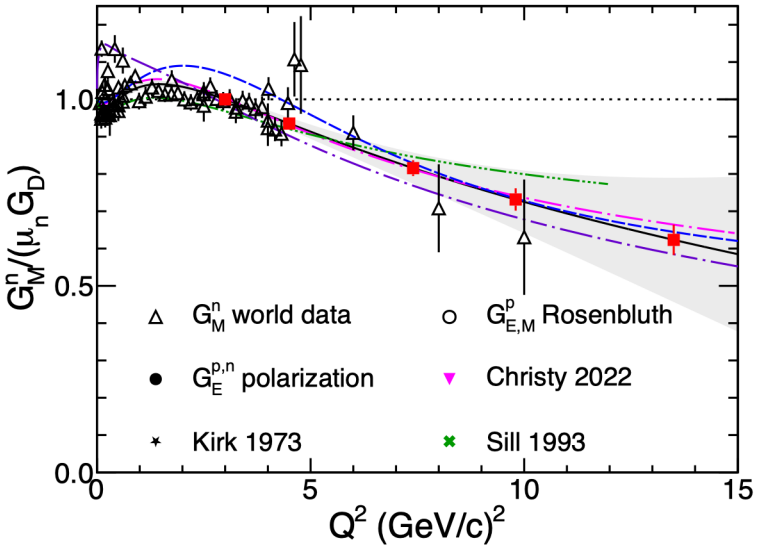

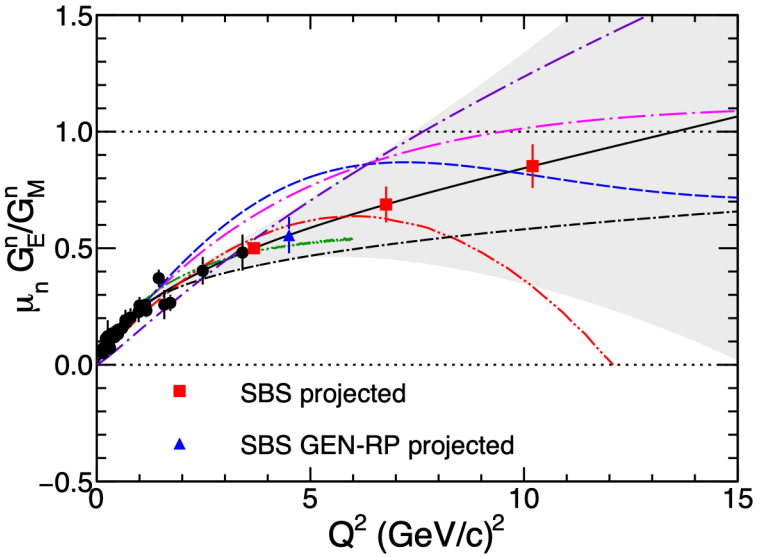

- Figure from "50 Years of QCD": https://inspirehep.net/literature/2617065 (Eur.Phys.J.C 83 (2023) 1125)
- GMN/nTPE (E12-09-019/E12-20-010): Oct. 2021-Feb. 2022
- GEN Helium-3: Oct. 2022-Oct. 2023
- GEN-RP: April-May, 2024
- GEP: April-August, 2025
- SBS projected uncertainties are shown arbitrarily on the 2018 global fit curves by Ye *et al.*
- G_M^n was already complete at the time this was published; projected uncertainties were already known
- G_E^n, G_E^p projections shown at the time were based on the experiment proposals

The Super BigBite Spectrometer in Hall A

Proton form factors ratio, GEp(5) (E12-07-109)

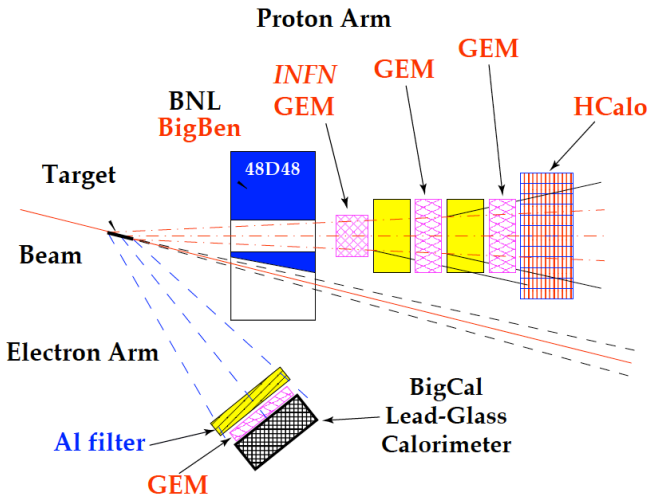

Neutron form factors, E12–09–016 and E12–09–019

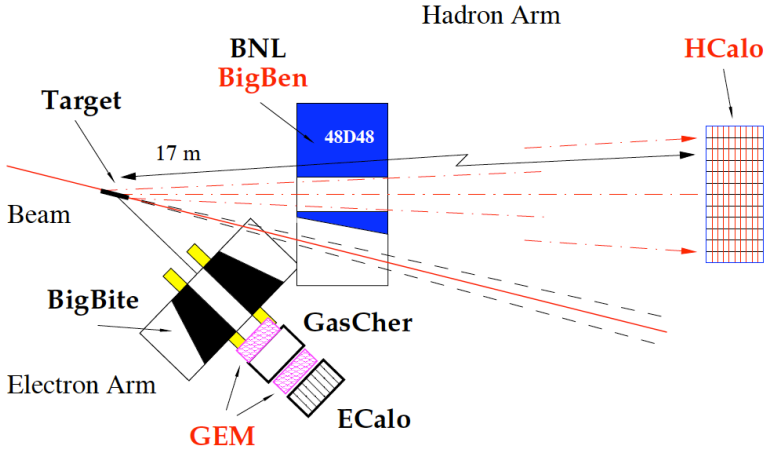

SIDIS transverse single-spin asymmetry experiment: E12-09-018

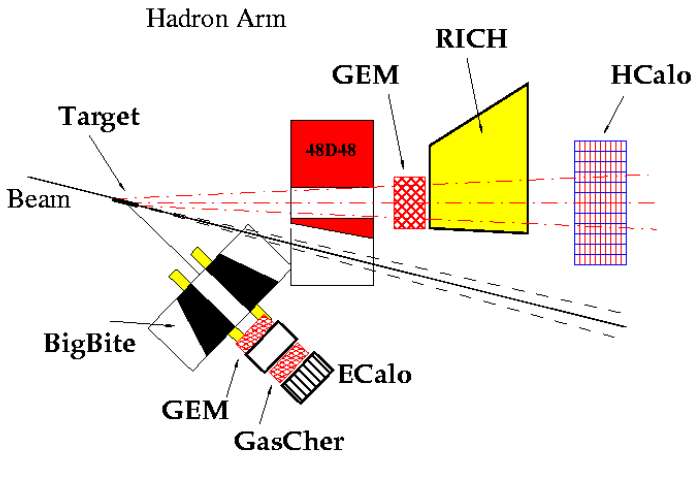

- What is SBS? → (up to) $\int BdL \approx 2.4\,T \cdot m$ dipole magnet with vertical bend, a cut in the yoke for passage of the beam pipe to reach forward scattering angles, and a flexible/modular configuration of detectors.
- Designed to operate at luminosities up to 10^{39} cm^{-2} s^{-1} with large momentum bite, moderate solid angle
- Five fully approved "large" experiments plus two fully approved "small" experiments, focused on high-Q^2 nucleon form factors, transverse SSAs in SIDIS
- Conditionally approved future program of "tagged DIS"—pion and kaon structure
- ***Large solid-angle + high luminosity @ forward angles = most interesting physics!***

The SBS neutron Form Factor Experiments (2021-2024)

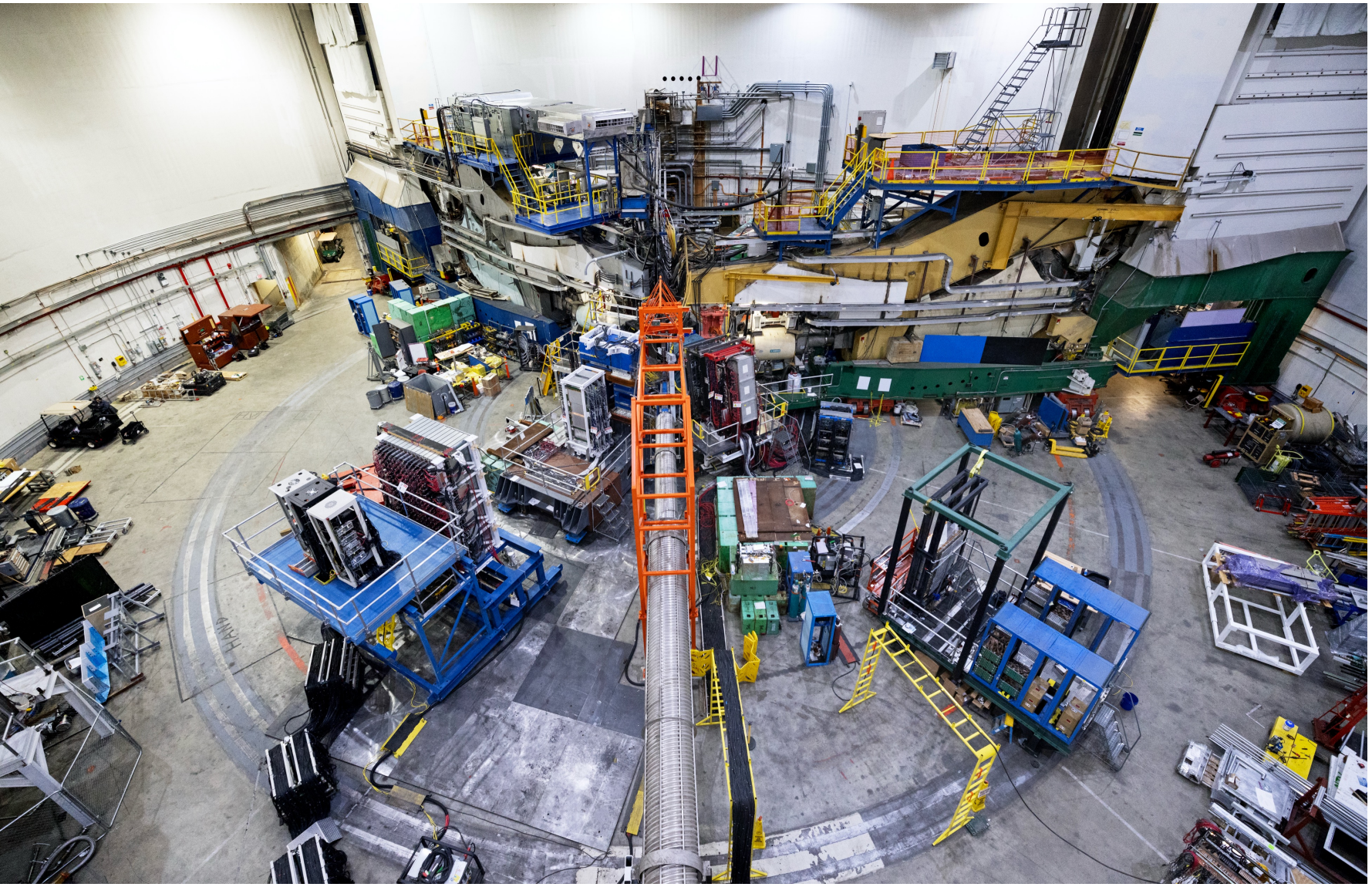

- GMN, GEN, GEN-RP all involve measurements of coincidence (e,e'N) reactions in quasi-elastic kinematics on light nuclear targets
- Common requirements include:
  - Scattered electron detection with tracking, PID, and full kinematic reconstruction
  - Nucleon detection and charge identification
- Key differences include:
  - Physics observables (cross section ratio versus polarized beam-target asymmetry versus recoil polarization)
- Dominant sources of uncertainty:
  - nucleon acceptance/detection efficiency systematics (GMN)
  - Statistics! (GEN/GEN-RP)
  - Low polarimetry FOM (GEN-RP)
  - Inelastic backgrounds (all)

Experiments E12-09-019/E12-20-010 (GMN/nTPE)

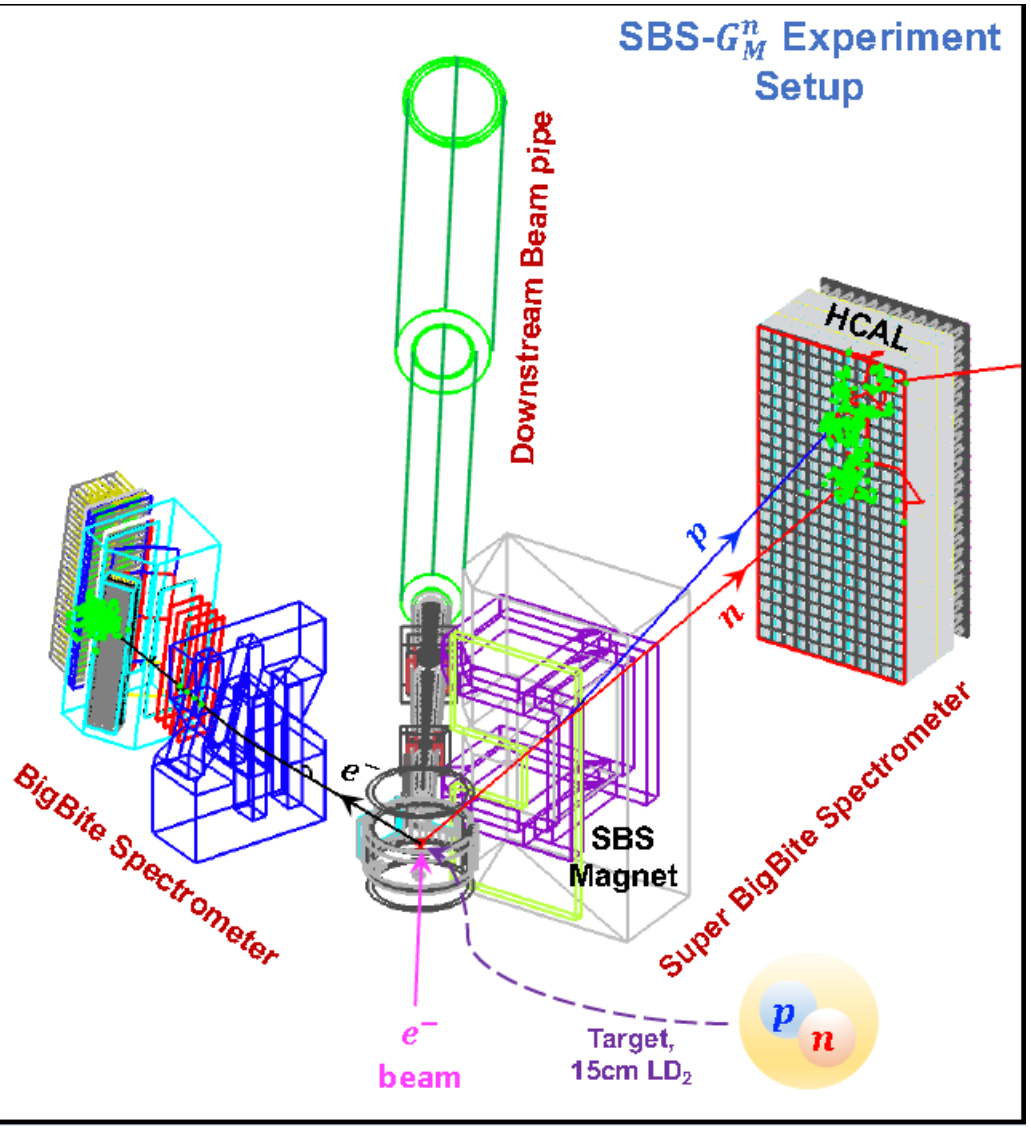

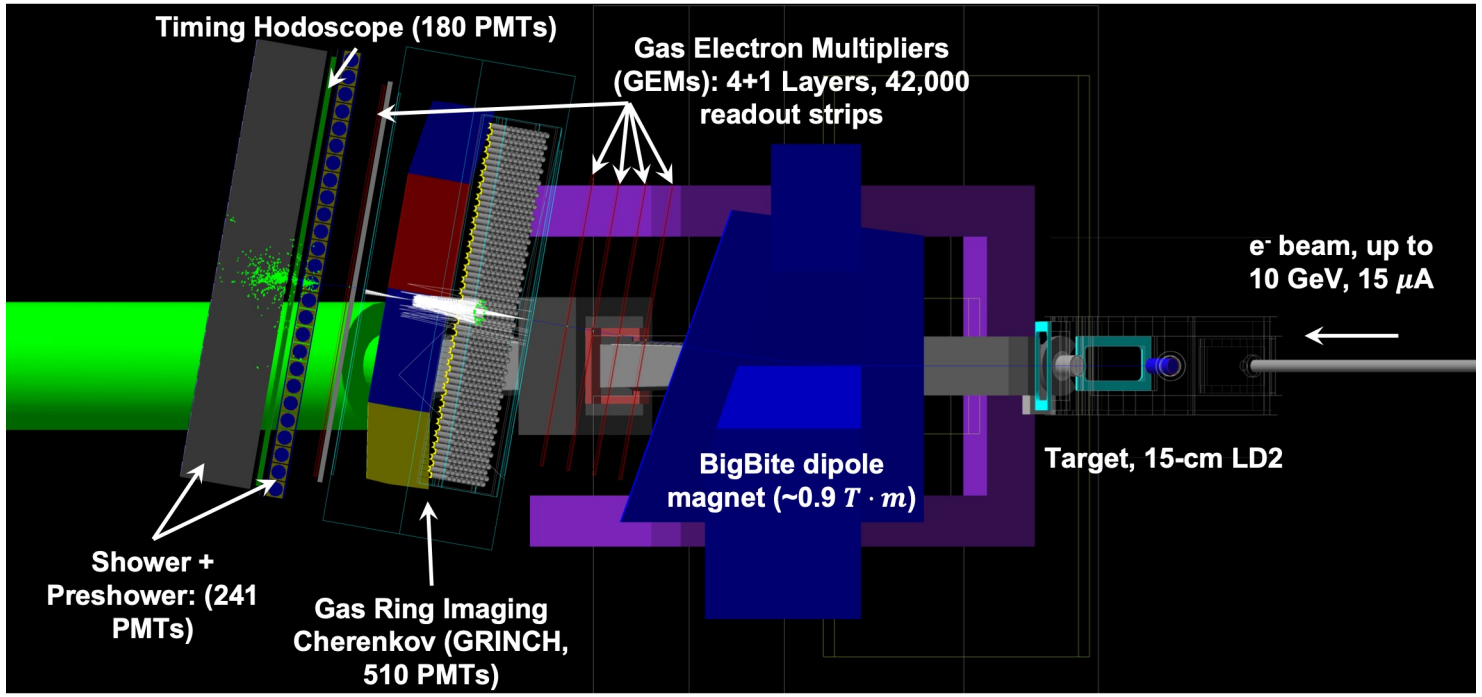

- Measure cross section ratio d(e,e'n)/d(e,e'p) on liquid deuterium.
- e^- arm: BigBite with upgraded detectors for high-luminosity running
- n/p arm: SBS with HCAL
- Ran Oct. 2021-Feb. 2022

Data/MC Fit to Δx Distribution: $Q^2 = 7.4\ (GeV/c)^2$

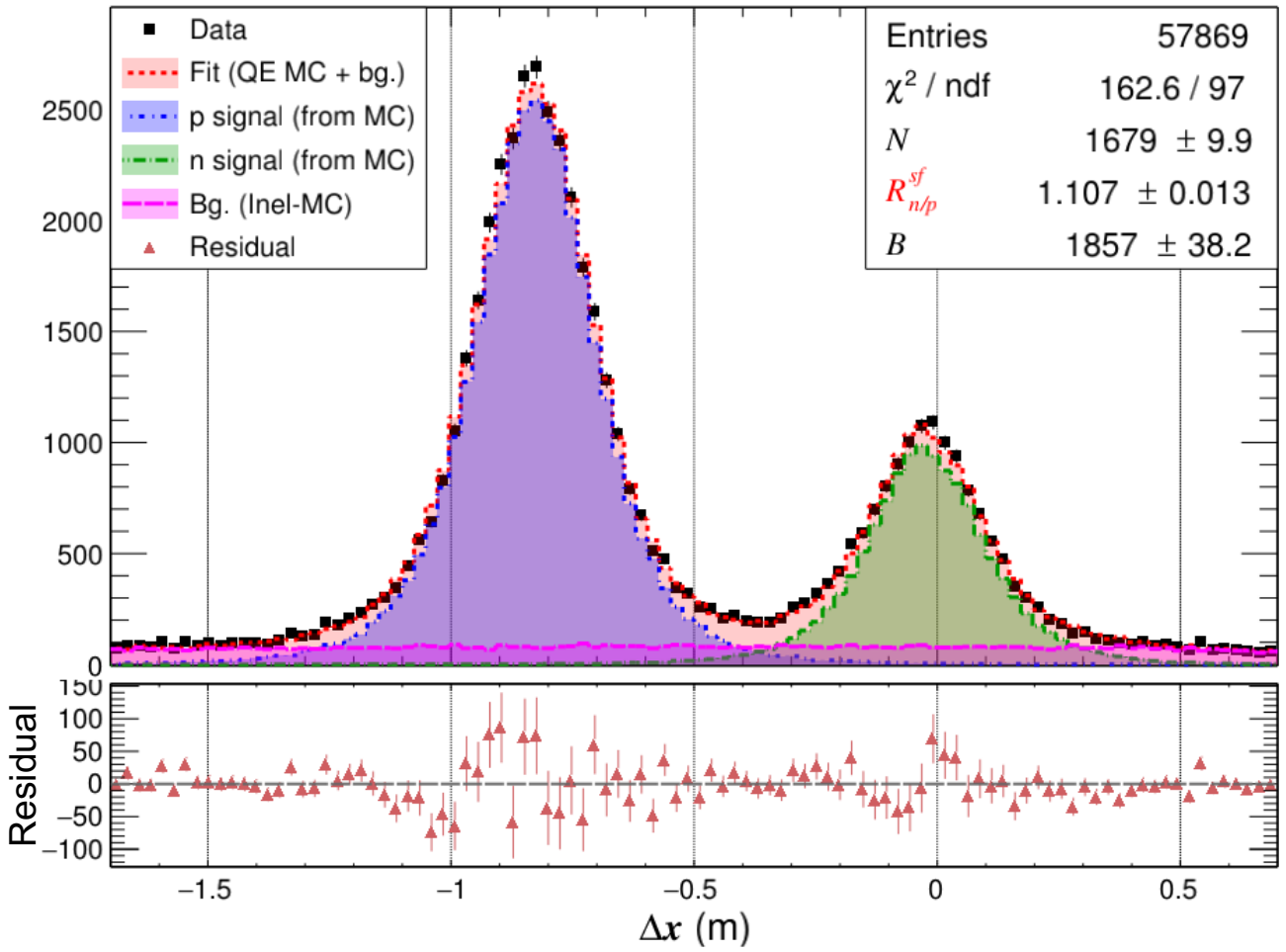

- Fit equation:

$$\text{Data} = N * (\text{p}^{\text{MC}}_{\text{signal}} + R^{sf}_{n/p} * \text{n}^{\text{MC}}_{\text{signal}}) + B * \text{Inel}^{\text{MC}}_{\text{bg}}$$

- Fit parameters:
  1. N – Overall proton (p) normalization.
  2. $R^{sf}_{n/p}$ – Relative neutron (n) to proton normalization.
  3. B – Overall background normalization.

- Agreement of fit looks good in the entire range of interest.

GMn Extraction from Data/MC Fit : $Q^2 = 7.4\ (GeV/c)^2$

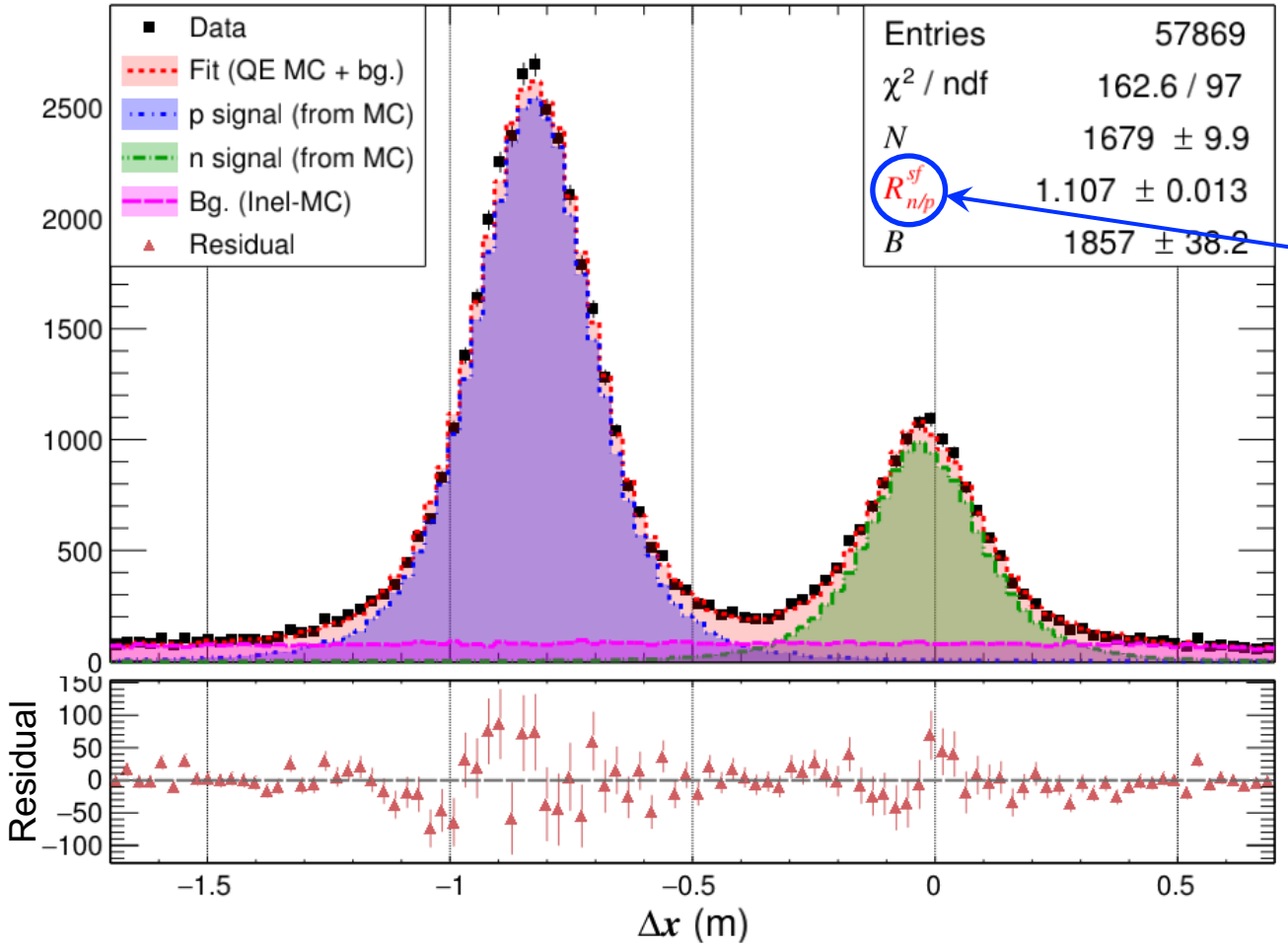

- Assumption:
  - Simulation accurately represents nuclear, radiative, and detector effects that are known to be present in data.
- Interpretation:
  - The fit parameter $R^{sf}_{n/p}$, i.e. the relative n/p normalization, is a measure of the discrepancy in the neutron to proton Born cross section ratio between simulation and data.
- GMn extraction:

$$R = \frac{\frac{d\sigma}{d\Omega}\Big|_{n(e,e')}}{\frac{d\sigma}{d\Omega}\Big|_{p(e,e')}} = R^{sf}_{n/p} * R_{MC}$$

$$\Rightarrow G^n_M = -\left[\frac{1}{\tau_n}\frac{\epsilon_n(1+\tau_n)}{\epsilon_p(1+\tau_p)}\sigma^p_{Red}R - \frac{\epsilon_n}{\tau_n}G^{n\,2}_E\right]^{\frac{1}{2}}$$

G_M^n analysis at world-record* $Q^2 = 13.6\ GeV^2$

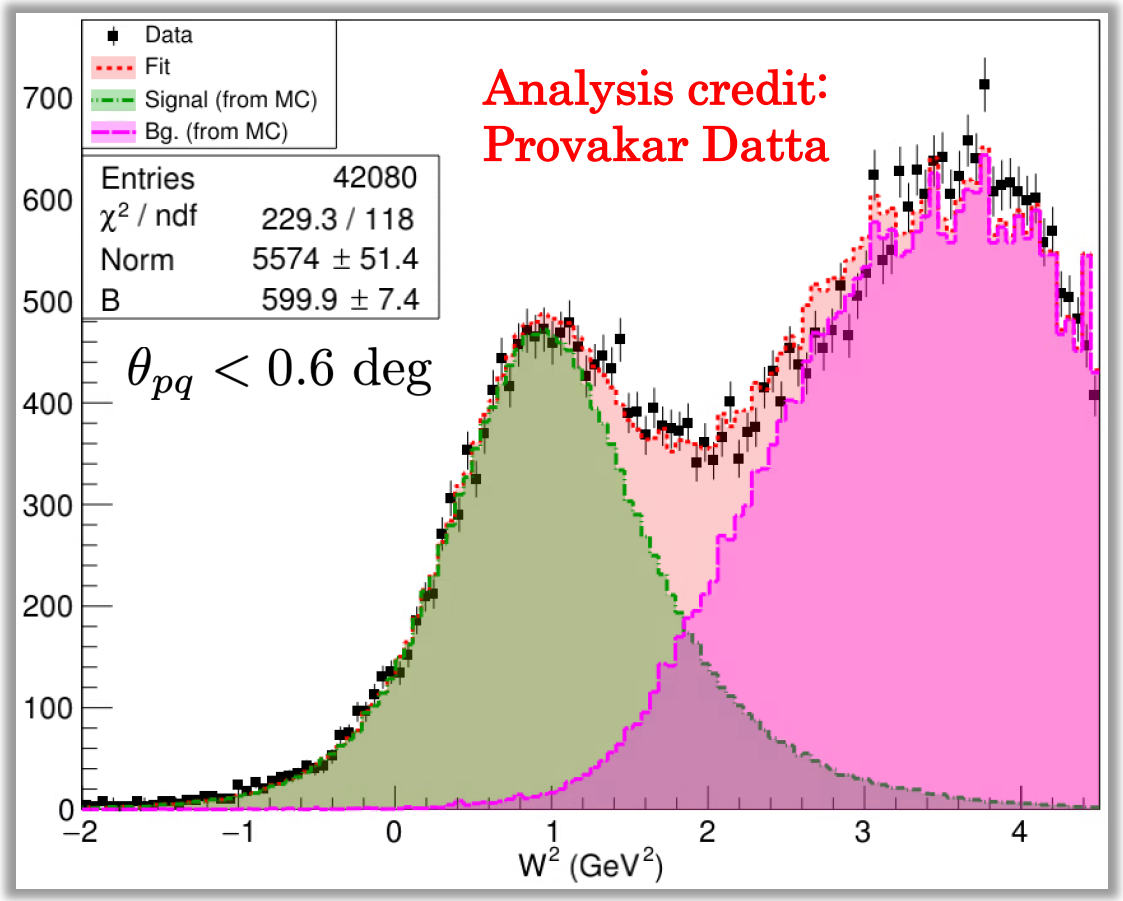

Q^2 = 13.6 (GeV/c)²

*--For a neutron form factor measurement

Q^2 = 13.6 GeV², 0.16 ≤ W^2 ≤ 1.44 GeV², Fiducial Cuts

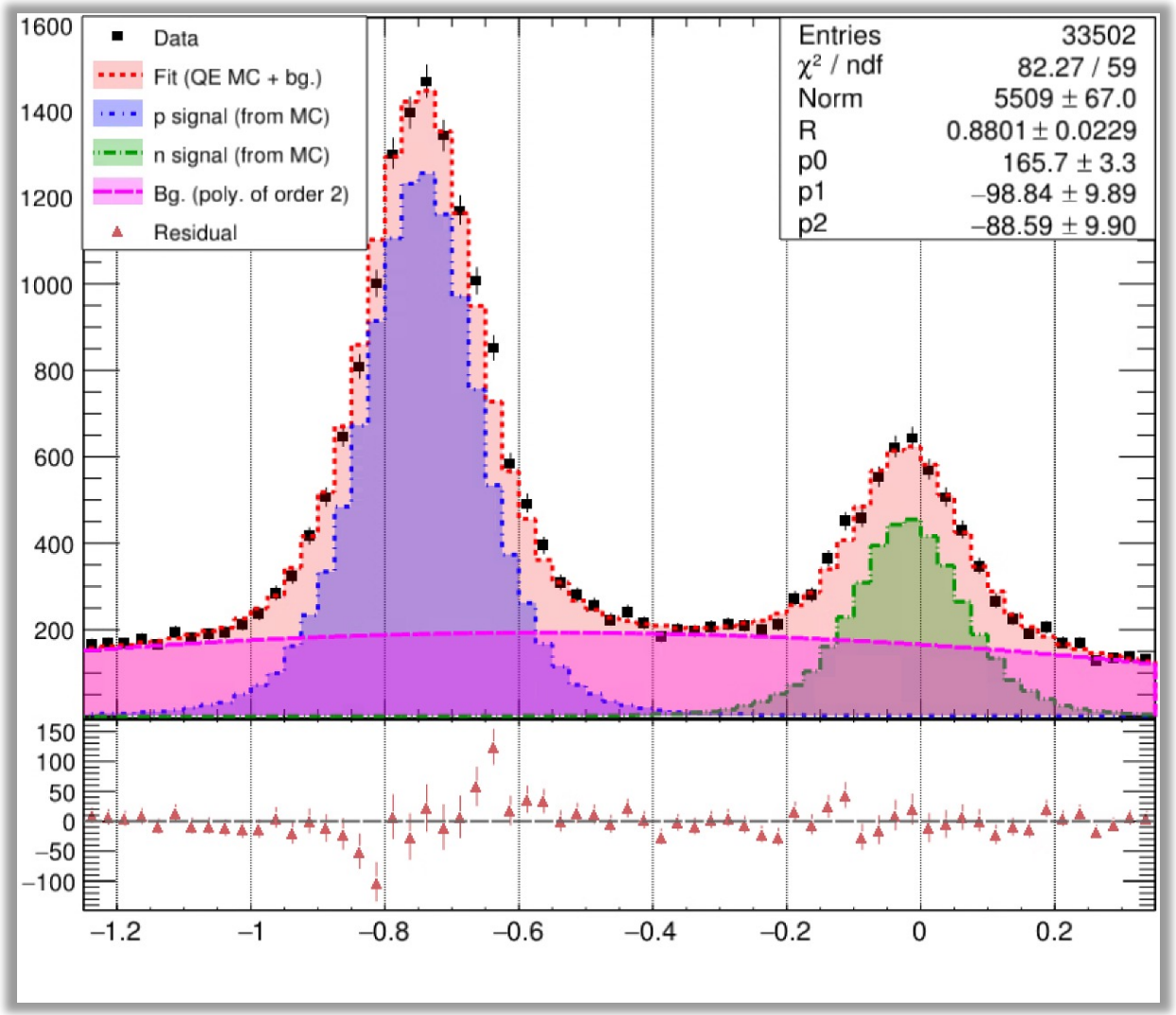

GMn—preliminary results (plots credit: P. Datta, LBNL)

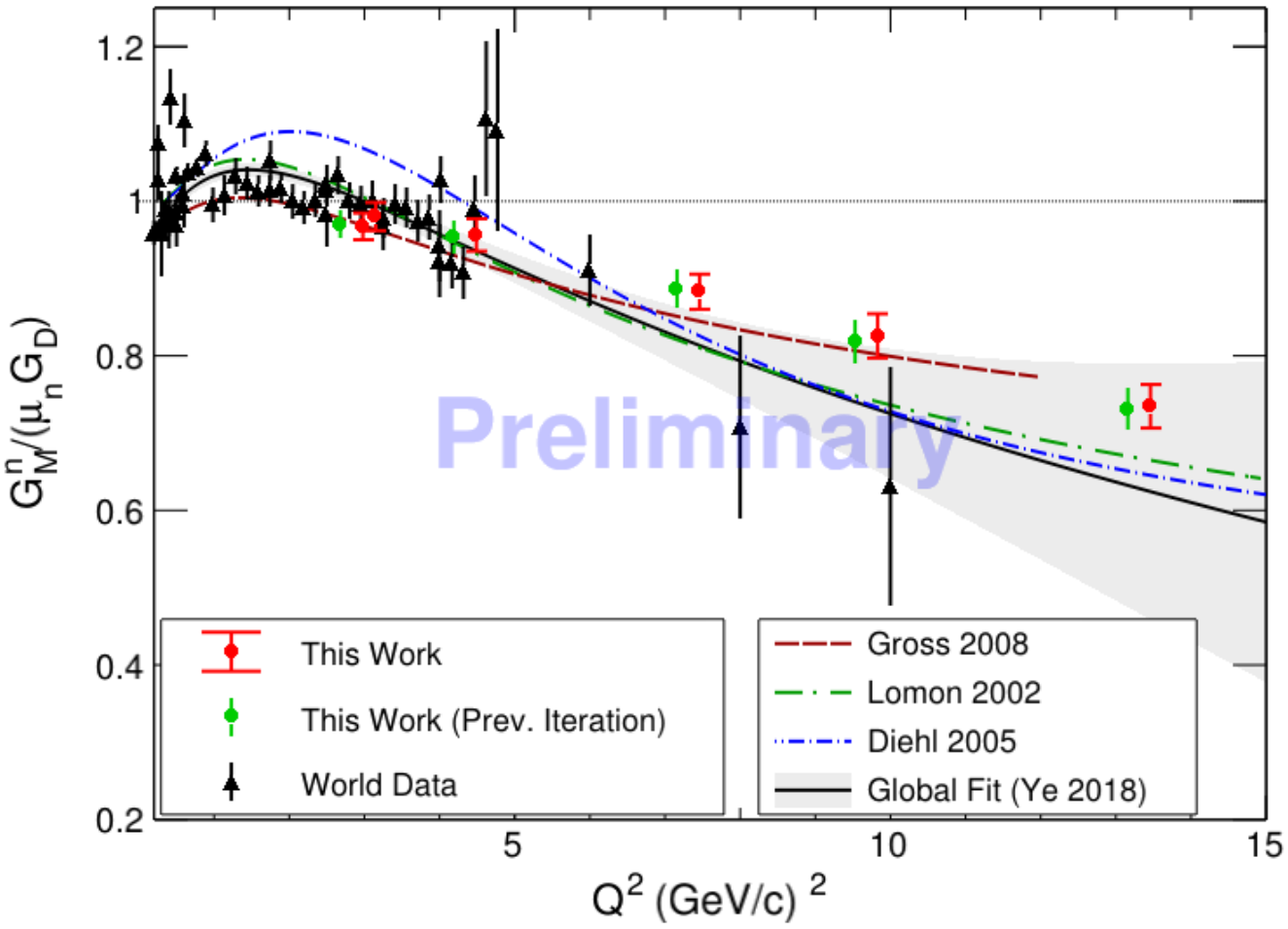

- Green = "pass 2"
- Red = "pass 3" (w/combined stat. plus syst. error)
- Biggest improvement from "pass 2" to "pass 3" was timing calibrations—physics results stable
- "Found data" at $Q^2 = 3$ GeV^2 tripled the statistics for the more optimal SBS field setting used at this Q^2
- We intend to publish the results from pass 3

3rd Pass of Reconstruction – Results

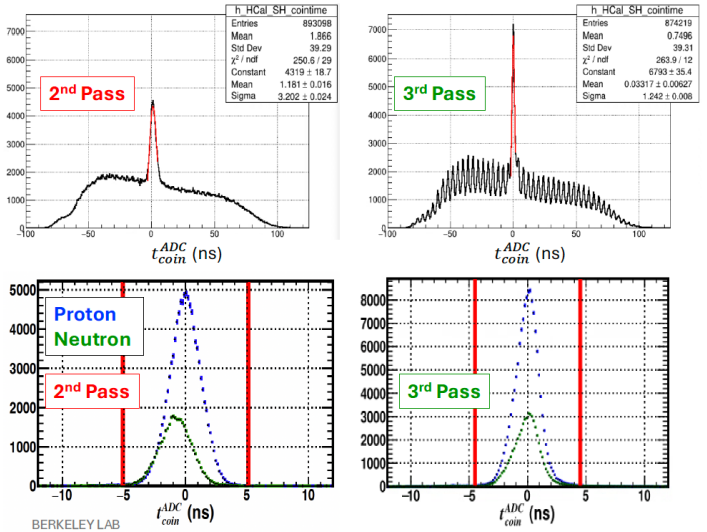

Greatly improved HCal-Shower ADC coincidence time resolution good enough to resolve the beam bunch structure.

Mitigation of position-dependent non-uniformity in HCal timing calibration better aligns the coincidence times for *D(e,e'p)* and *D(e,e'n)* events.

BERKELEY LAB

31

51	11595	10/24/2021	16:38	17:00	LD2	1.75	5		
52	11596	10/24/2021	17:07		LD2	1.75	50	N/A	junk - DAQ keeps on going down in rate
53	11597	10/24/2021	17:15	19:30	LD2	1.75	50	Y	32.4 junk - DAQ keeps on going down in rate
54	11598	10/24/2021	19:41	20:06	Dummy	6.5	50	Y	4 Production Run - Cycle 4
55	11599	10/24/2021	20:08	20:23	Dummy	6.5	50	Y	2.7 Production Run - Cycle 4

nTPE experiment: Precision Rosenbluth Separation of $en \rightarrow en$

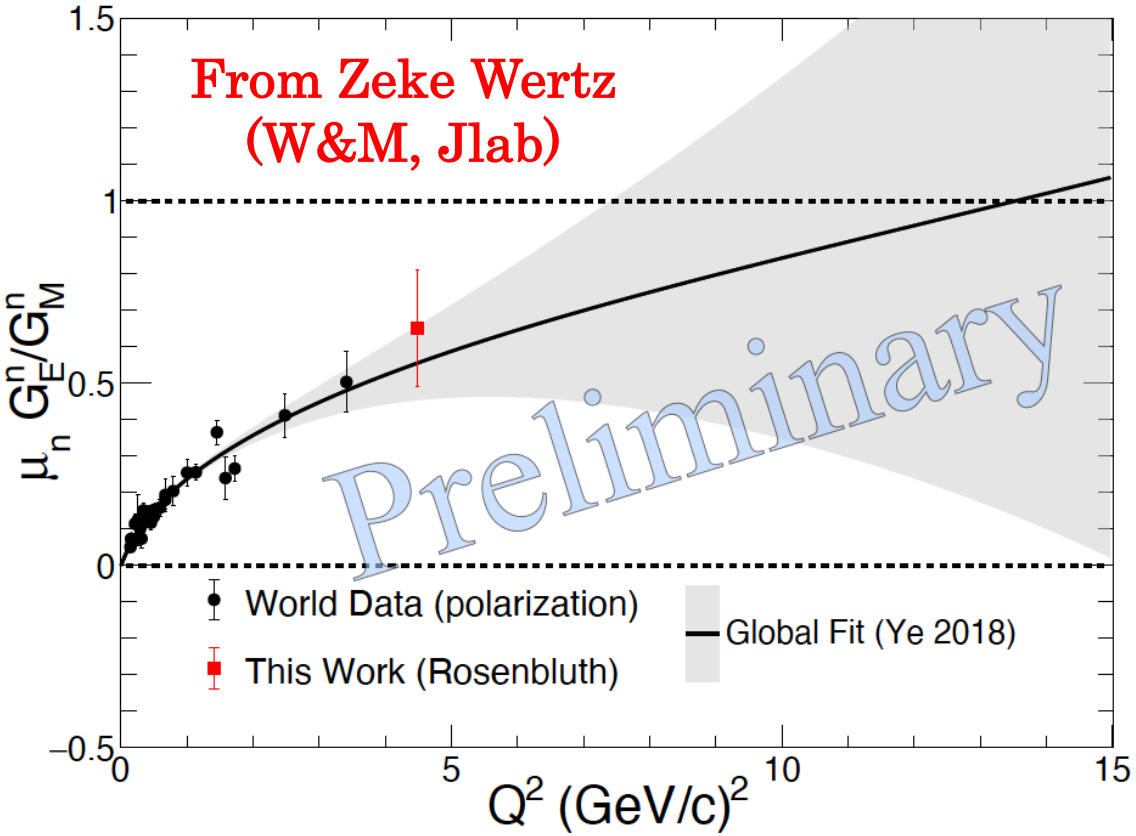

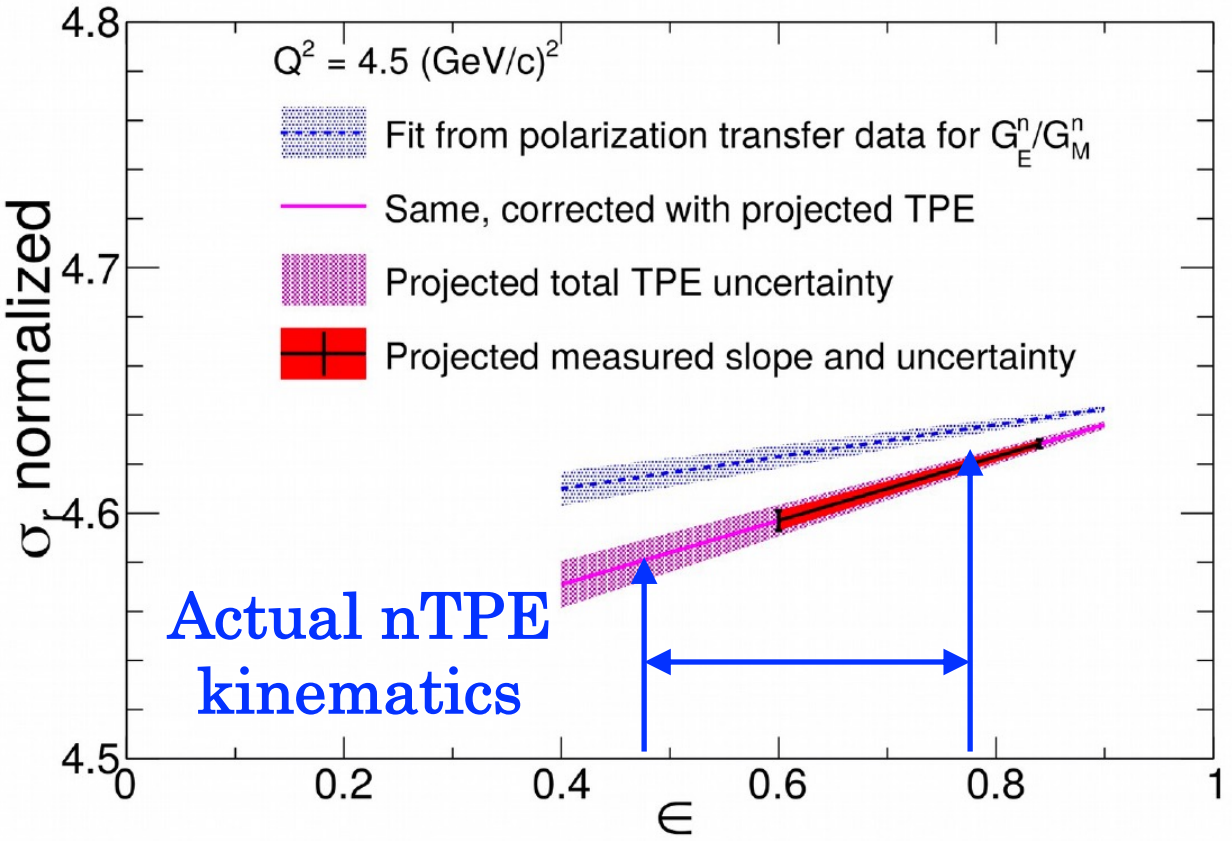

- Left: $\mu_n G_E^n/G_M^n$ world data and preliminary result from **Zeke Wertz thesis**
- Right: projected nTPE sensitivity from proposal 12-20-010 (**Eric Fuchey contact**)
- Actual kinematics have $\Delta\epsilon \approx 0.3$, compared to 0.24 from the proposal

The Jefferson Lab Thesis Prize, 2025

From left: David Dean, Provakar Datta, Elizabeth Lawson, Loana "Maria" Niculescu, and Matthew Shepherd pose for a group photo after Datta wins the thesis award during the Jefferson Lab User Organization (JLUO) annual meeting award ceremony held inside the CEBAF Center auditorium at Jefferson Lab in Newport News, Va., on June, 25, 2025. (Aileen Devlin | Jefferson Lab)

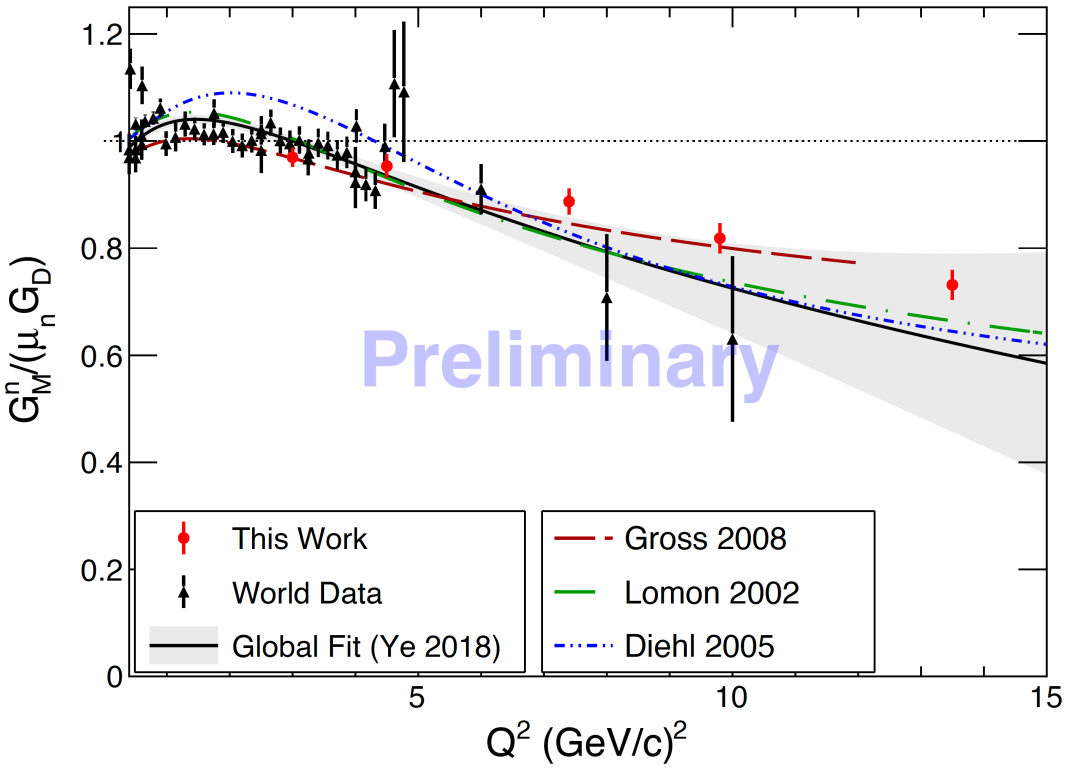

Preliminary results for neutron magnetic form factor (normalized to "standard dipole") from the prize-winning thesis

- Thesis: https://inspirehep.net/literature/2853798
- JLab press release: https://www.jlab.org/news/releases/built-hand-proven-datta

E12-09-016: G_E^n/G_M^n to 10 GeV^2 using polarized ^{3}He(e,e'n)pp

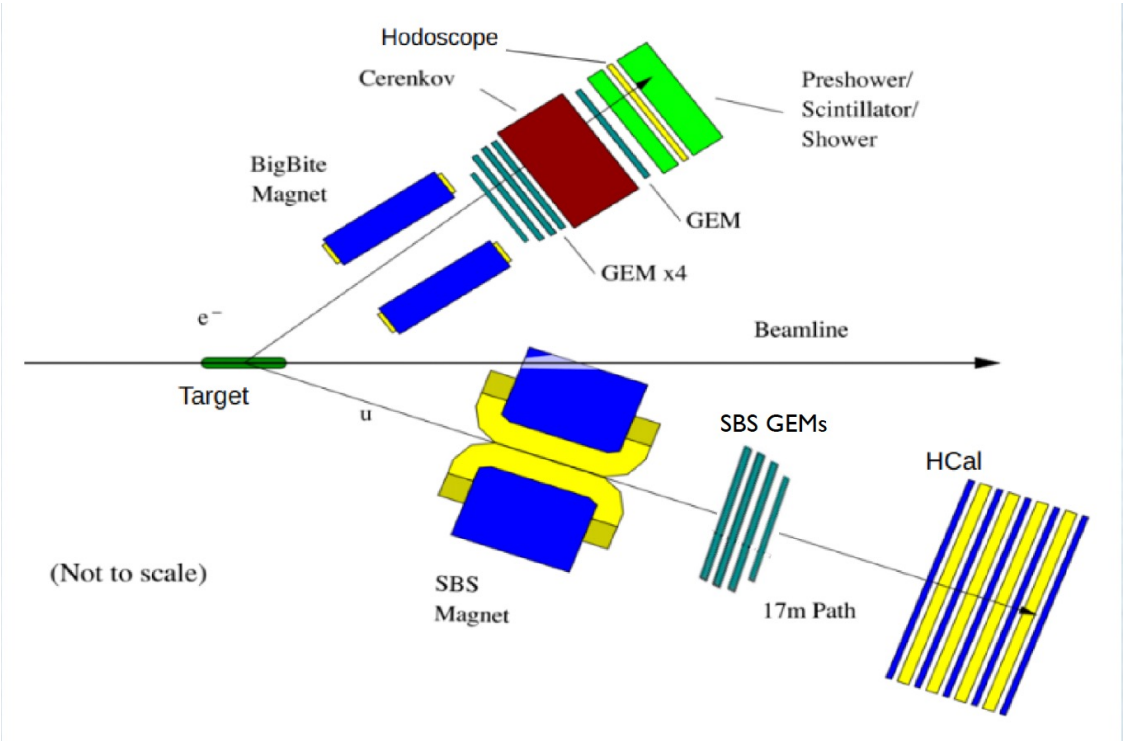

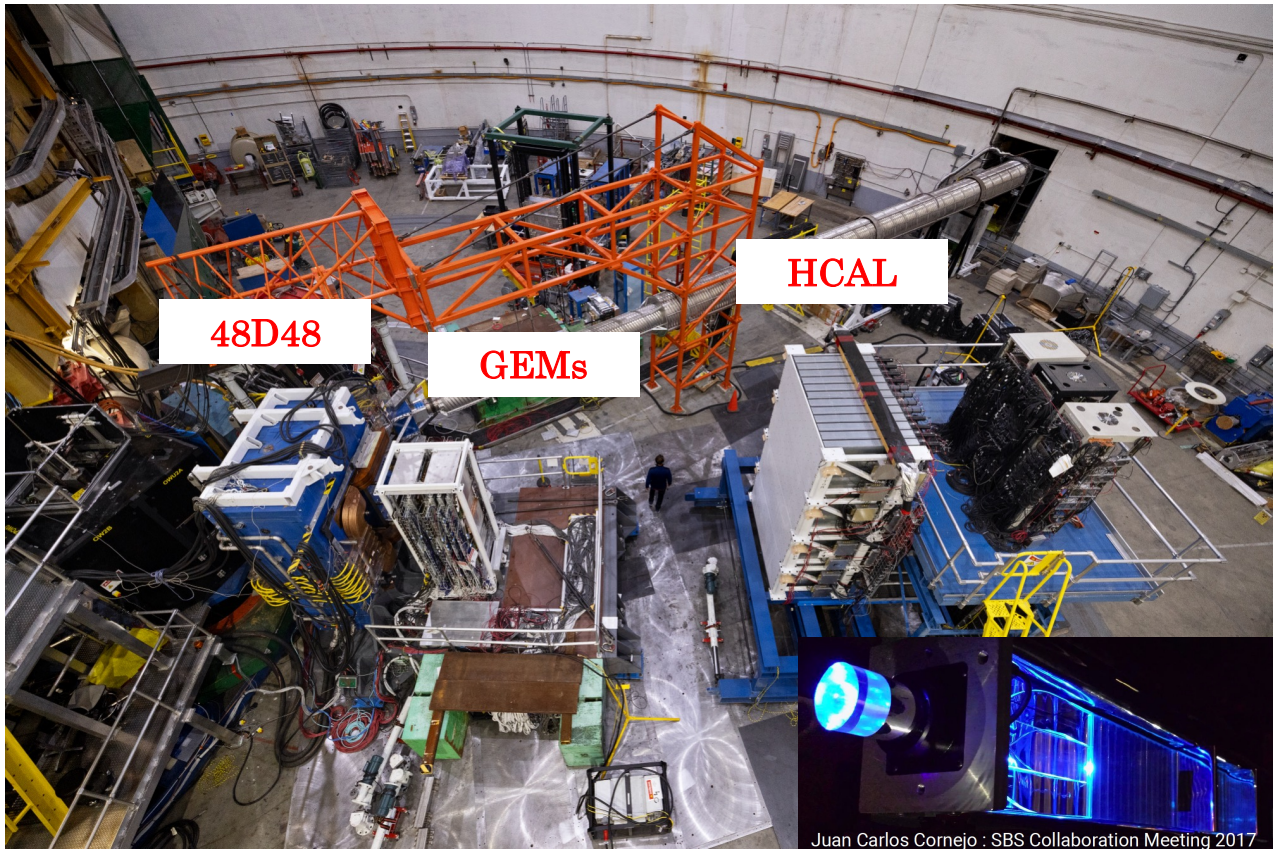

- Same detector configuration as GMN (E12-09-019) (with GEMs added to SBS for commissioning)
- High-luminosity polarized ^{3}He target with convection-driven circulation of polarized gas.
- Measurement to 10 GeV^2 has enormous discrimination power among theoretical models
- **Data-taking completed Oct. 2022-Oct. 2023!**

- Note: the photo above was taken in GEN-RP configuration
- GEN had HCAL 17 m from target to optimize coincidence time-of-flight for background rejection

The SBS-GEN polarized Helium-3 target

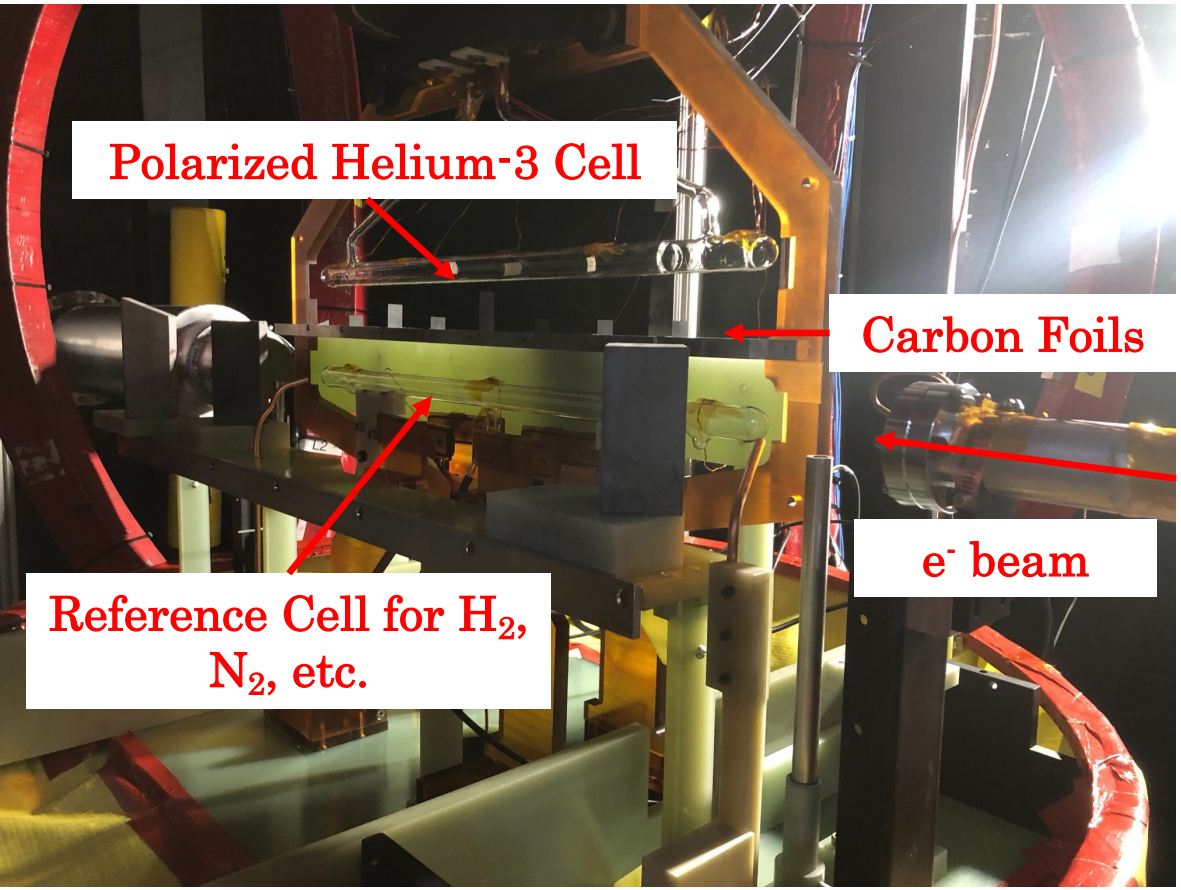

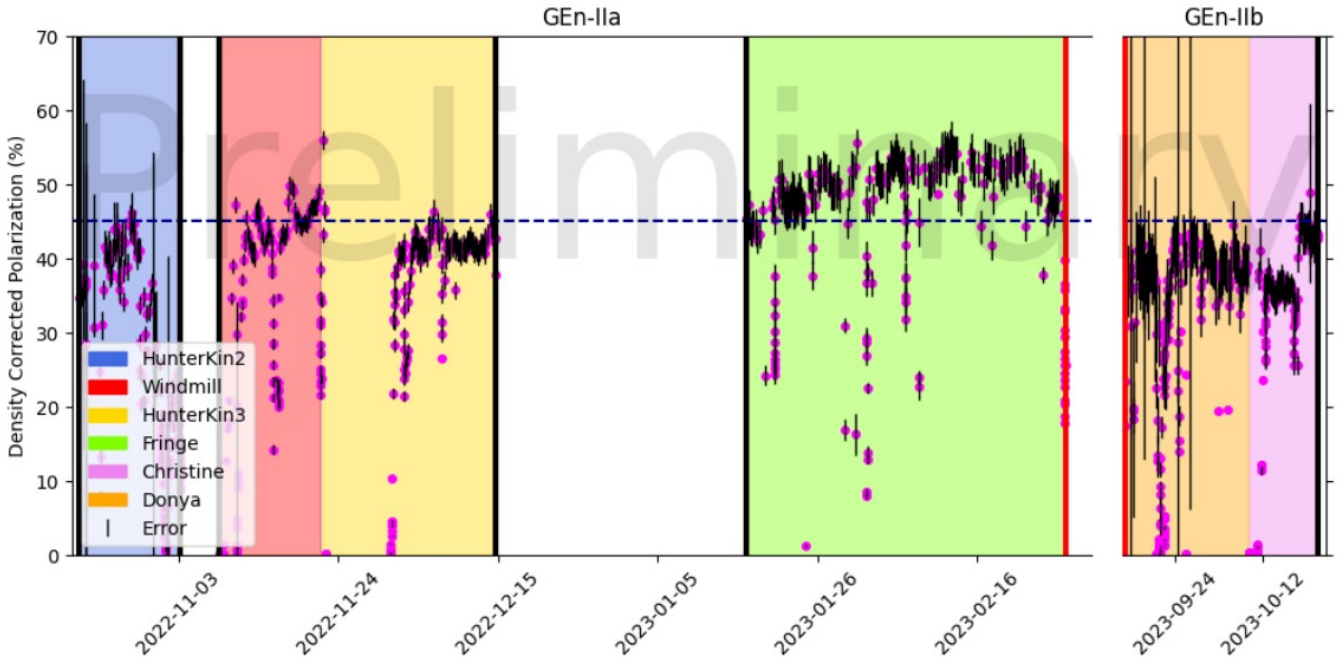

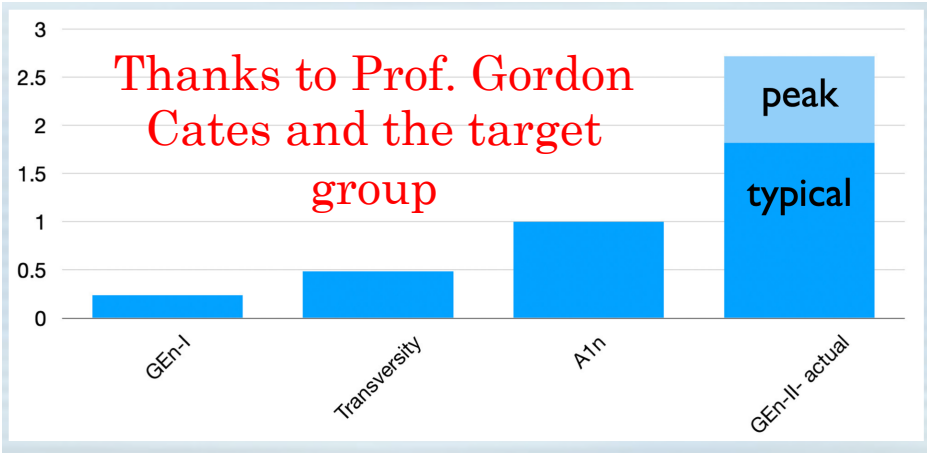

- Above, left: Inside the target enclosure
- Above, right: preliminary target polarization results
- Below, right: estimated FOM compared to previous experiments

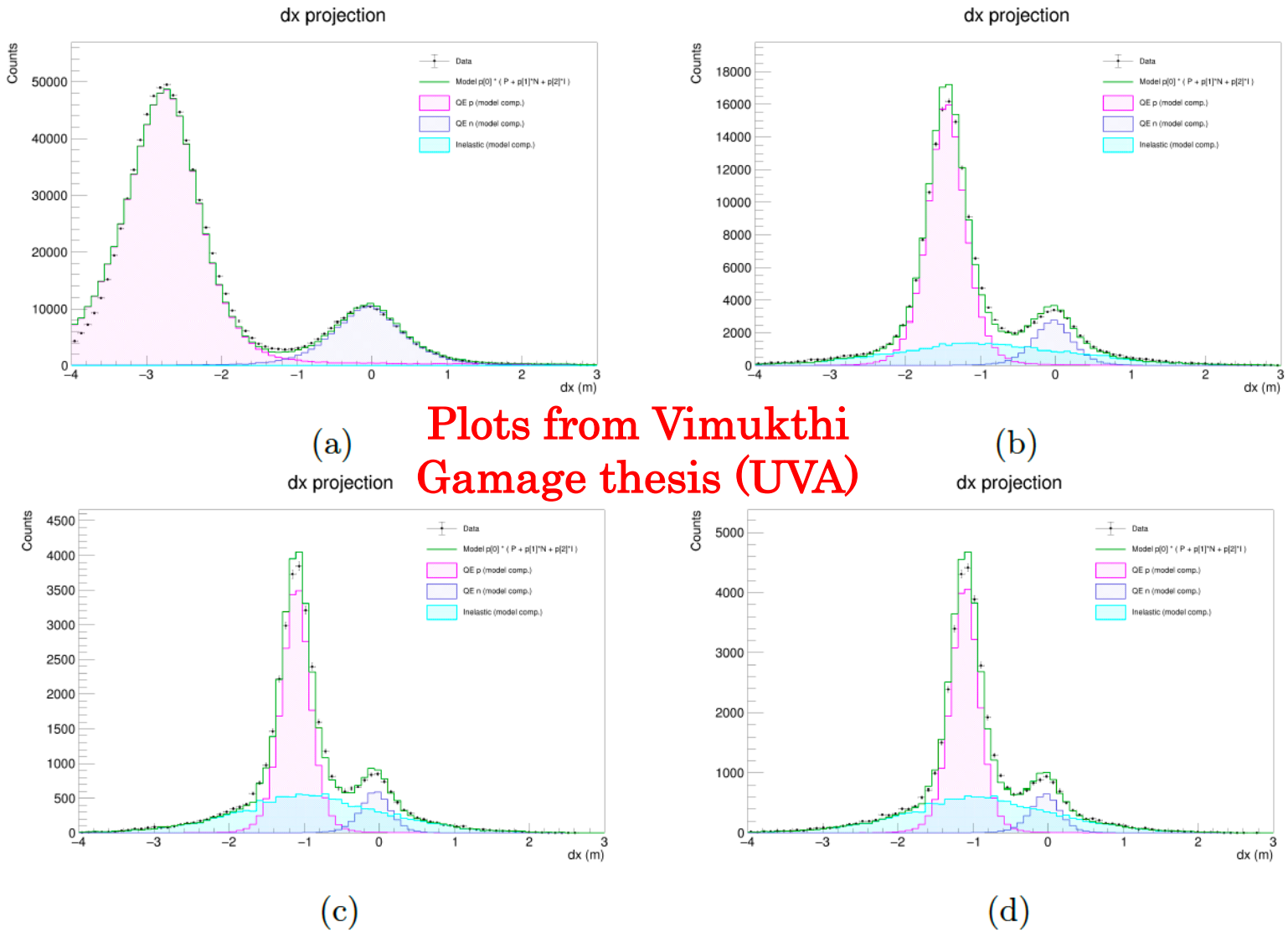

Plots from Vimukthi Gamage thesis (UVA)

Figure 6.6: Δx projection distributions showing inelastic and proton contamination for each kinematic point.(a) Kin2 (b) Kin3 (c) Kin4a (d) Kin4b

- Quasi-elastic event selection and inelastic background contamination estimates
- Kin. 2 → $Q^2 = 3.0$ GeV^2
- Kin. 3 → $Q^2 = 6.8$ GeV^2
- Kin. 4a → $Q^2 = 9.8$ GeV^2 (spring 2023 running)
- Kin. 4b → $Q^2 = 9.8$ GeV^2 (fall 2023 running)
- Inelastic contamination limits both statistical precision and accuracy of the result at highest Q^2
- Data with SBS GEMs help understand the signal and (charged) background shapes (next slide)

Raw asymmetry at $Q^2 = 3\ GeV^2$ (plot credit: Vimukthi Gamage thesis (UVA))

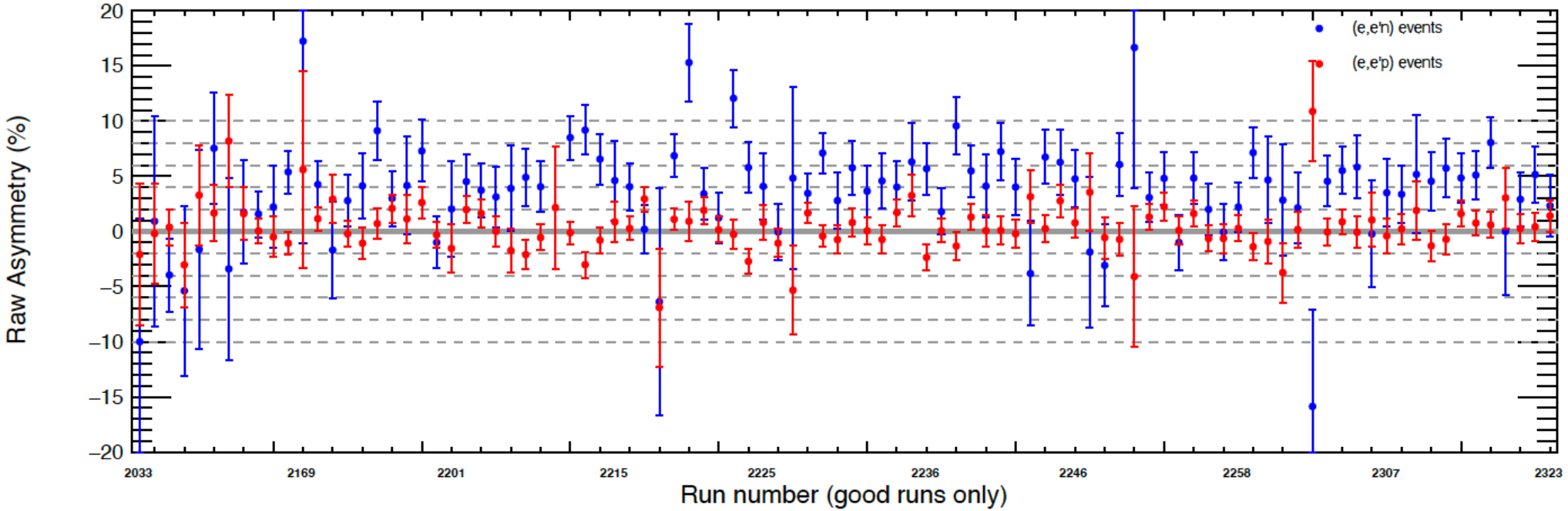

Figure 5.14: Run by run asymmetry for Kin2 after accounting for the half-wave plate and accelerator settings. Certain runs are excluded from the analysis due to various quality issues including helicity measurement malfunctions.

- Neutron (proton) asymmetry "large" ("small") as expected for ^{3}He target

Understanding GEn-II detector performance with SBS GEMs, I

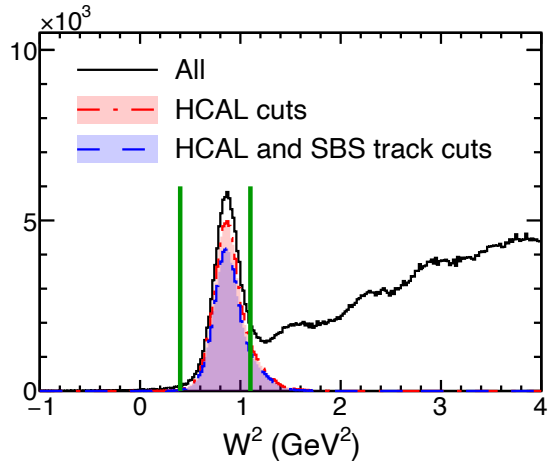

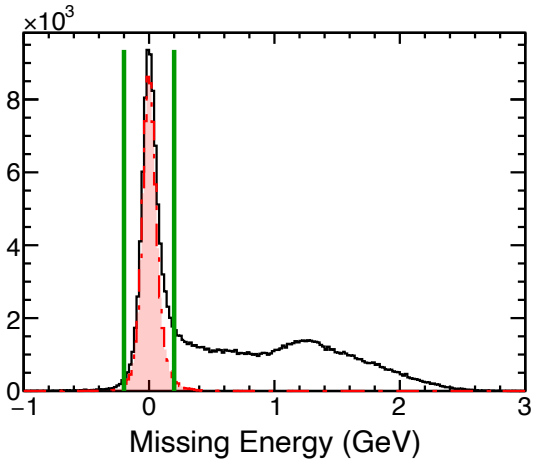

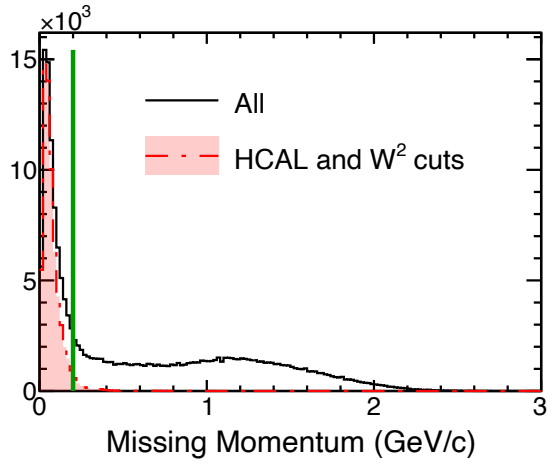

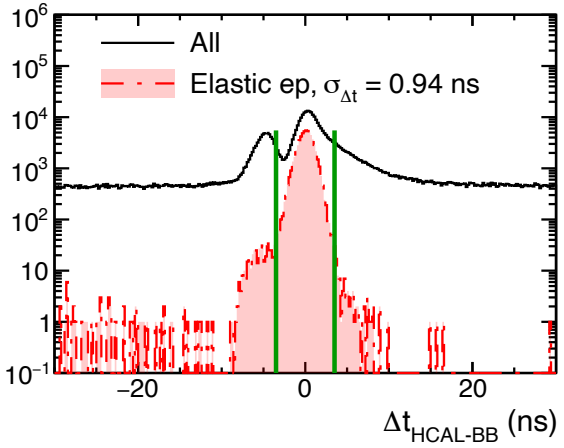

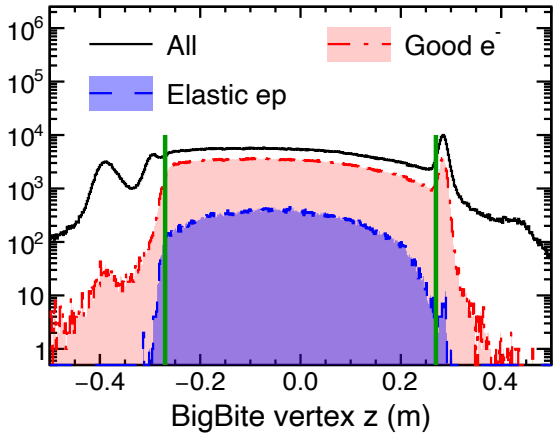

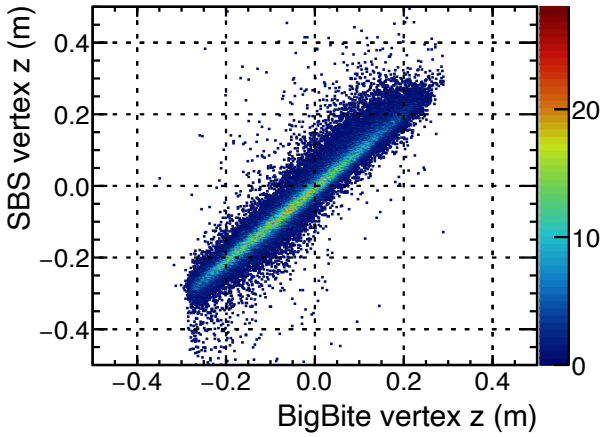

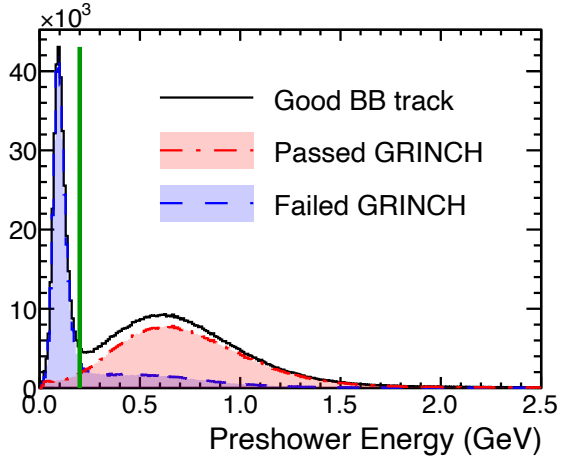

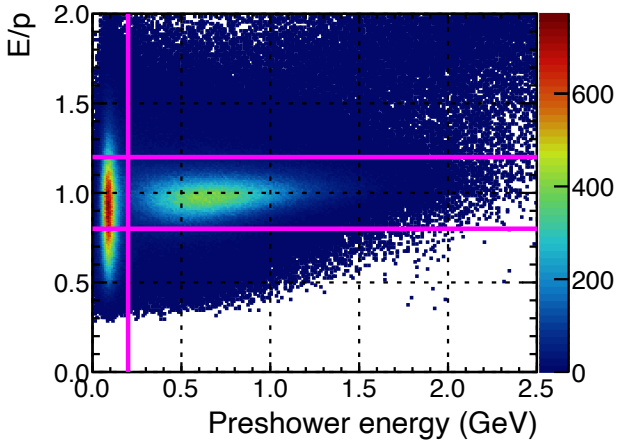

- H_2 reference cell data from $Q^2 = 3$ GeV^2 with tracking in SBS

Understanding GEn-II detector performance with SBS GEMs, II—High-Q^2 data

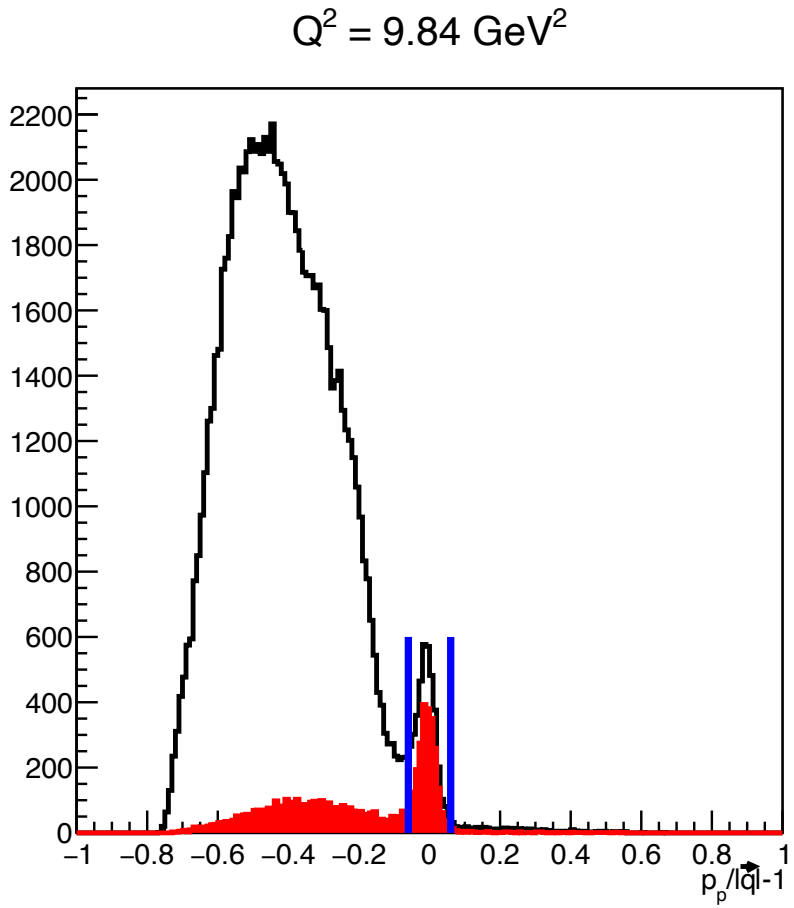

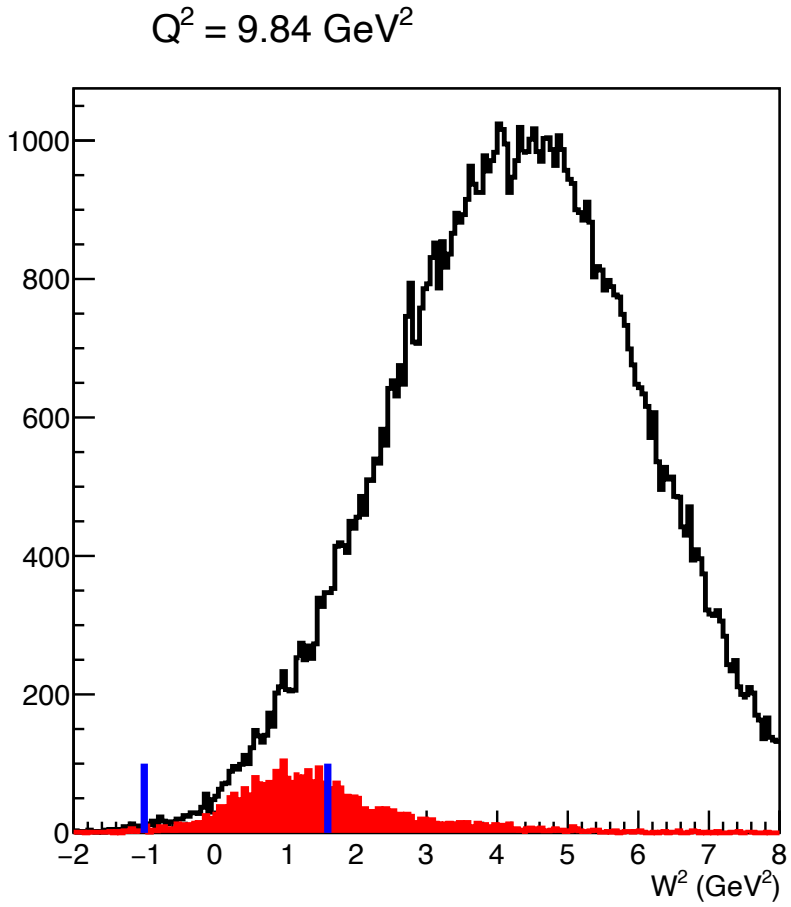

- Left: fractional deviation of proton momentum from magnitude of $\vec{q}$-(three) vector from BigBite, **without** and **with** W^2 **cut**
- Right: W^2, **without** and **with cut** on $\frac{p_p}{|\vec{q}|} - 1$

- This is Helium-3 data (with a positively charged track in SBS), at the highest Q^2
- (Surprisingly?) clean (quasi-)elastic ^{3}He(e,e'p)np event selection with full kinematic reconstruction in both arms (missing energy, missing momentum, etc)→Too bad we can't do this for neutron events!
- Helps understand signal and background shape with large Fermi smearing and inelastic background!
- QE W^2 distribution

E12-17-004 (GEN-RP): G_E^n/G_M^n to 4.5 GeV² via charge-exchange recoil polarimetry

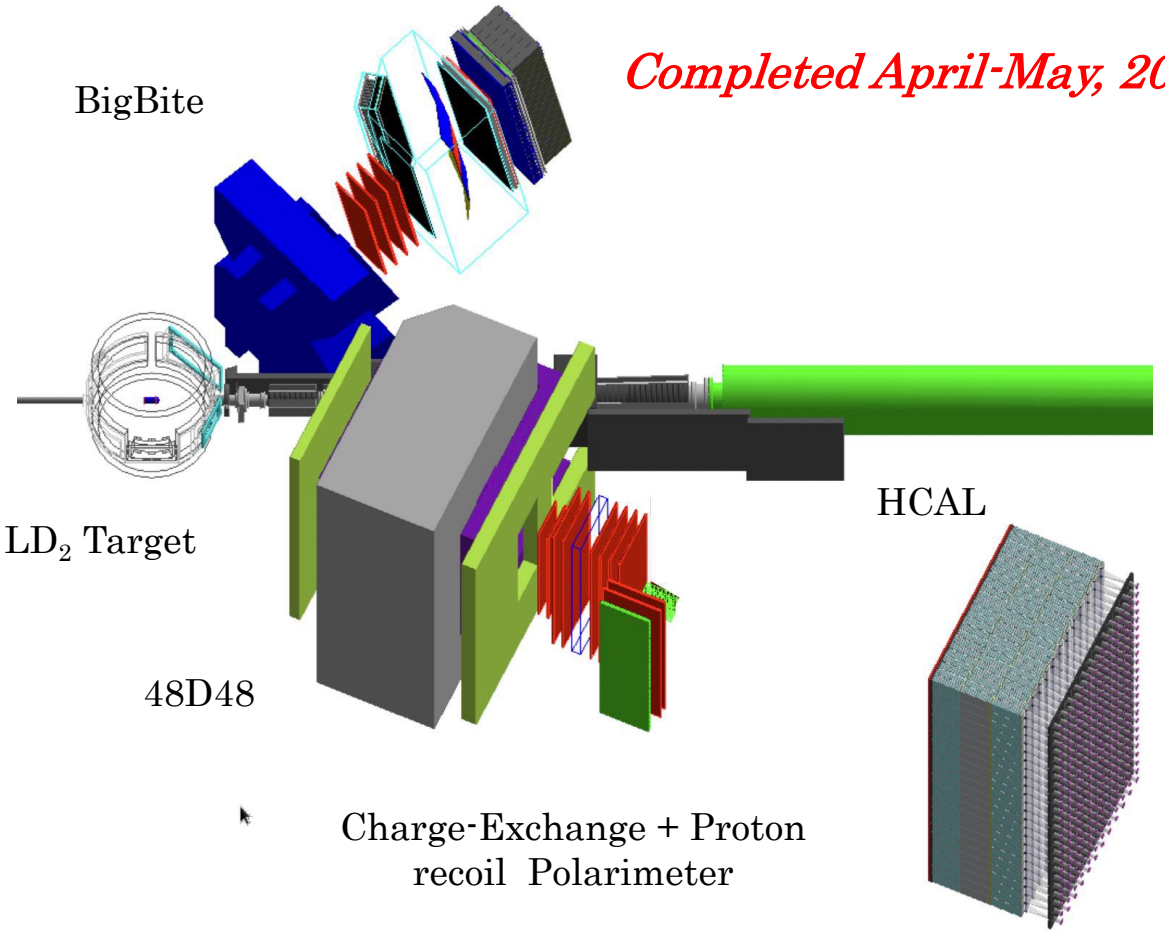

Completed April-May, 2024

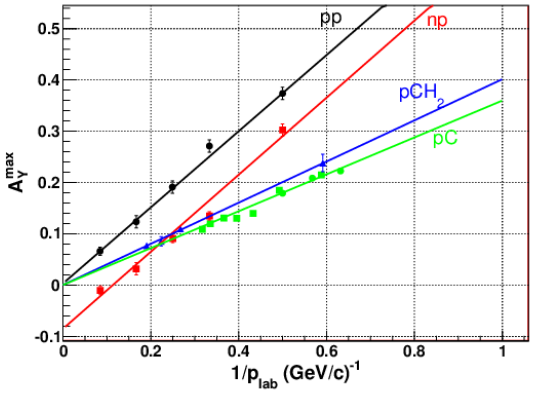

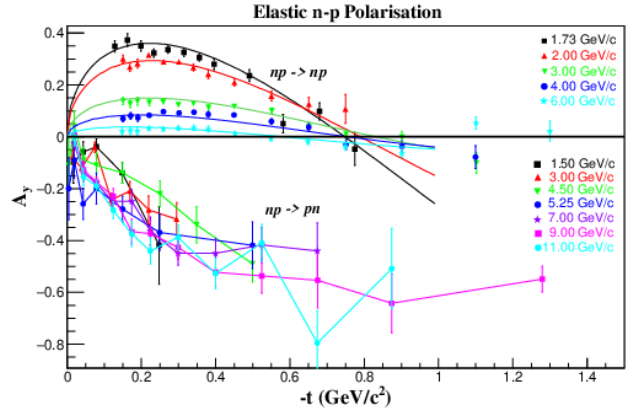

Analyzing powers for np, pp, pA scattering vs. initial momentum (left) and vs. transferred momentum (right)

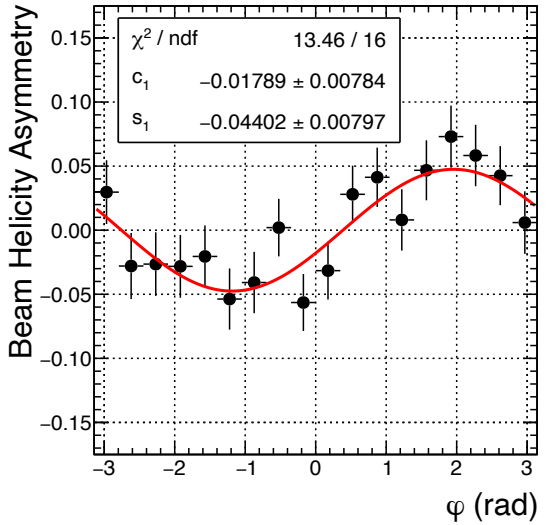

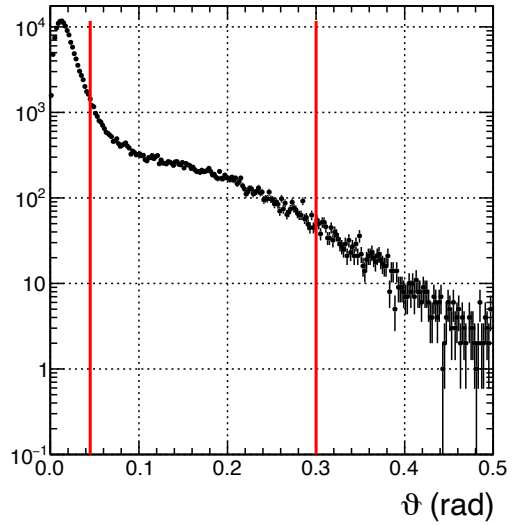

Above: LH_2 elastic asym. from GEN-RP

- E12-17-004 layout (above) and projected results (right):
  - First use of charge-exchange polarimetry in a FF experiment
- E12-20-008 approved as add-on to measure K_{LL} for $\gamma n \to \pi^- p$

GEN-RP Analysis Progress—Quasi-Elastic Data

Charge-Exchange Event Separation

- The hadrons coming from the target goes through the SBS magnet
- Using the precise q-vector generated using BB information we can calculate the expected position of the hadron(if not deflected from the SBS magnet) on the analyzer plate(or the HCAL)
- With the deflection from the SBS magnet we can see two separate peaks for Neutrons and Protons
- We can not use the HCAL as a reliable method of distinguishing the particles like it's done in other SBS experiments (GEn-II or GMn) because of the possible deflections analyzer in the middle, specially for the charge-exchange events
- Neutron events can be further isolated from Protons using the condition of not having a track before analyzer

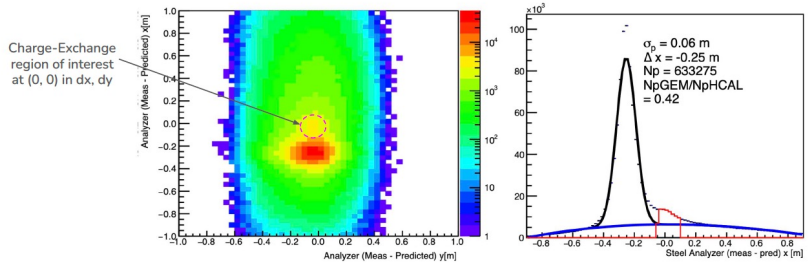

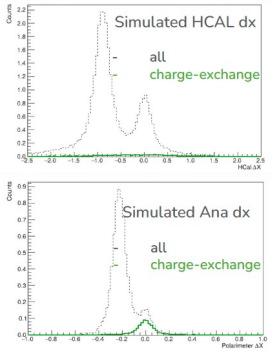

Simulations: Andrew Cheyne

Charge-Exchange channel Asymmetry

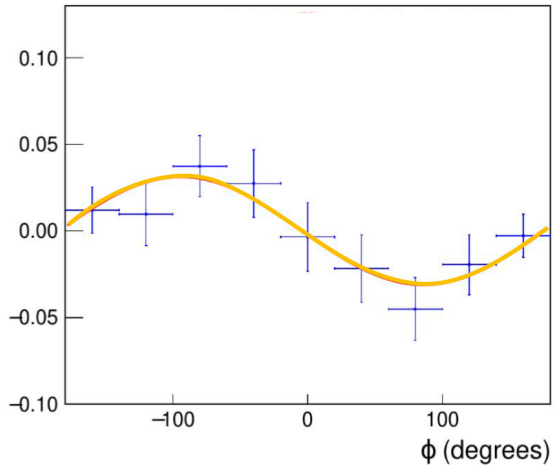

More work needs to be done for better isolation of the charge-exchange channel

Credits: David Hamilton

- "Online" asymmetry results promising, but a long, difficult, and statistically challenged analysis lies ahead
- Isolation of charge-exchange (chEx) channel difficult—backgrounds are significant and relative rate of chEx events is low
- First full cooking pass after a lot of calibration work by students recently completed!
- **Slides credit: Bhashita Dharmasena (UVA), Hall A Winter meeting, 2026**

Current status of G_E^n measurements from the SBS program

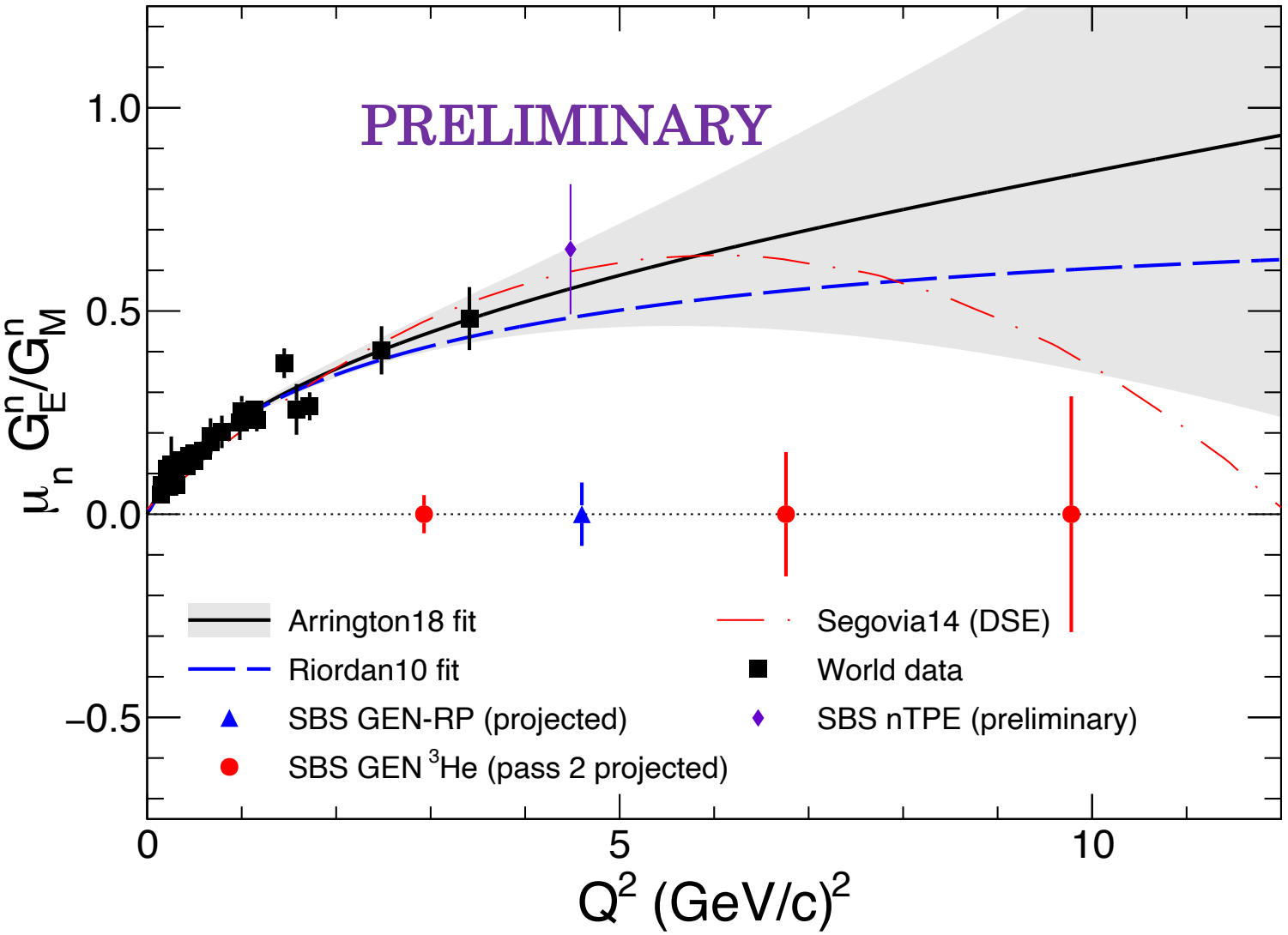

- Projected uncertainties (statistical only) are shown arbitrarily at zero for GEn-II/GEN-RP
- GEn-II (polarized Helium-3) uncertainties are "worst-case" based on actually reconstructed statistics in 2nd analysis pass (V. Gamage thesis, UVA)
- GEN-RP uncertainty is taken from proposal estimate (first full cooking pass recently completed)
- **nTPE preliminary result is based on Zeke Wertz Ph.D. thesis (W&M)**
- Uncertainties statistics-limited for GEn-II/GEN-RP and systematics-limited for "nTPE"

SBS GEP—Original motivation and “flagship” experiment

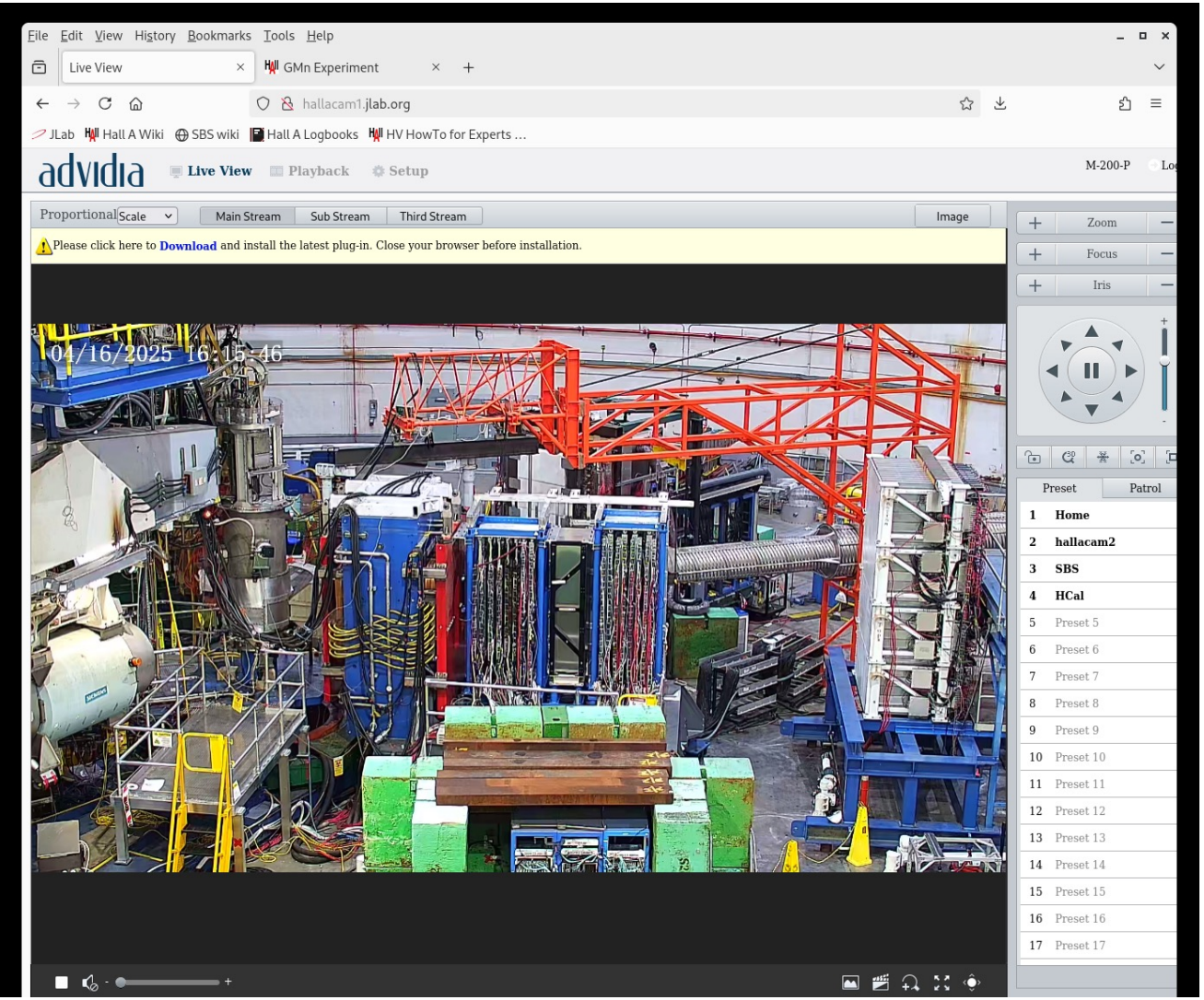

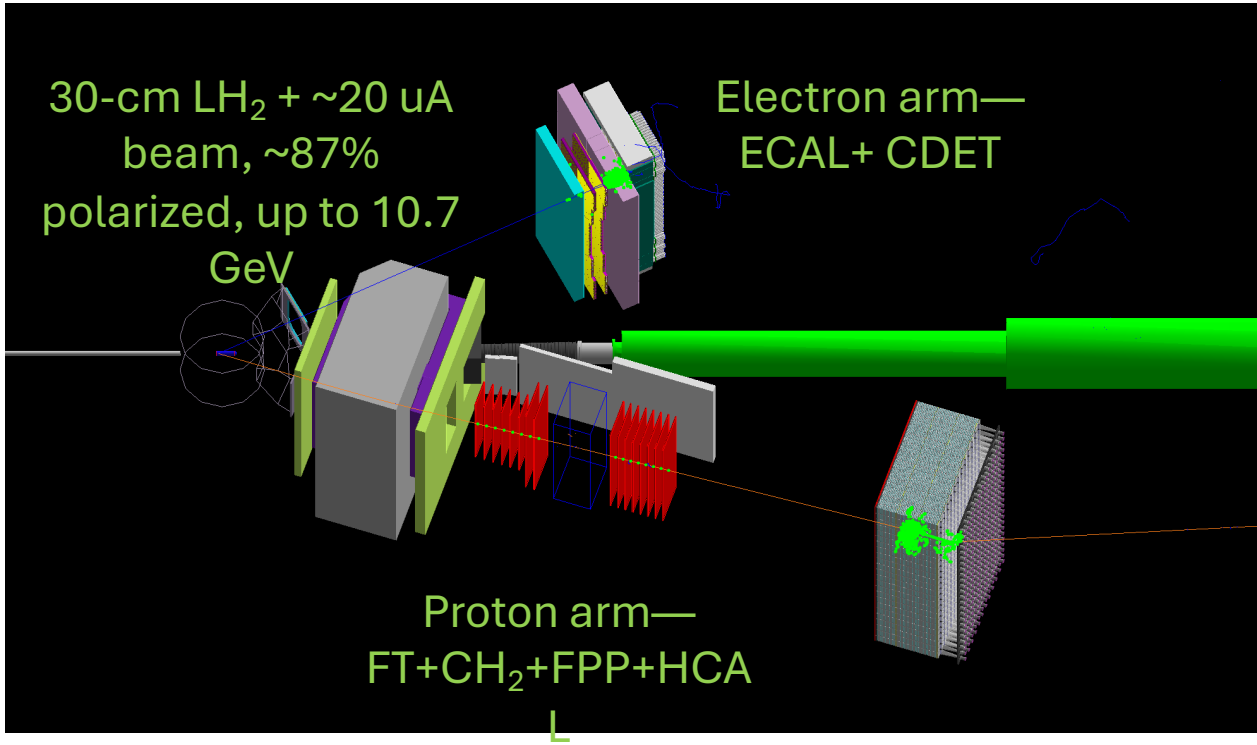

- Left: Hall Camera During GEP
- Right: A simulated elastic *ep* event in *g4sbs*
- Ran April-August, 2025
- Designated “High Impact Experiment” by PAC41

The SBS High-Temperature ECAL: Performance

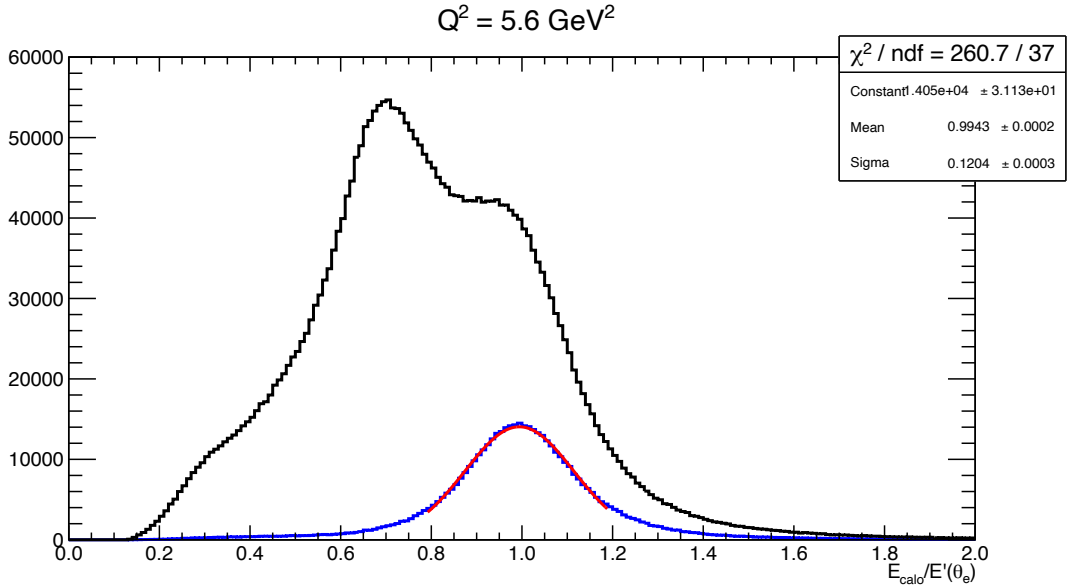

- Above: ~10-12% energy resolution, stable throughout the run
- Right: Photos taken during post-experiment disassembly
- Thermal annealing concept WORKED (although we put nowhere near the radiation dose on ECAL that this heating system was designed for)
- Energy resolution was STABLE and sufficient for our trigger needs

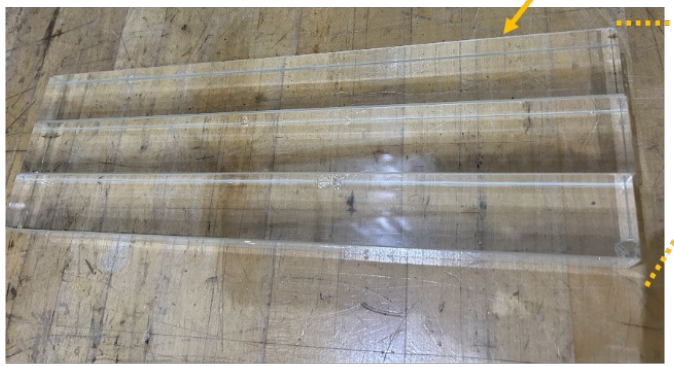

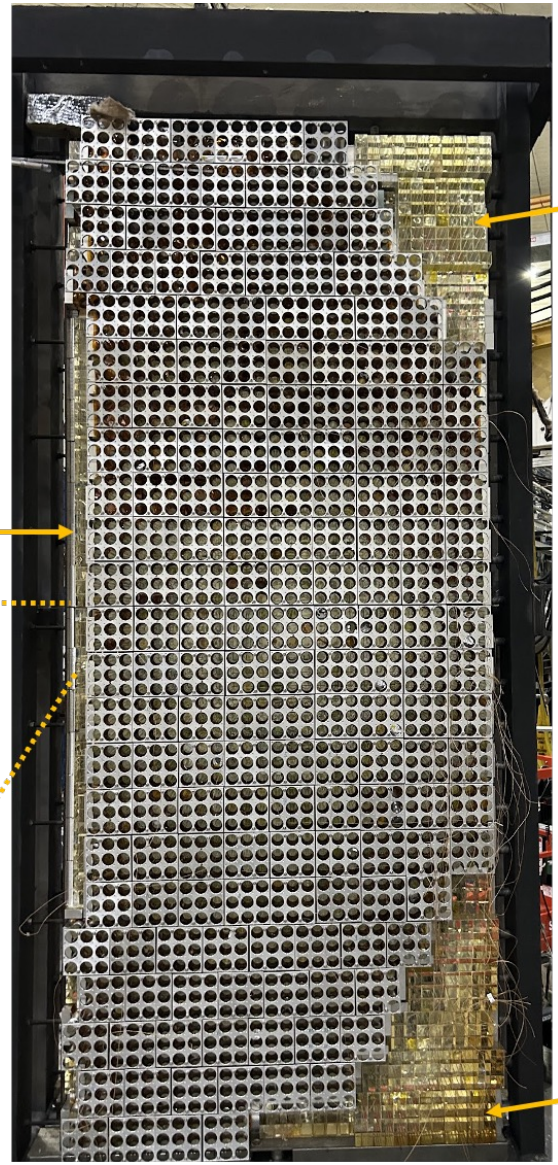

GEP Experiment Event Reconstruction Challenges

Slide credit: A. Rathnayake

- Main challenge by far is *GEM tracking* under high occupancy (space and time signal pileup) and low signal to background ratios
- The hit comes from the large number of combinatorics → high computational times + (fake hits + fake tracks)
- 1D cluster formation and 2D hit reconstruction is especially affected by high occupancy → lots of *fake hit* reconstruction
- Tracking portion itself is done in field-free regions → straight lines; hence not the most complicated part *if* the hits fed in are mostly *true/real* proton hits

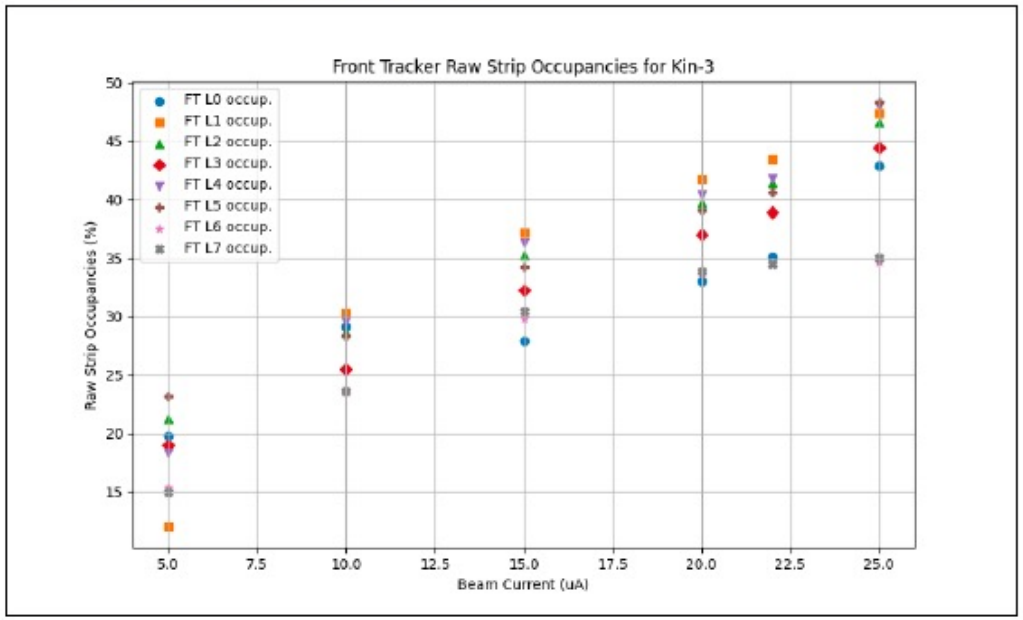

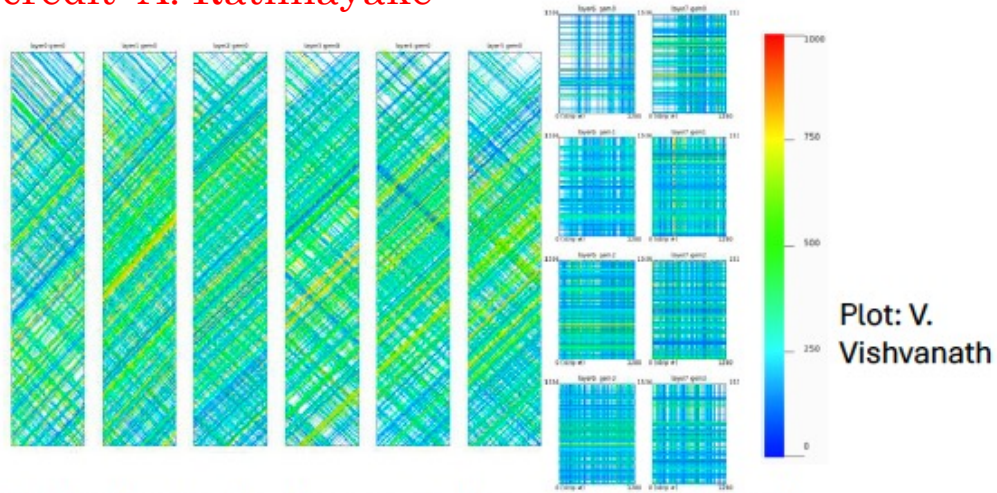

Plot: V. Vishvanath

Front Tracker strips fired in an event color coded in ADC strength.
22 uA on LH2 target; one of the highest background cases in SBS.

15 uA run elastic yield

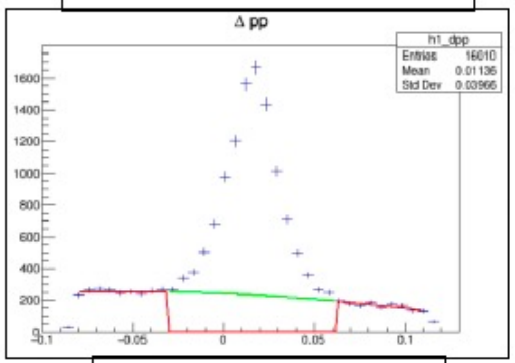

Heep yield/C = **24K**

22 uA run elastic yield

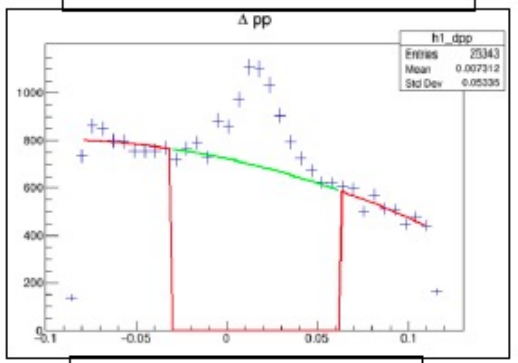

Heep yield/C = **11K**

Reconstruction Challenges—Not just GEMs! Pile-up in ECAL/HCAL FADC waveforms

- Current algorithm finds the first peak above threshold and stops
- **In some cases, an obviously better-timed pulse comes later**

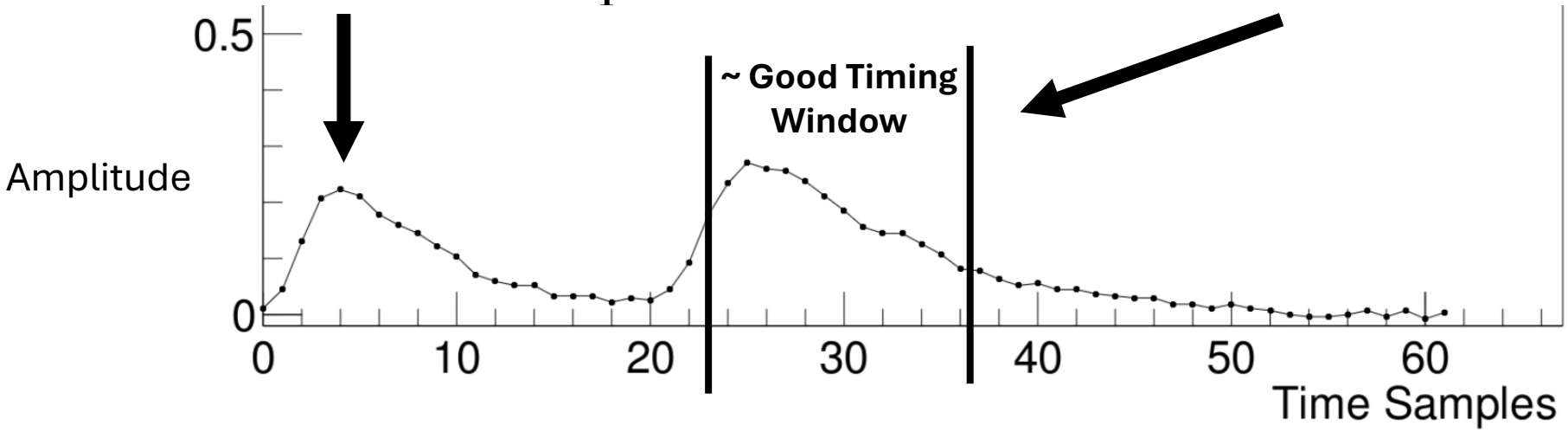

Kip Hunt (UConn) improving FADC waveform analysis

- **Pile-ups with multiple pulses**

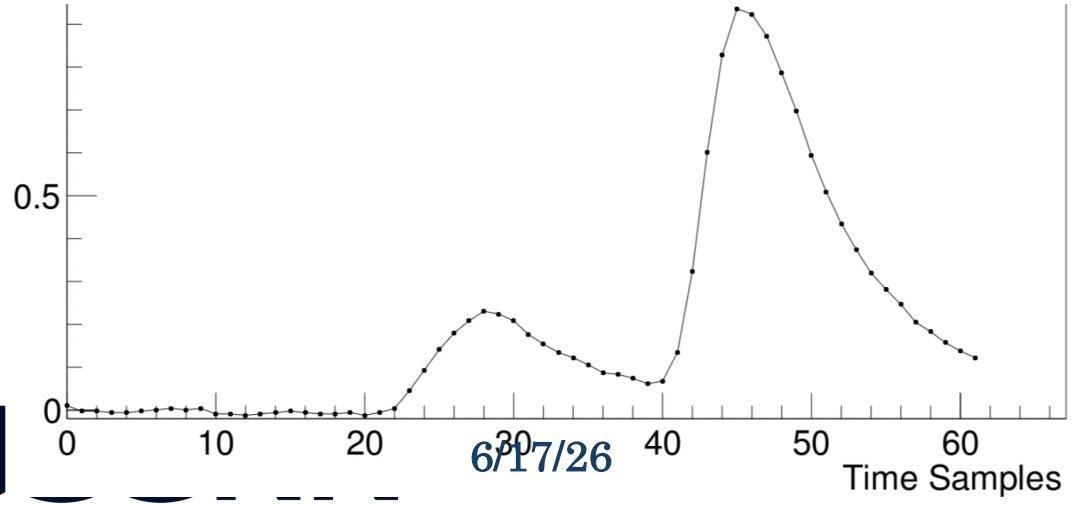

- **Overlapping pulses**

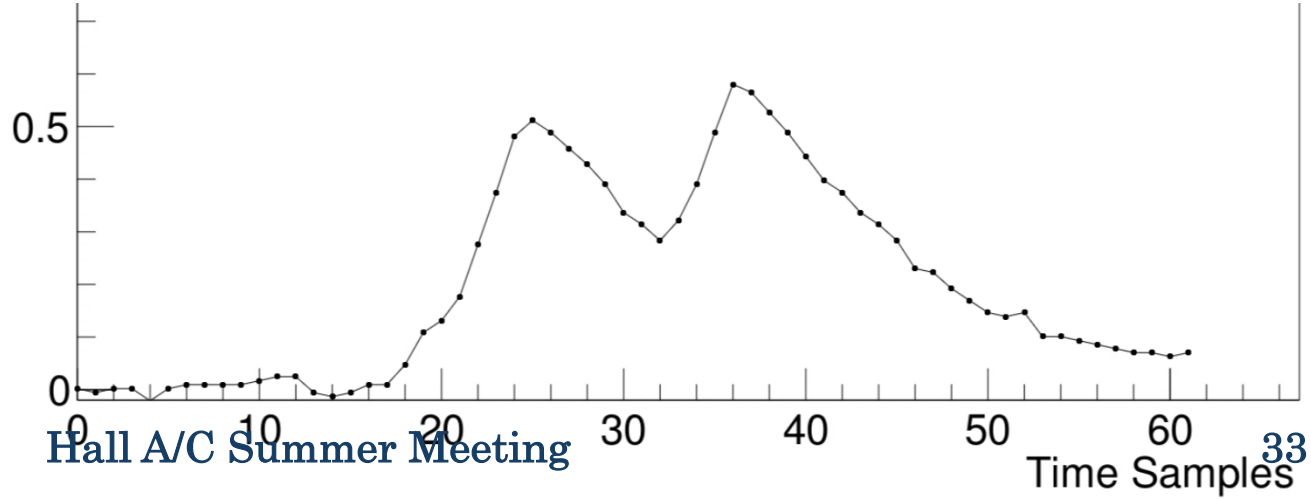

Elastic Event Selection (ideal)

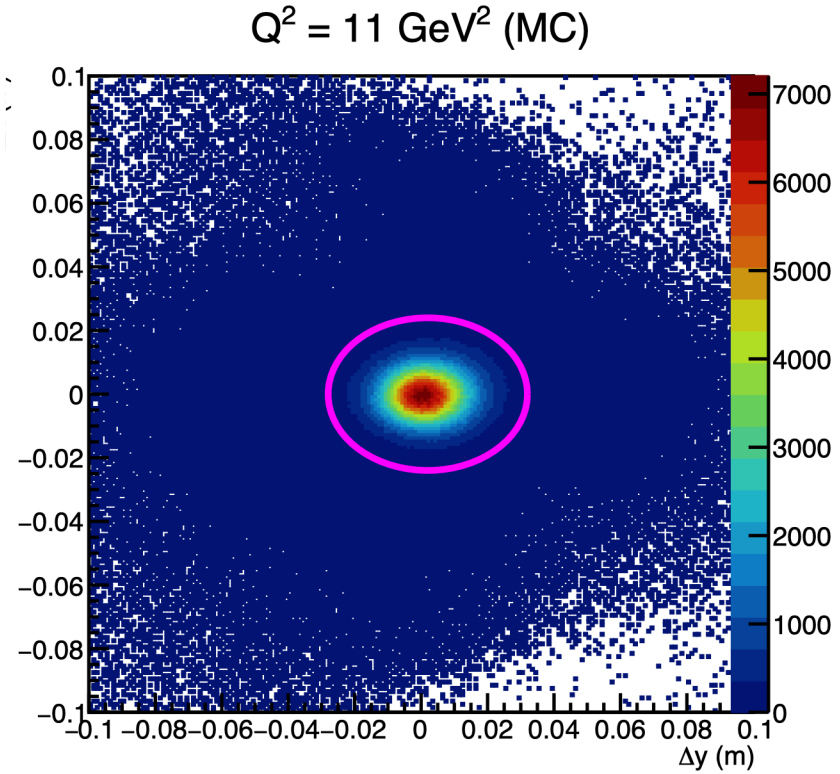

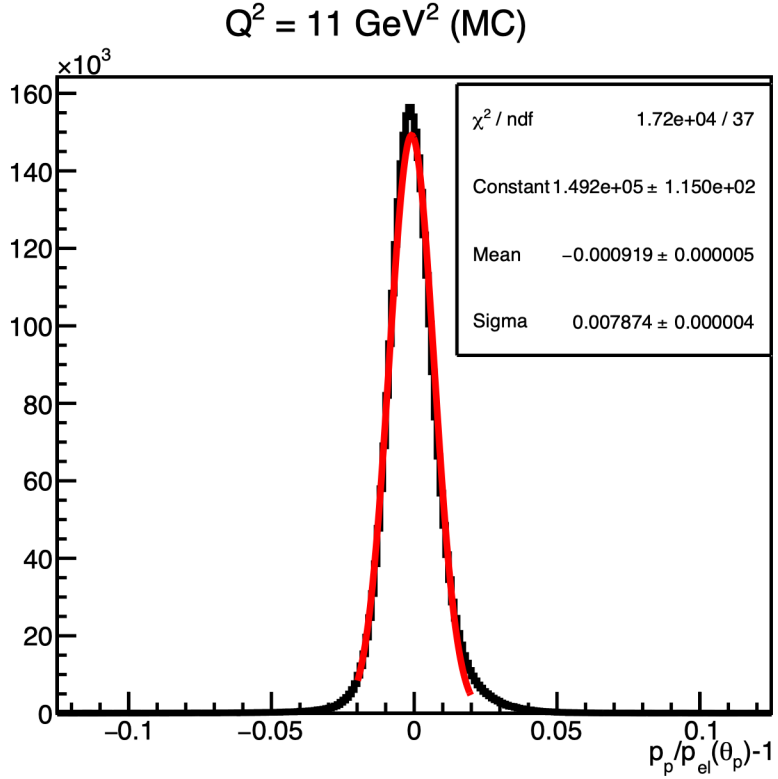

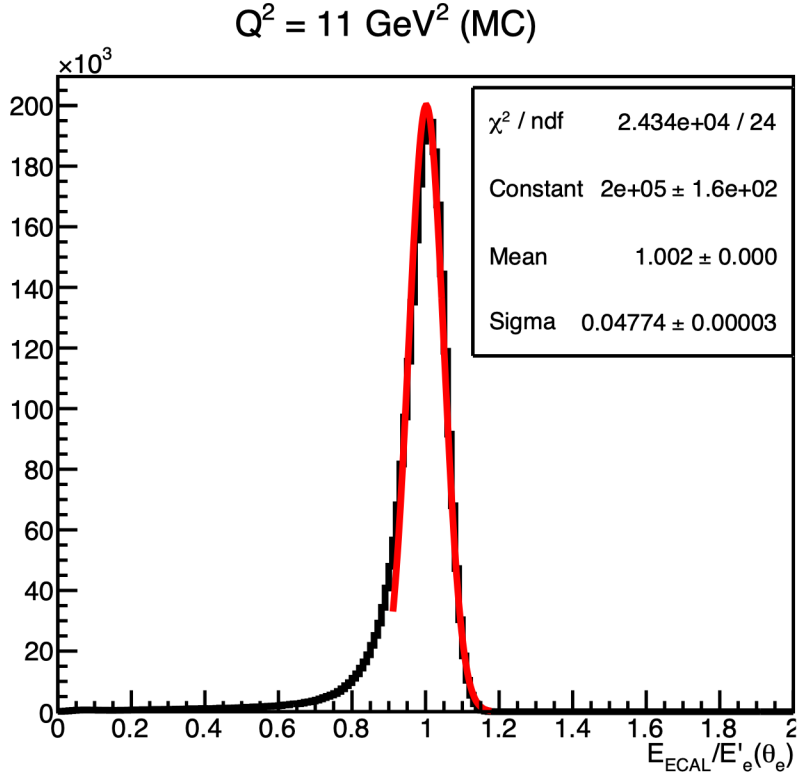

- Left to right:
  - $(\Delta y, \Delta \mathrm{x})\ (\sigma_{\Delta y}, \sigma_{\Delta \mathrm{x}}) = (1\ cm, 8\ mm)$
  - $\frac{\sigma_p}{p} \approx 0.8\%$
  - $\frac{\sigma_{Ecalo}}{E'_e} \approx 4.8\%$

Expected elastic event selection performance in the "ideal" scenario from MC: no background, no alignment uncertainty, no magnetic field and/or optics modeling uncertainty

Elastic Event Selection (real), II (w/*ad hoc* corrections on $\Delta x, \Delta y$)

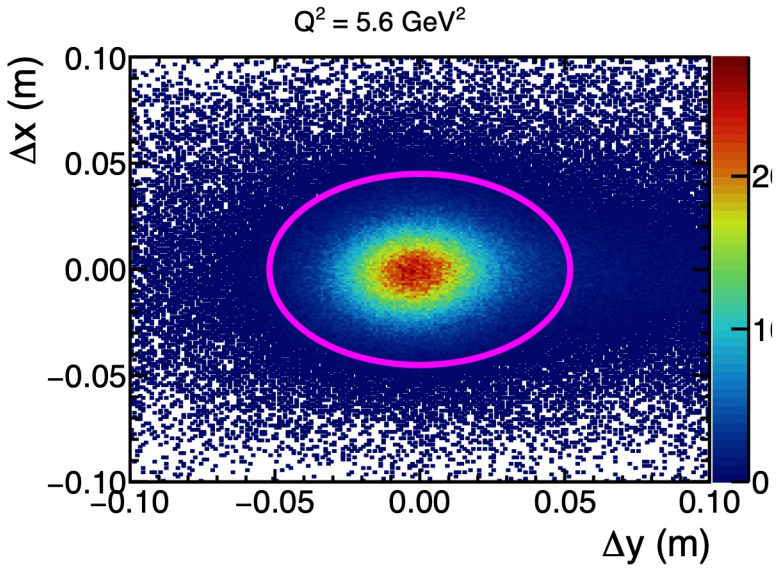

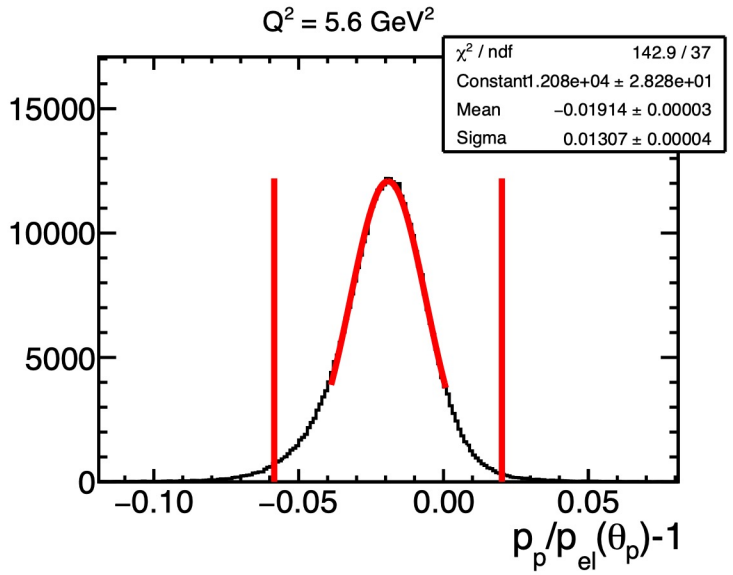

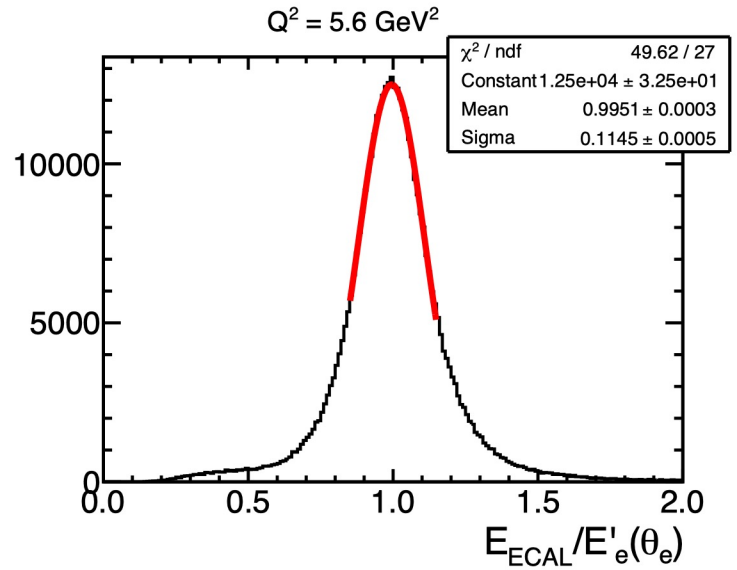

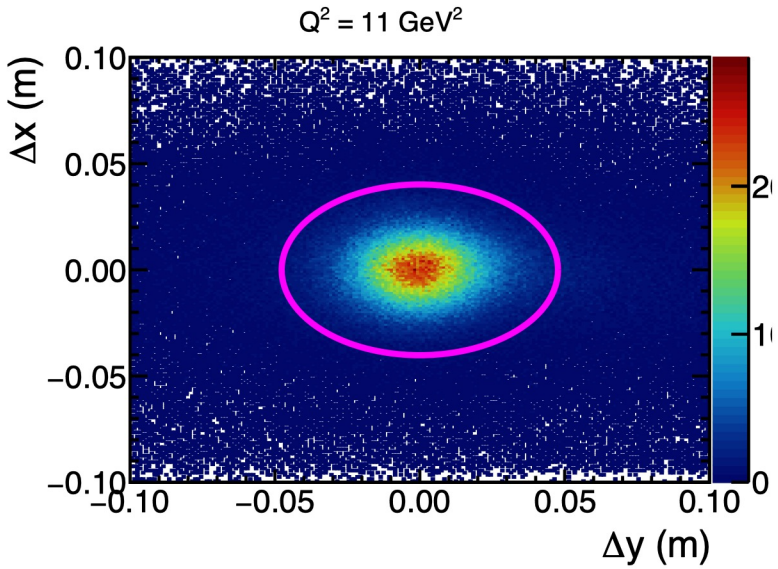

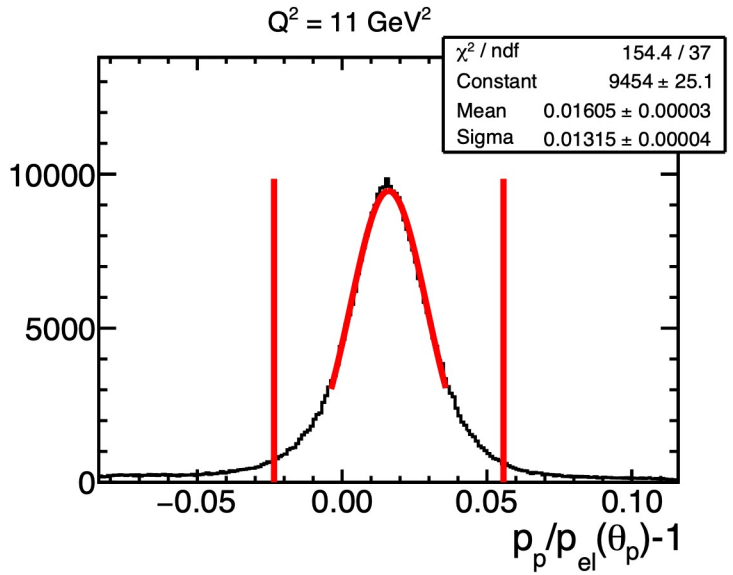

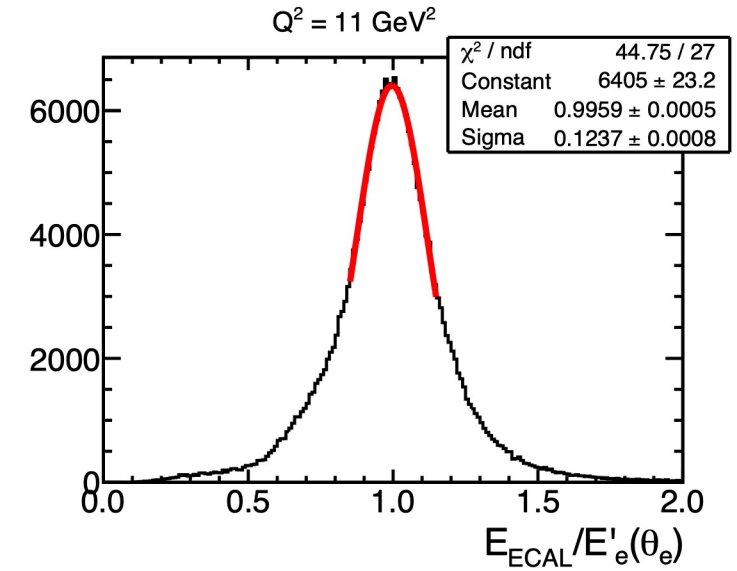

Polarimeter Reconstruction (ideal)

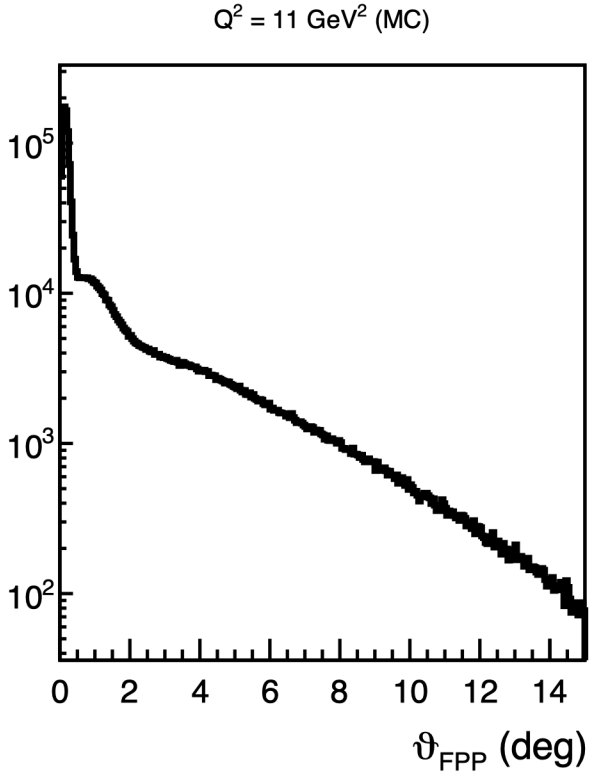

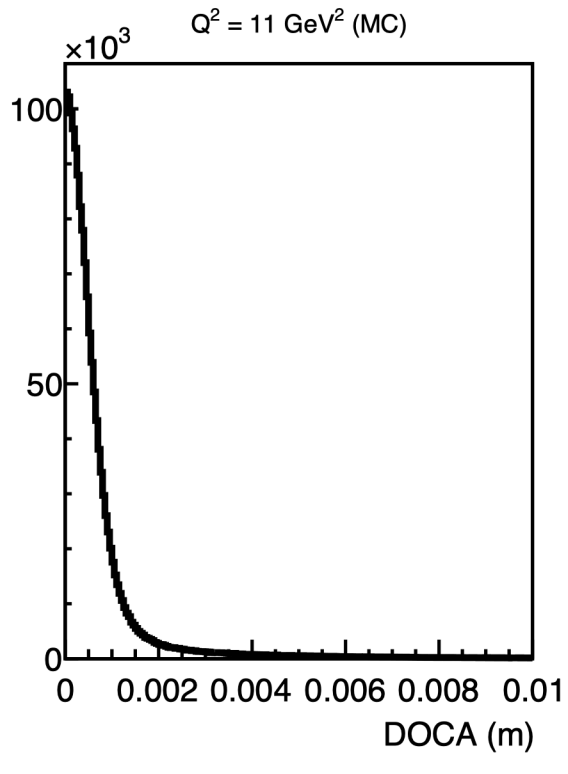

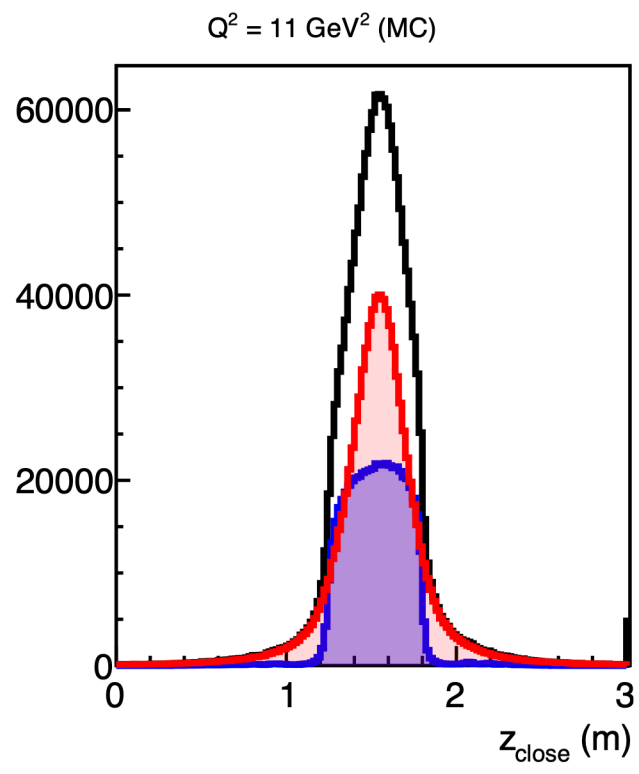

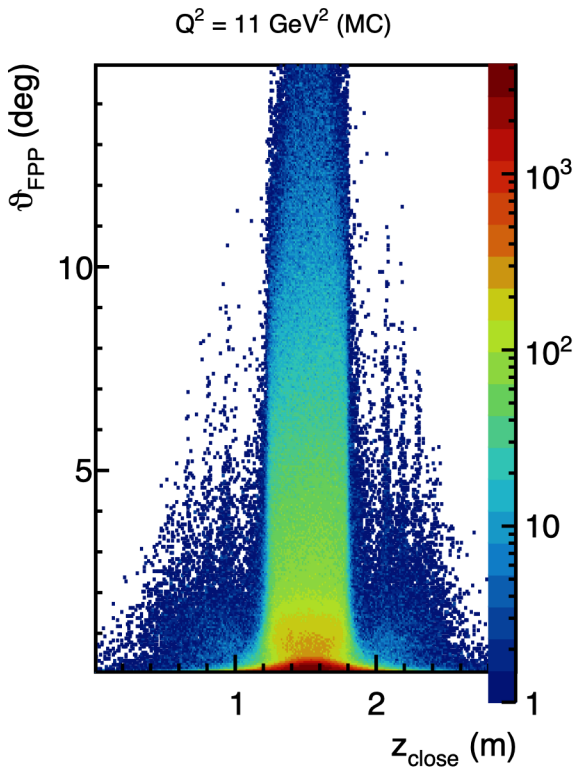

- Left to right: polar scattering angle, distance-of-closest-approach, z coordinate of closest approach, correlation between ϑ, z_{close}

Polarimeter Reconstruction (real)

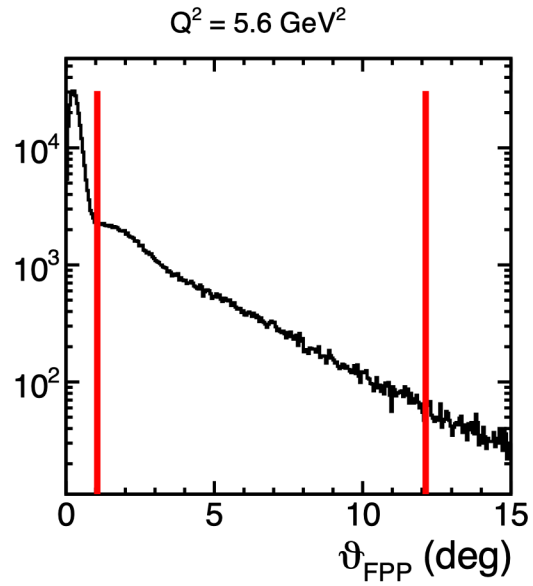

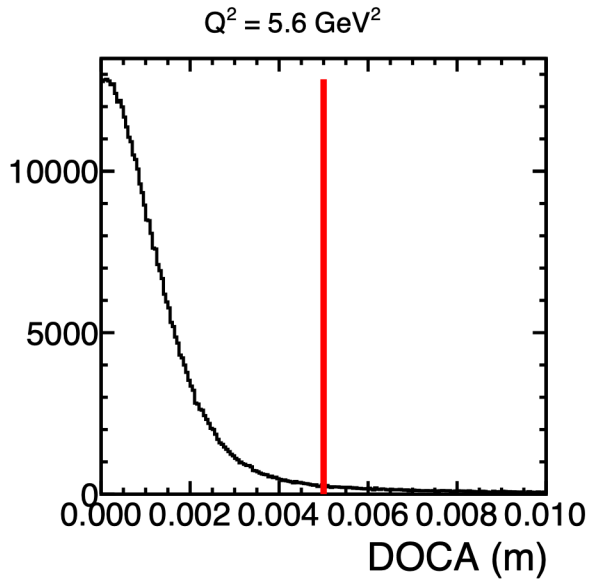

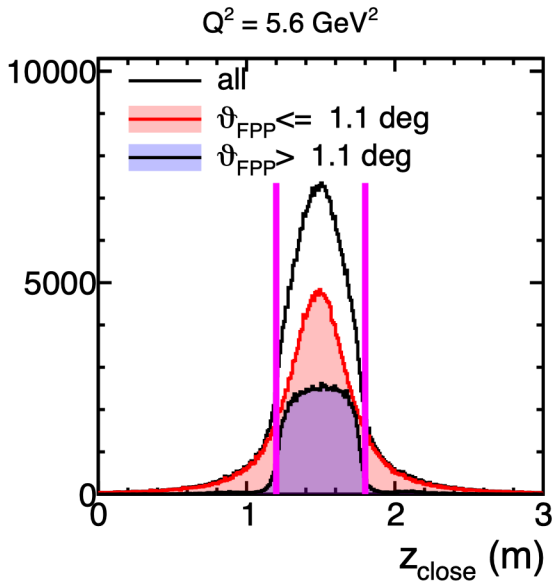

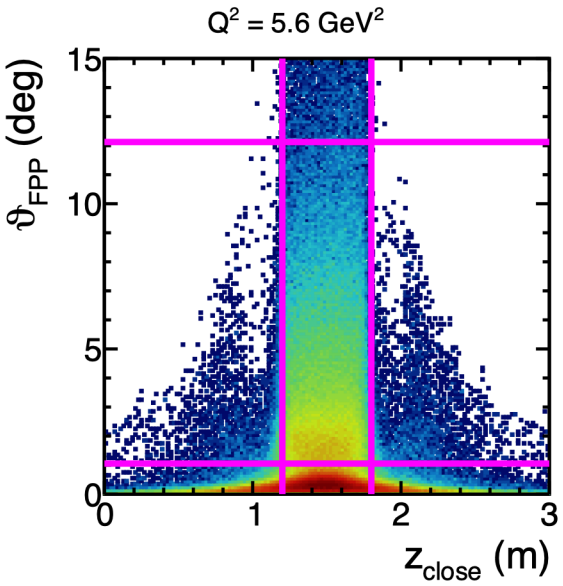

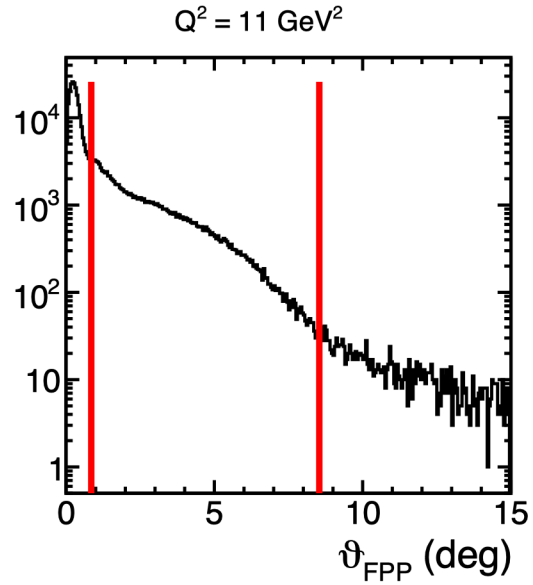

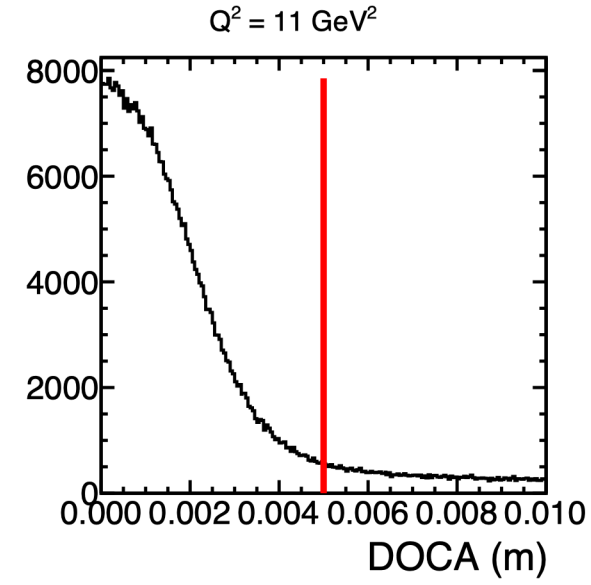

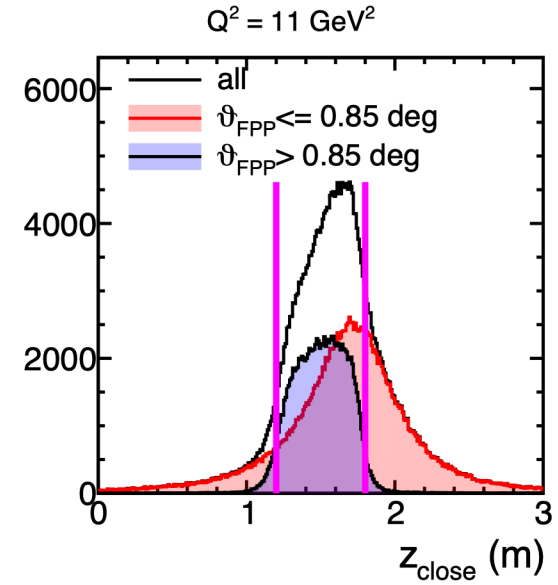

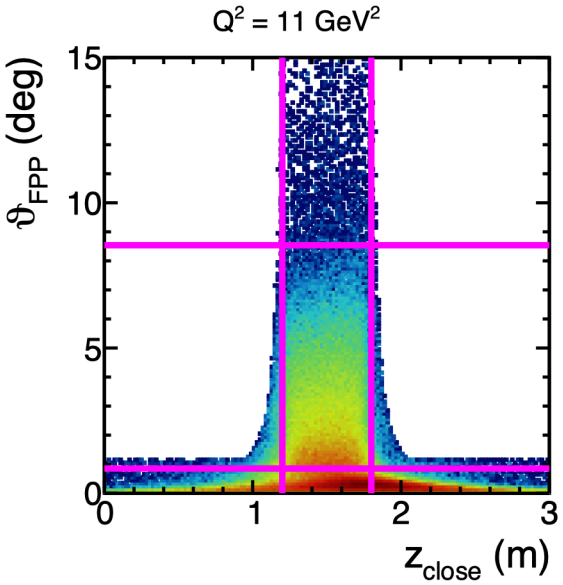

Polarimeter asymmetry at $Q^2 = 11$ GeV^2: measured vs. projected

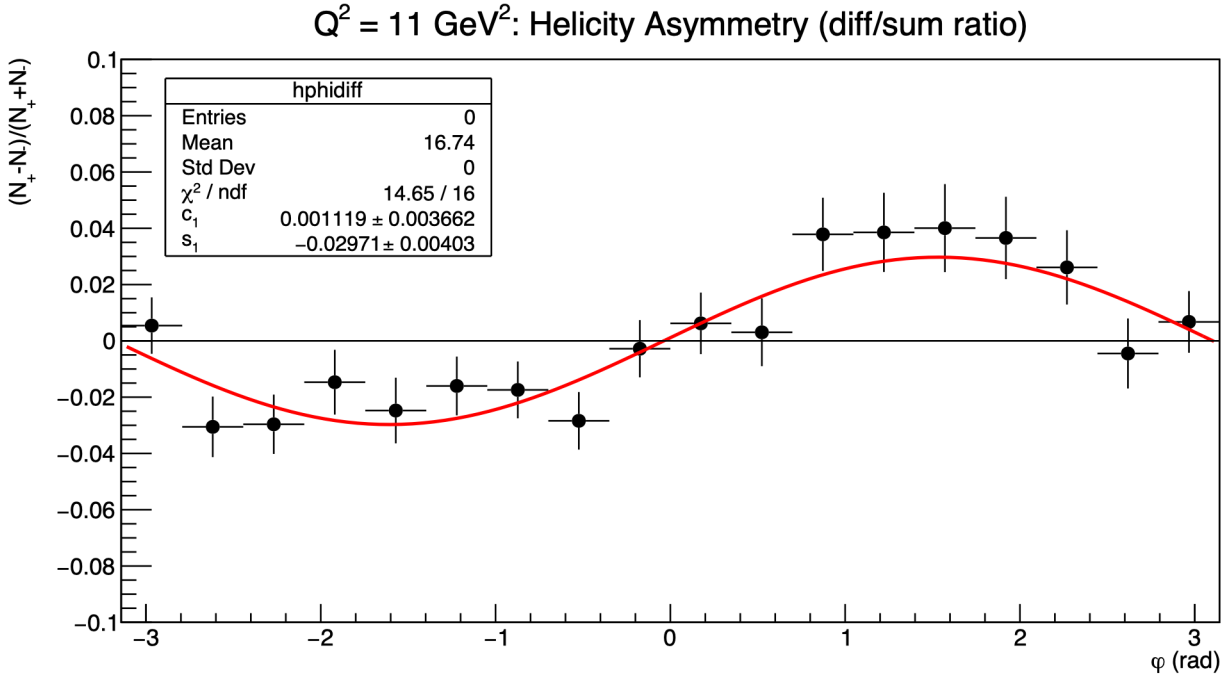

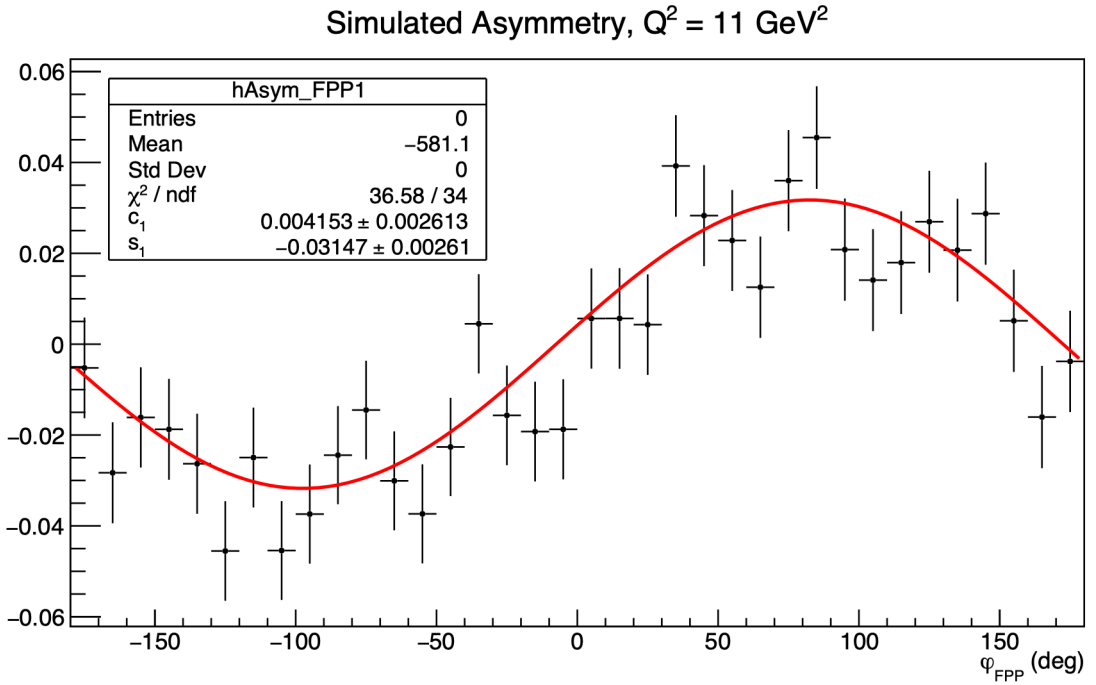

- Left: Real data asymmetry from ~140k elastic ep events with scattering angles in the useful range $0.07 \leq p_T(GeV) \leq 1.0$ (this represents approximately 1/4$^{\text{th}}$ of "worst case" statistics accounting for polarimeter efficiency)
- Right: Asymmetry from ~440k simulated events with scattering angles in the useful range (note this is not supposed to represent full proposal statistics!)
- Consistency of measured and simulated asymmetries suggests analyzing power is good and consistent with (extrapolated) GEp-III parametrization

SBS GEP—summary of data collected and range of outcomes for high-Q^2 result

- Total charge collected (live-time corrected):
  - $Q^2 = 5.6\ GeV^2$: 3.7 C
  - $Q^2 = 11\ GeV^2$: 94.2 C
- Raw data volume ~6.1 PB (~60% of total SBS FF program)
- Estimate several mega-CPU-hour per reconstruction pass
- "Worst case" assumes no further improvements in reconstruction efficiency
- "Best case" assumes 70% overall detection/trigger/reconstruction efficiency
- Current analysis efforts are focused on detector calibrations, reconstruction efficiency and speed improvements, including AI/ML deployment, toward a first full reconstruction pass in calendar 2026

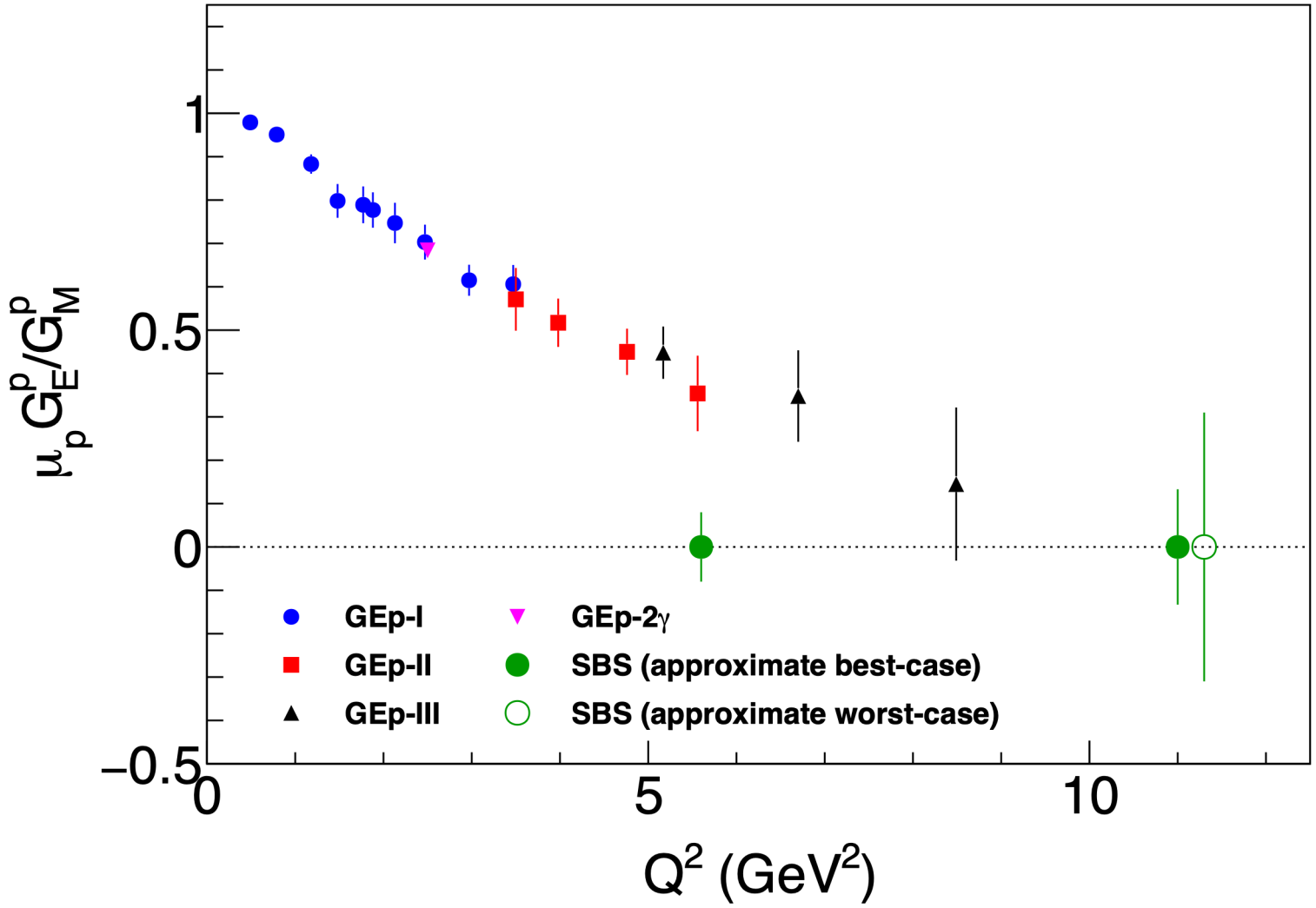

Summary and Conclusions

- SBS FF program occupied the floor of Hall A continuously for four years (2021-2025), generating roughly 10 PB of raw data volume
- Despite many challenges and setbacks, the goals for Q^2 coverage were largely met, while falling somewhat short of proposal goals in statistical precision for the highest Q^2 polarization measurements.
- G_M^n/nTPE analyses are both relatively mature–systematics are being finalized and publications are in preparation
- GEn-II (GEN-RP) recently completed third (first) full reconstruction passes incorporating recent improvements in detector timing calibrations→should improve background rejection especially for high-Q^2 G_E^n
- GEP reconstruction is difficult and computationally expensive→ we're targeting a first full cooking pass by the end of 2026. Backgrounds extreme, calibrations difficult, but event selection is clean, "online" asymmetries look good, and the range of physics outcomes is already more or less understood
- Many SBS instrumentation papers are already in the works, including one already published on the BigBite Calorimeter (P. Datta and K. Evans led this effort): https://doi.org/10.1016/j.nima.2026.171669 (and also https://inspirehep.net/literature/3108638)
- Lots of remaining analysis work, stay tuned for results!
- Large remaining approved physics program with SBS (SIDIS/TDIS) and new ideas in development!

Backups

HCAL proton detection efficiency benchmarked with LH_2 elastic data

Vertical **Horizontal**

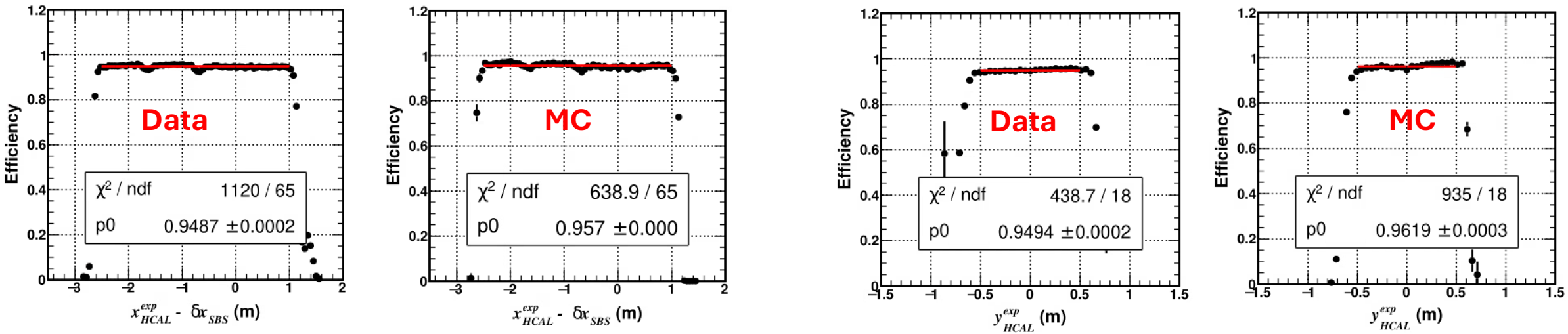

- HCAL detection efficiency non-uniformity built into MC by position-dependent re-weighting of MC events
- Absolute neutron detection efficiency calibration was not possible with our data—rely on MC for this
- Very high and similar proton and neutron detection efficiencies baked into HCAL design, limiting the systematic uncertainty
- Fiducial cuts minimize/eliminate acceptance mismatch
- Agreement with other world data at lower Q^2 gives confidence in our MC simulation

Total Systematic Error Budget (Preliminary)

Table 2: Estimated contributions (in percent) to systematic error on R and $\frac{G_M^n}{\mu_n G_D}$.

	Error Sources	Q^2 (ϵ)				
		3 (0.72)	4.5 (0.51)	7.4 (0.46)	9.9 (0.50)	13.5 (0.41)
$\Delta(R)_{sys}$	Inelastic Cont.	0.33	0.75	0.84	0.75	2.67
	Nucleon Det. Effi.	2.00	2.01	2.01	2.02	2.02
	Radiative Corr.	2.31	3.32	3.77	3.87	5.47
	Cut Stability	0.16	0.15	0.40	0.67	0.60
	FSI	0.04	0.01	0.02	0.02	0.03
	Total	3.08	3.95	4.37	4.48	6.44
$\Delta(\frac{G_M^n}{\mu_n G_D})_{sys}$	Inelastic Cont.	0.17	0.38	0.42	0.37	1.34
	Nucleon Det. Effi.	1.00	1.00	1.01	1.01	1.01
	Radiative Corr.	1.16	1.66	1.88	1.94	2.73
	Cut Stability	0.03	0.07	0.20	0.33	0.30
	FSI	0.02	0.00	0.01	0.01	0.01
	σ_{Red}^p	0.82	0.92	1.35	1.52	1.33
	G_E^n	0.55	0.65	0.62	0.66	0.55
	Total	1.83	2.27	2.64	2.79	3.53

Density interpretations of Form Factors: electron scattering from a static charge distribution

$$\begin{aligned}
\frac{d\sigma}{d\Omega} &= \left(\frac{d\sigma}{d\Omega}\right)_{Mott} |F(\mathbf{q})|^2 \\
\left(\frac{d\sigma}{d\Omega}\right)_{Mott} &\equiv \frac{\alpha^2(\hbar c)^2}{4E_e^2 \sin^4\frac{\theta}{2}} \frac{E_e'}{E_e} \cos^2\frac{\theta}{2} \\
F(\mathbf{q}) &= \int \rho(\mathbf{x}) e^{i\mathbf{q}\cdot\mathbf{x}} d^3x
\end{aligned}$$

$$\begin{aligned}
G_E &\equiv F(\mathbf{q}) = \int \rho(\mathbf{x}) e^{i\mathbf{q}\cdot\mathbf{r}} d^3\mathbf{r} \\
&= \int \rho(\mathbf{r}) \left(1 + i\mathbf{q}\cdot\mathbf{r} - \frac{(\mathbf{q}\cdot\mathbf{r})^2}{2} + \ldots\right) d^3\mathbf{r} \\
&= \int_0^\infty \rho(r) r^2 dr \int_0^\pi \sin\theta d\theta \left(1 + i|\mathbf{q}| r\cos\theta - \frac{1}{2}\mathbf{q}^2 r^2 \cos^2\theta + \ldots\right) \\
G_E &\approx 1 - \frac{1}{6}\mathbf{q}^2 \int r^2 \rho(r) d^3\mathbf{r} = 1 - \frac{1}{6}\mathbf{q}^2 \langle r^2 \rangle
\end{aligned}$$

- In the one-photon-exchange approximation in QED (equivalent to the first Born approximation in nonrelativistic quantum scattering theory), the cross section factorizes as the product of the "Mott" cross section, and the square of the *form factor* $F(\boldsymbol{q})$, equal to the Fourier transform of the charge density with respect to the three-momentum transfer $\boldsymbol{q} = \boldsymbol{k} - \boldsymbol{k}'$
- The Mott cross section represents the theoretical cross section for scattering of ultrarelativistic, spin-1/2 electrons from a point-like, spin-less target of charge *e*.
- In the non-relativistic limit, $Q^2 \ll M^2$, we have the correspondence: $|F(\vec{q})| = G_E(Q^2)$
- The mean square charge radius of the proton is minus 6 times the first derivative of $G_E(Q^2)$ at zero Q^2

Density interpretations of Form Factors: 3D (Kelly 2002)

Nonrelativistic interpretation:

$$\rho_{ch}^{NR}(r) = \frac{2}{\pi}\int_0^\infty dQ\, Q^2 j_0(Qr) G_E(Q^2),$$

$$\mu\rho_m^{NR}(r) = \frac{2}{\pi}\int_0^\infty dQ\, Q^2 j_0(Qr) G_M(Q^2),$$

Rest-frame density is Fourier Transform of "intrinsic FF" in wavenumber space:

$$\rho(r) = \frac{2}{\pi}\int_0^\infty dk\, k^2 j_0(kr)\tilde{\rho}(k).$$

(Model-dependent) Relativistic prescription to relate Sachs FF to intrinsic FF:

$$\tilde{\rho}_{ch}(k) = G_E(Q^2)(1+\tau)^{\lambda_E}, \qquad \lambda_E = \lambda_M = 2$$

$$\mu\tilde{\rho}_m(k) = G_M(Q^2)(1+\tau)^{\lambda_M},$$

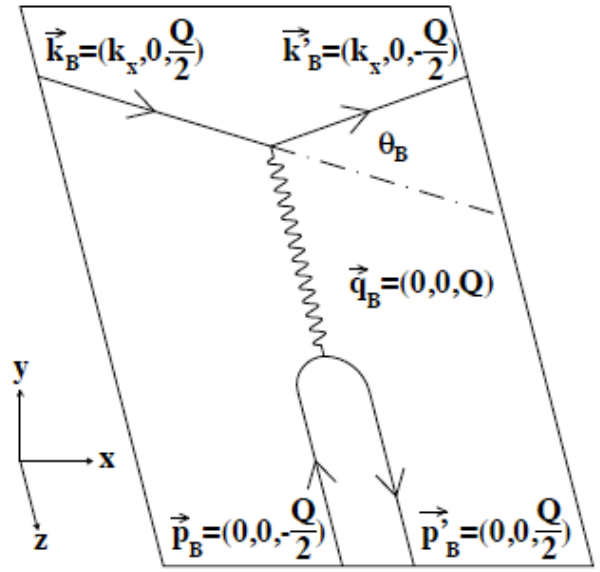

Figure 1-2: Elastic scattering in the Breit frame

Interpret Sachs FF as FT of Breit-frame density. Rest frame wavenumber related to Q^2 by boost along momentum transfer:

$$k^2 = \frac{Q^2}{1+\tau} \qquad \tau = \frac{Q^2}{4M^2}$$

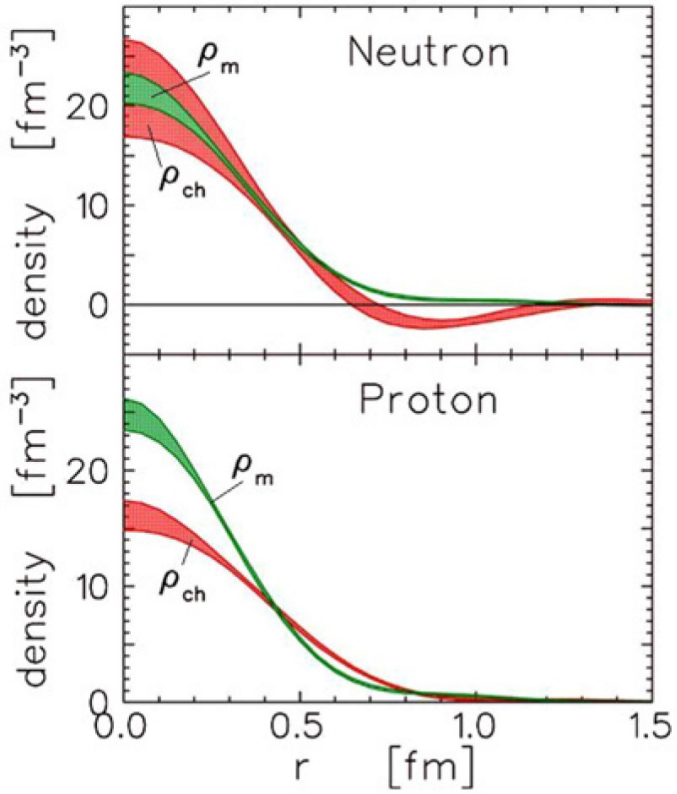

J. J. Kelly: PRC 66, 065203 (2002)

Statistical requirements: asymmetries vs. cross section measurements

Cross sections:

$$\sigma \propto N$$

$$\Longrightarrow \frac{\Delta\sigma}{\sigma} = \frac{1}{\sqrt{N}}$$

To measure a cross section with a relative statistical precision of 1%, you need 10,000 events.

Asymmetries:

$$\Delta A = \sqrt{\frac{1-A^2}{N}}$$

$$\frac{\Delta A}{A} = \sqrt{\frac{1-A^2}{NA^2}}$$

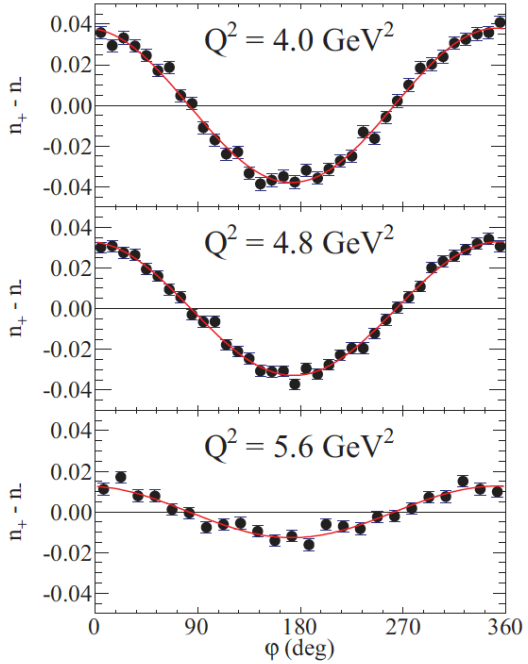

FIG. 6. (Color online) Focal-plane helicity-difference asymmetry $n_+ - n_- \equiv (N_{\text{bins}}/2)[N^+(\varphi)/N_0^+ - N^-(\varphi)/N_0^-]$, where N_{bins} is the number of φ bins and $N^{\pm}(\varphi)$, $N_0^{\pm}$ are defined as in Eq. (4), for the three highest Q^2 points from GEp-II. Curves are fits to the data. See text for details.

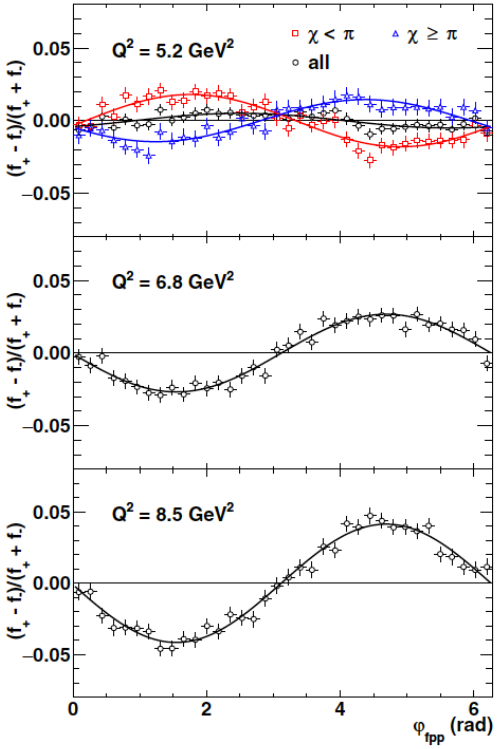

FIG. 10. Focal plane helicity difference/sum ratio asymmetry $(f_+ - f_-)/(f_+ + f_-)$, defined as in Eq. (20), for the GEp-III kinematics, for FPP1 and FPP2 data combined, for single-track events selected according to the criteria discussed in Sec. III B 2. Asymmetry fit results are shown in Table V. The asymmetry at $Q^2 = 5.2$ GeV^2 is also shown separately for events with precession angles $\chi < \pi$ and $\chi \geq \pi$, illustrating the expected sign change of the $\sin(\varphi)$ term.

- Example: Typical asymmetry magnitude in a recoil proton polarimeter at ”high” momentum is ~few percent.
- To measure a 5% asymmetry with a relative precision of 1%, one needs $N = 10{,}000 \times \frac{1-A^2}{A^2} \approx 4\times10^6$ events!

→ Asymmetry measurement must maximize beam and/or target polarization, and luminosity × acceptance!

Polarization Transfer Method

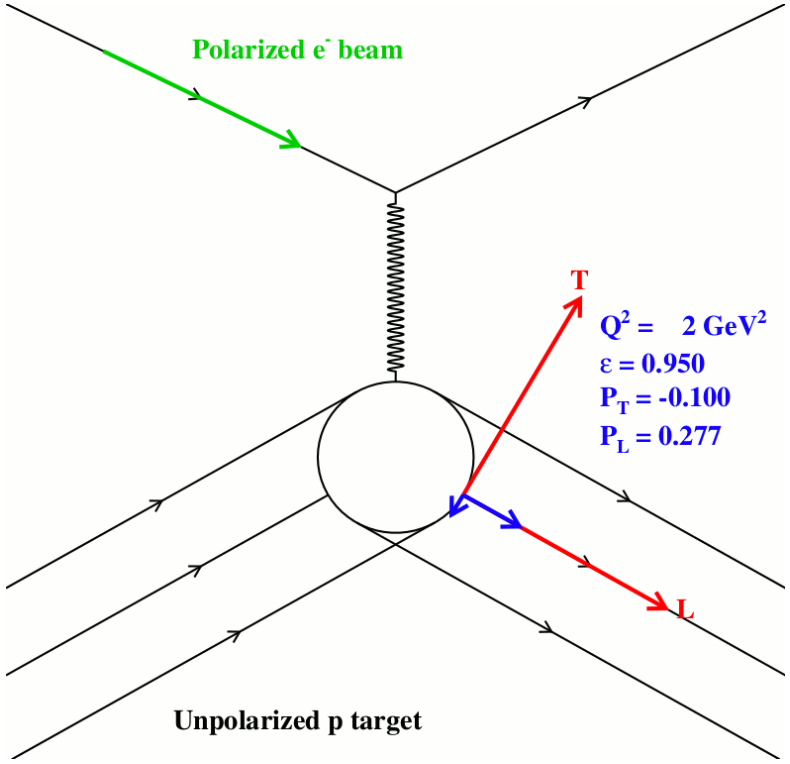

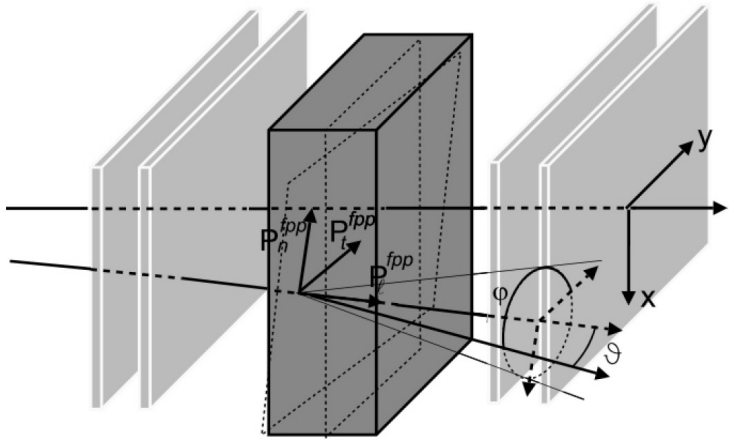

FIG. 9. Principle of the polarimeter, showing a noncentral trajectory through the front chambers, scattering in the analyzer, and a track through the back chambers; ϑ is the polar angle, and φ is the azimuthal angle from the y direction counterclockwise.

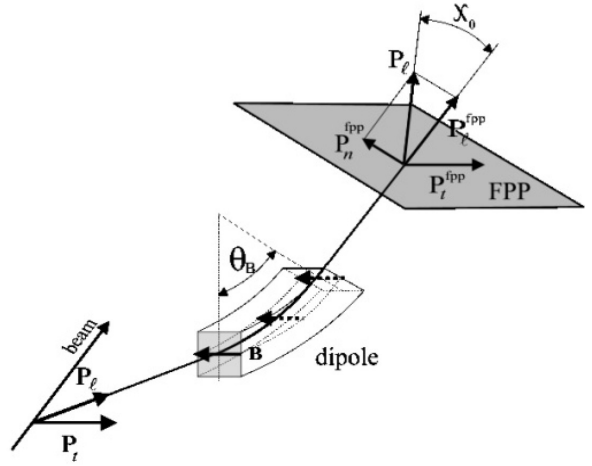

FIG. 15. Precession of the polarization component P_ℓ in the dipole of the HRS by an angle χ_θ.

- Based on spin-orbit coupling in proton-nucleus scattering

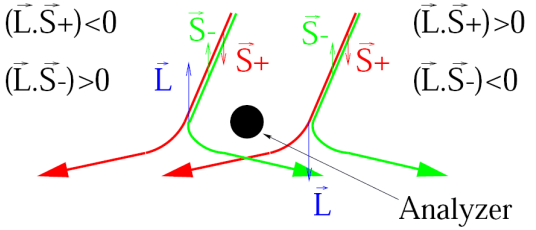

If more S+ than S- ($+P_x^{fpp}$) ...

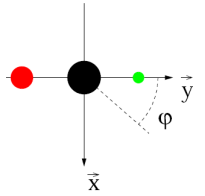

... more events left than right

- A spin-1/2 particle, such as a proton, is preferentially deflected by the nuclear spin-obrit force along the direction of $\vec{p}\times\vec{S}$, where $\vec{p}$ is the incident proton momentum, and $\vec{S}$ is the proton spin.
  - A spin-orbit force is insensitive to longitudinal polarization!
  - Precession in a magnetic field rotates P_L into a transverse component that can be measured
- Azimuthal asymmetry in the angular distribution of secondary scatterings measures $\vec{S}$

Toward high-Q^2: Fixed-target Electron Scattering Kinematics @11 GeV

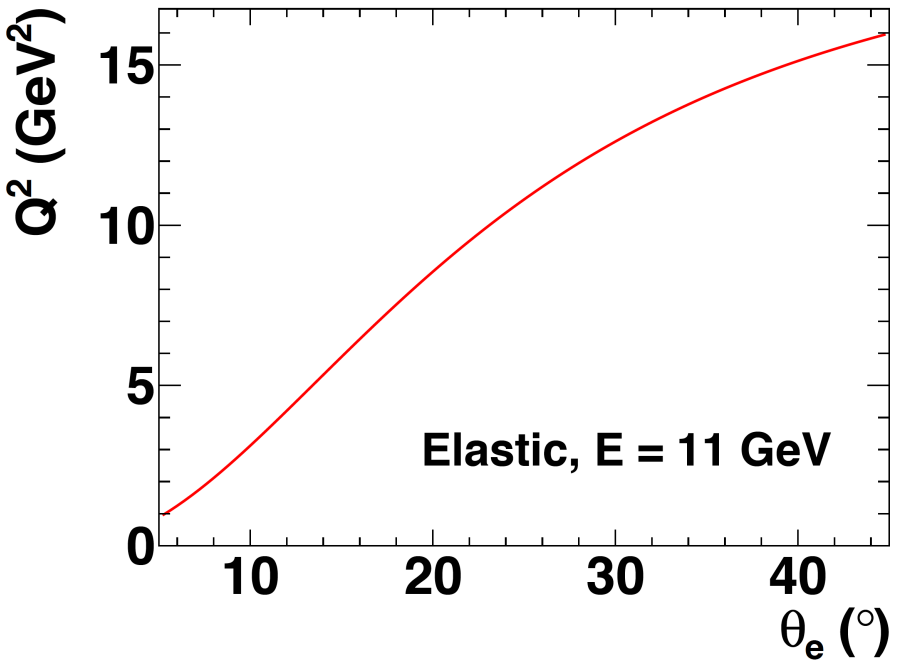

- Particles associated with the partonic (or other) degree of freedom that absorbed the virtual photon are found predominantly near the direction of the momentum transfer **q**
- *Partonic interpretation of electron scattering data is accessible at large Q^2 → particles of interest are located at forward angles and high momentum*

- Measurements of high-Q^2 elastic FFs, SIDIS, DVCS, etc involve coincidence N(e,e'X) (electroproduction) reactions, where X =
  - N' (elastic or quasi-elastic)
  - h (SIDIS or DVMP)
  - γ (DVCS)
- Virtual photon angle decreases as "inelasticity" and Q^2 increase:

$$Q^2 = 2M\nu x_{Bj}$$

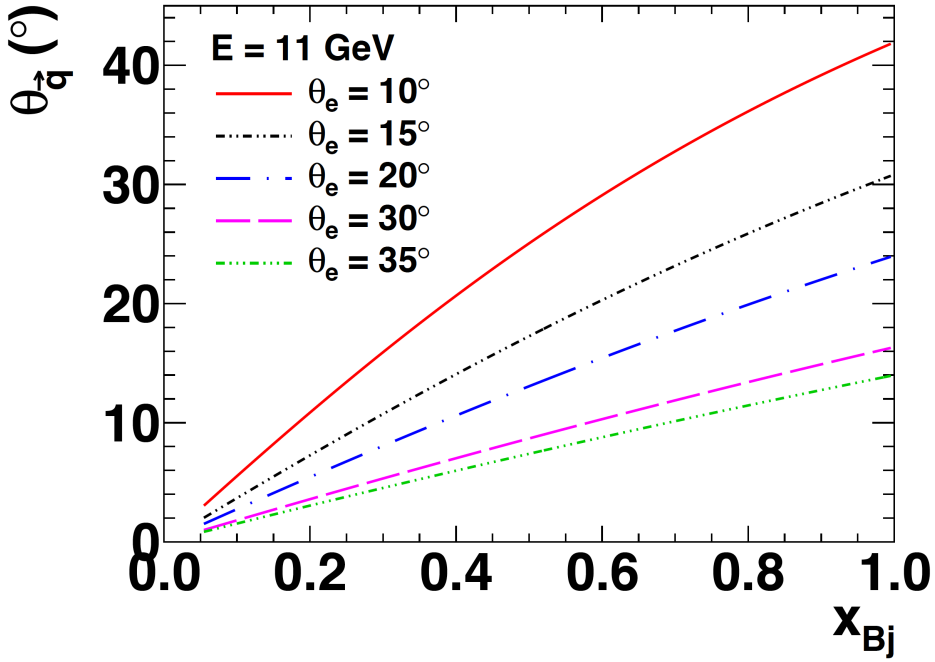

JLab detector landscape

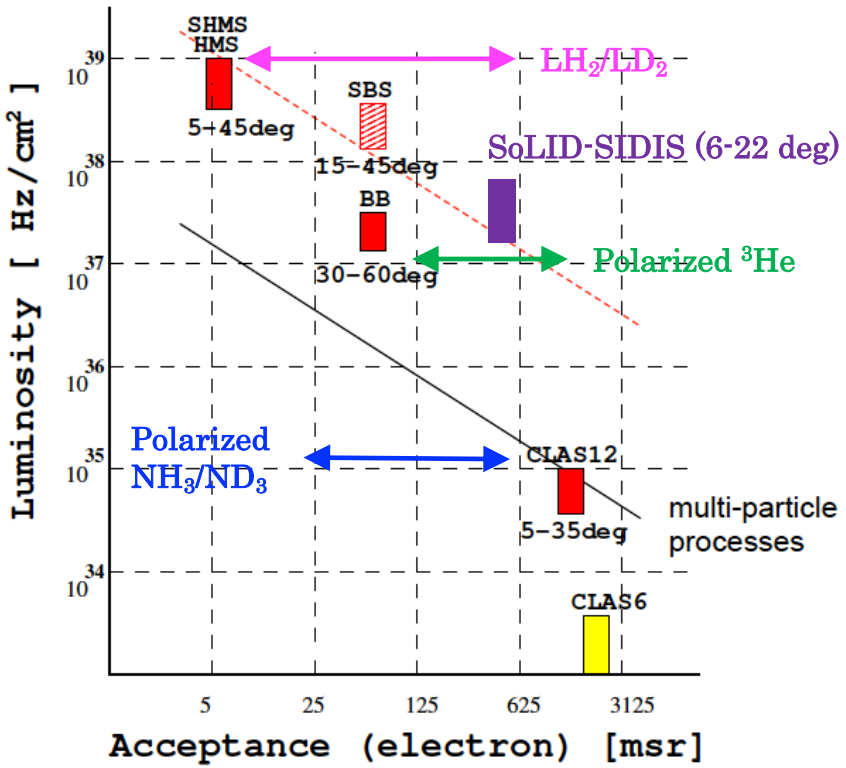

A range of 10^4 in luminosity.

A big range in solid angle:
from 5 msr (SHMS)
to about 1000 msr (CLAS12).

==========

The SBS is in the middle:
for solid angle (up to 70 msr)
and high luminosity capability.

In several A-rated experiments SBS was found to be the best match to the physics.

GEM allows a spectrometer with open geometry (->large acceptance) at high L.

- Complementary equipment/capabilities of Halls A, B, C allow optimal matching of (Luminosity x Acceptance) of the detectors to the luminosity capabilities of the targets, including state-of-the-art polarized target technology.

Helium-3 as an Effective Polarized Neutron Target

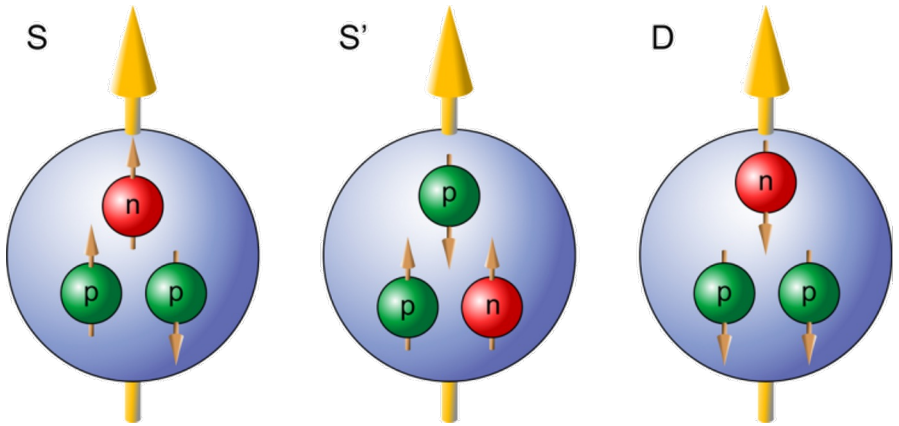

$$A_{^3\mathrm{He}} = P_n(1-f_p)A_n + P_p f_p A_p$$
$$P_n = 0.86^{+0.036}_{-0.02}$$
$$P_p = -0.028^{+0.009}_{-0.004}$$
$$f_p = \frac{2\sigma_p}{\sigma_{^3\mathrm{He}}}$$

Effective nucleon polarization approximation for DIS on Helium-3:
Scopetta, Phys. Rev. D 75, 054005 (2007)

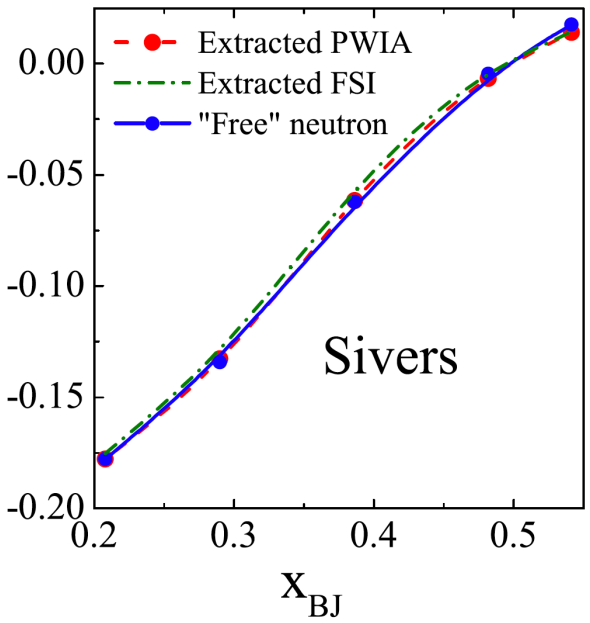

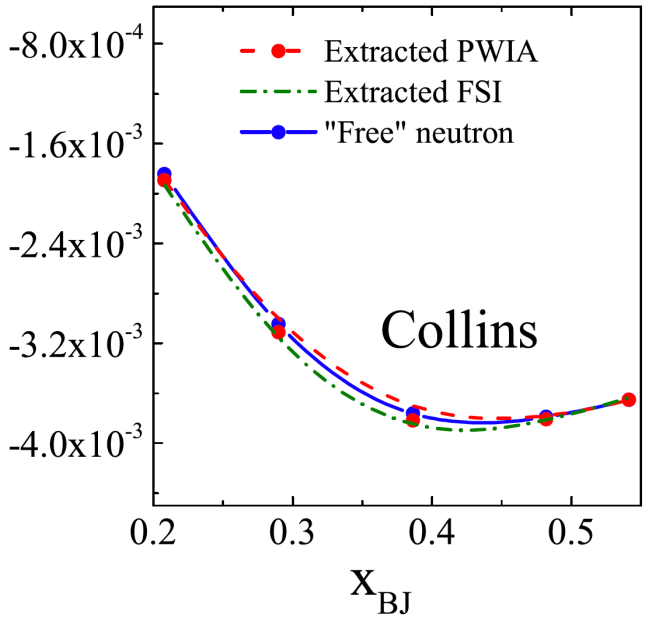

Del Dotto *et al.*, Phys. Rev. C 96, 065203 (2017)

- Effect of nuclear FSI on extraction of neutron Collins and Sivers effects from SIDIS on ^{3}He under good theoretical control
- Advantages of Helium-3 for study of polarized neutron:
  - Protons almost unpolarized
  - High luminosity capability (up to several 10^{37} cm^{-2} s^{-1})
  - Small holding field → small systematics of target spin flips

SBS Apparatus, I: Hadron Arm

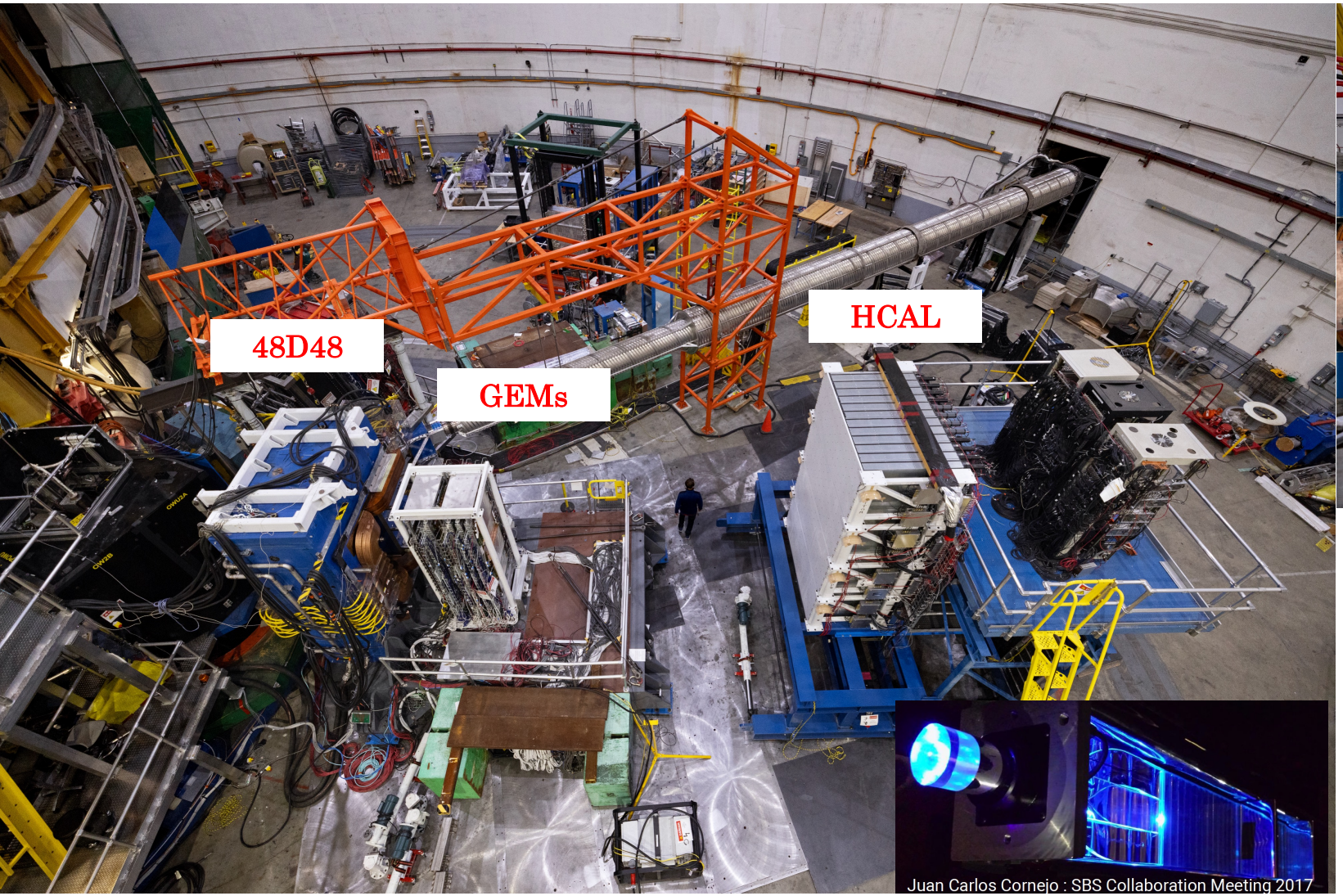

Common to ALL SBS experiments:

- 48D48 magnet: dipole with a cut in iron yoke for passage of the beam → reach forward scattering angles
- Hadron Calorimeter (HCAL) → efficient detector for high-energy hadrons (protons, neutrons, pions, etc)
- Gas Electron Multipliers (GEMs) → high-rate charged-particle tracking

Polarization transfer and the ratio $\mu_p G_E^p / G_M^p$: 6 GeV era Hall A/C results

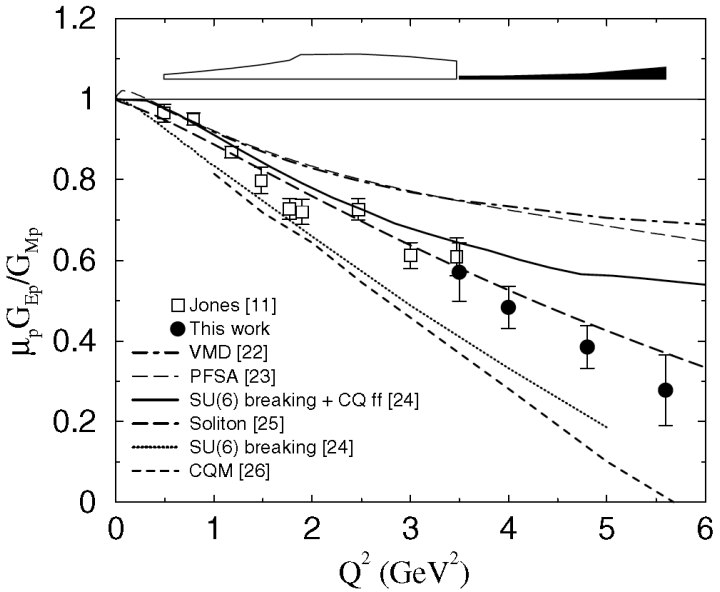

FIG. 2. The ratio $\mu_p G_{E_p}/G_{M_p}$ from this experiment and Jones *et al.* (Ref. [11]), compared with theoretical calculations. Systematic errors for both experiments are shown as a band at the top of the figure.

Gayou *et al.*, PRL 88, 092301 (2002) ("GEp-II")

- Figures at right are from Punjabi *et al.*, PRC 71, 055202 (2005)

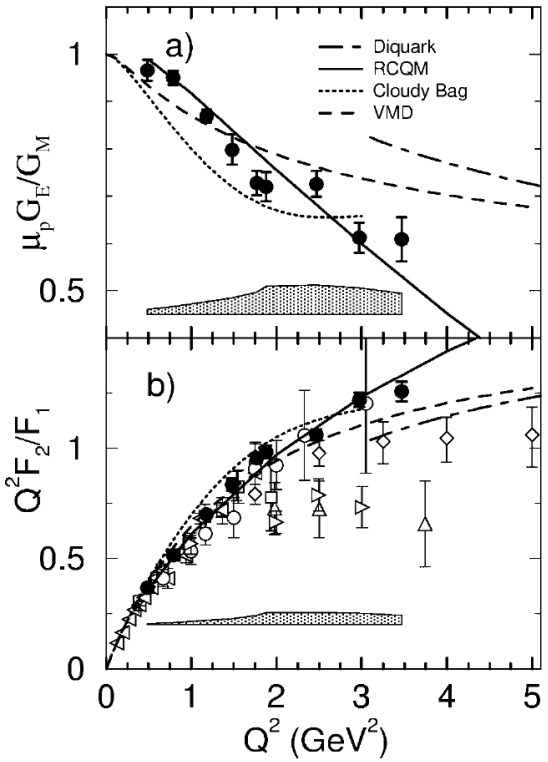

FIG. 2. (a) The ratio $\mu_p G_{E_p}/G_{M_p}$ from this experiment, compared with theoretical calculations. (b) The ratio $Q^2 F_{2_p}/F_{1_p}$ for the same data, compared to the same theoretical models as in (a) and world data; symbols as in Fig. 1. In both (a) and (b) the absolute value of systematic error from this experiment is shown by the shaded area.

Jones *et al.*, PRL 84, 1398 (2000) ("GEp-I")

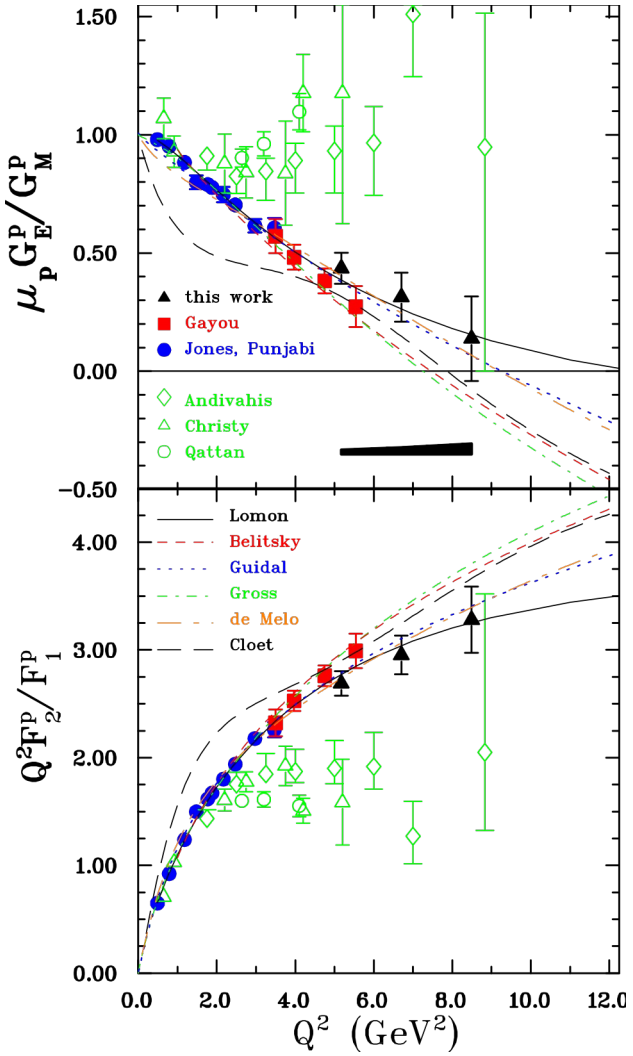

Puckett *et al.*, PRL 104, 242301 (2010)

The Problem with Rosenbluth Separations

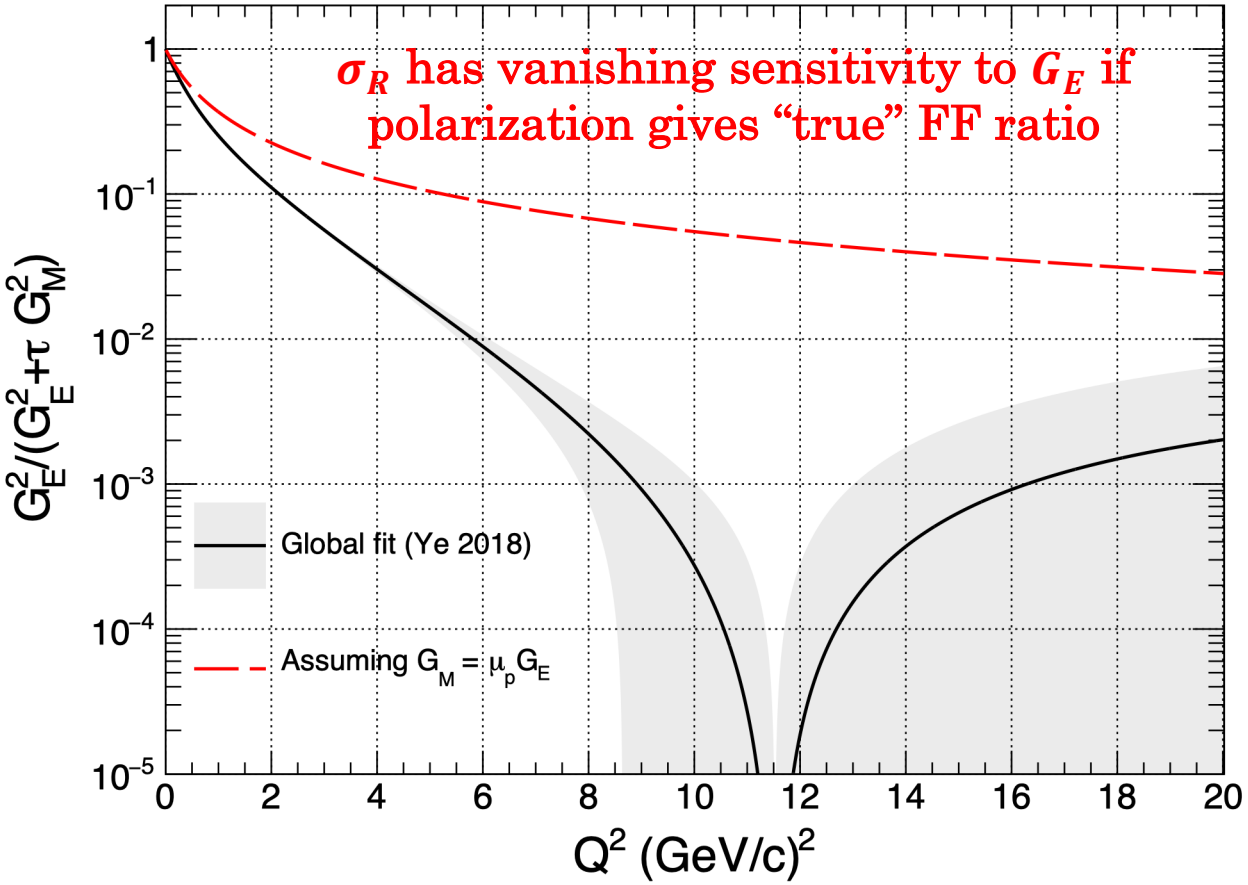

Maximum Fraction of the Reduced Cross Section Carried by the electric term versus Q^2 (50 years of QCD: EPJ C 83:1125 (2023))

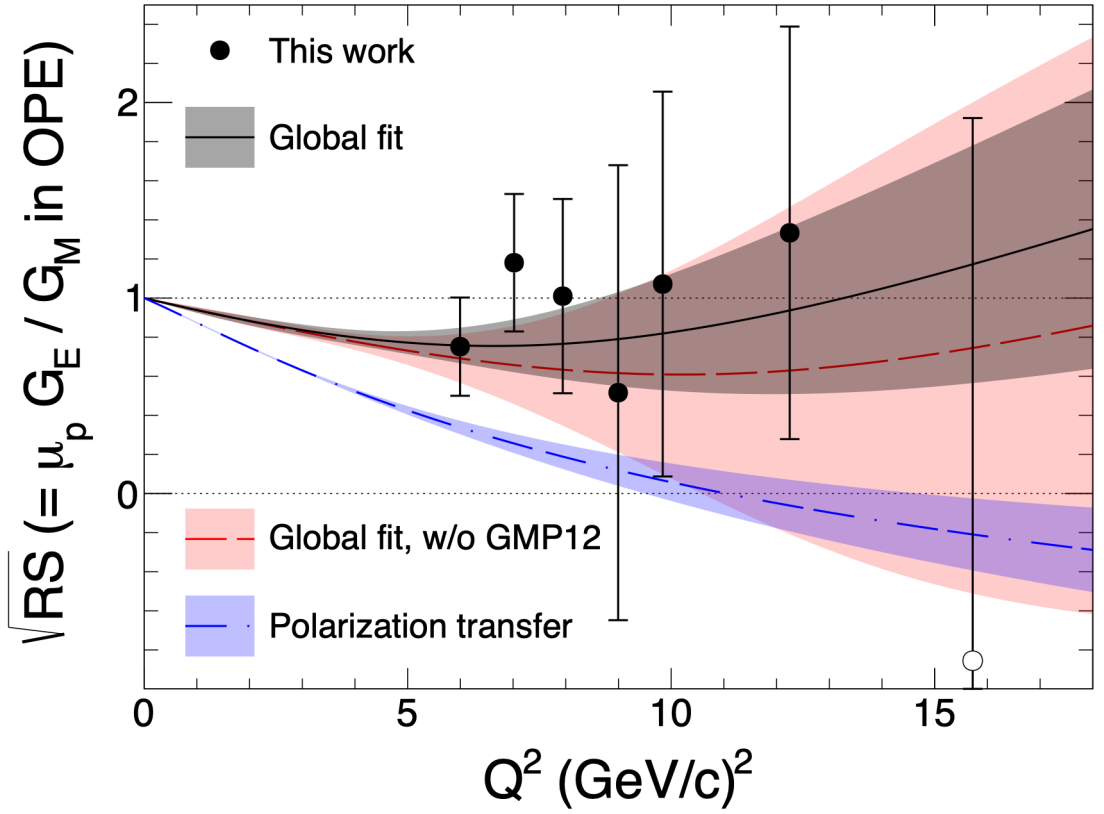

High-Q^2 Rosenbluth Separations from Hall A: Christy *et al.*, **Phys. Rev. Lett.** 128, 102002 (2022)

SBS GEN analysis: Moller Polarimetry: Faraz Chahili and Don Jones

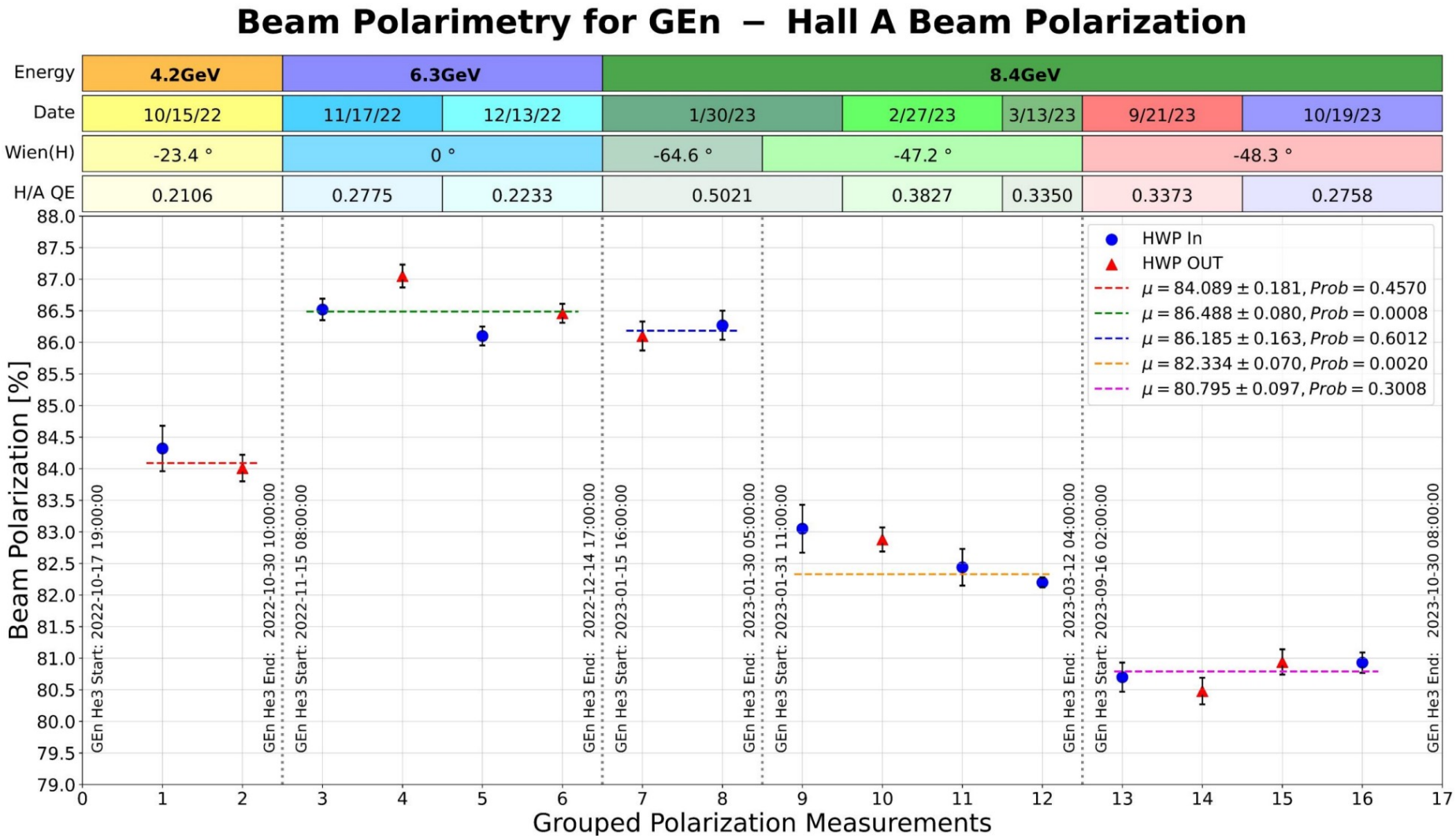

The SBS Collaboration (Photo from July 2023 Collab. Meeting at JLab)

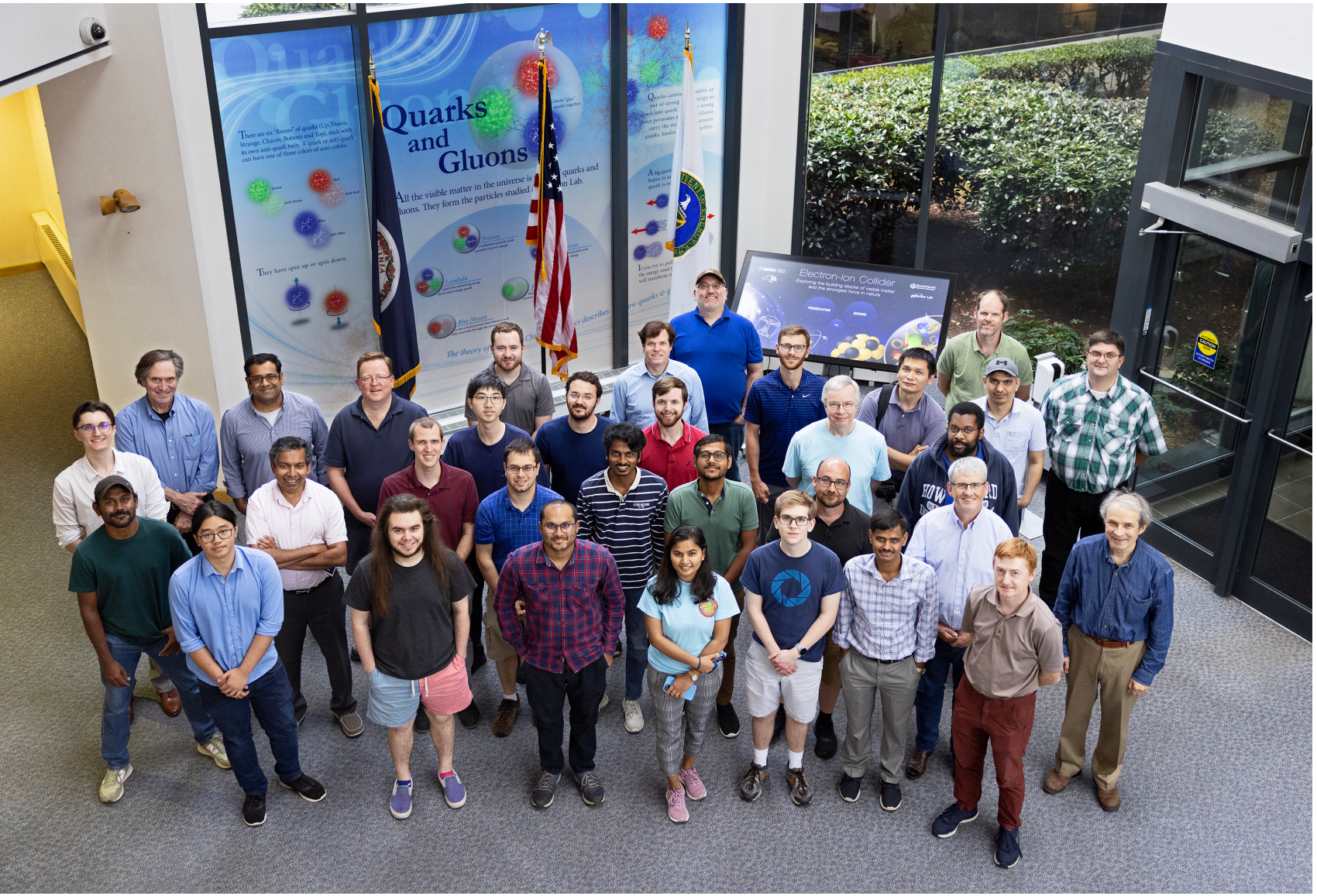

- Approximately 100 members from 20+ institutions, including, but not limited to (and in no particular order):
  - UConn
  - UVA
  - W&M
  - JLab
  - Glasgow U
  - Hampton U
  - U. Mass Amherst
  - CNU
  - Carnegie Mellon
  - Northern Michigan U
  - INFN
  - Virginia Tech
  - LBNL
  - Syracuse
  - Ohio U
  - Temple
  - Others…
- NOTE: this photo only shows ~1/4th of our active members!

FPP Kin. 1 azimuthal distribution and asymmetry

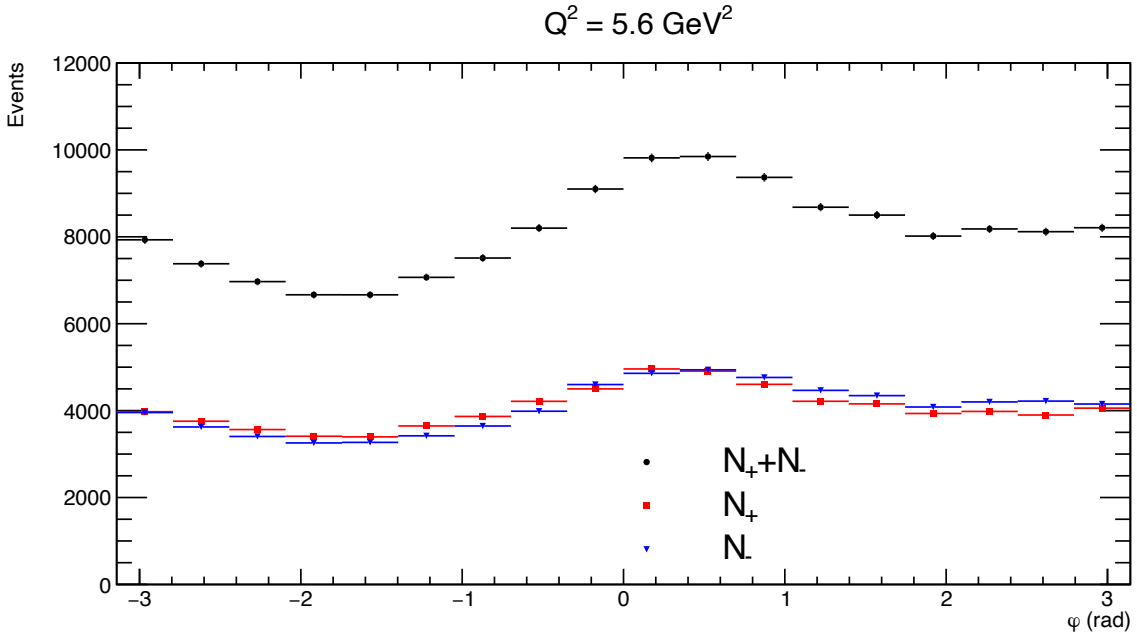

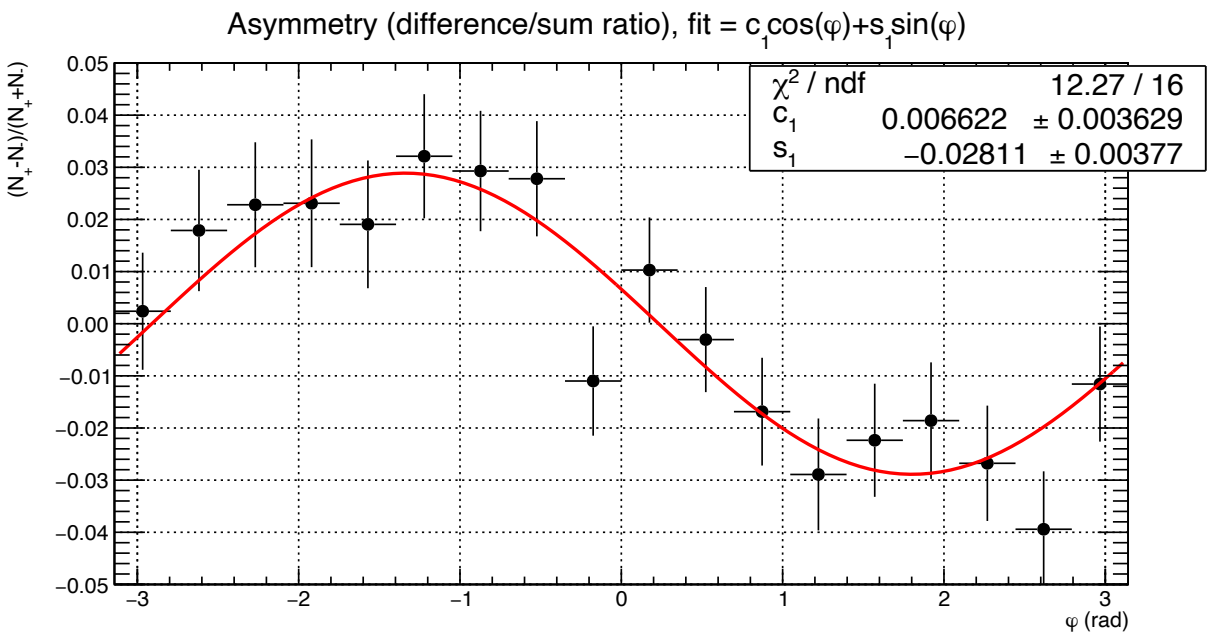

- Left: FPP azimuthal angle distribution passing all exclusivity and other cuts; for helicity sum and individual helicity states—large instrumental asymmetry due to nonuniform acceptance/efficiency
- Right: Helicity asymmetry: difference/sum ratio and cancellation of false asymmetry
- Asymmetry amplitude and relative sign/magnitude of sine and cosine asymmetries are consistent with expectations, with low statistical significance
- NOTE: both asymmetry signs are reversed for this Q^2 due to not accounting for correlation between IHWP state and absolute beam polarization sign as determined by Moller measurement.
- No evidence (yet) for analyzing power increase due to HCAL energy sensitivity—result is consistent with GEp-III

The high-temperature ECAL: motivation

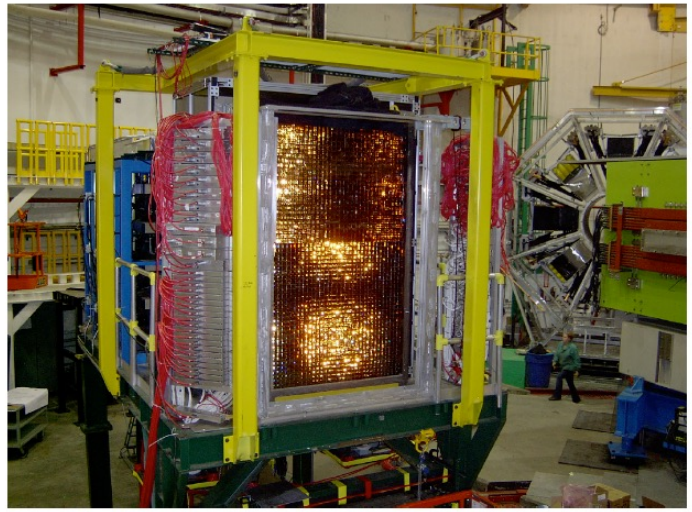

Figure G.1: BigCal in Hall C with the front opened, February 2008.

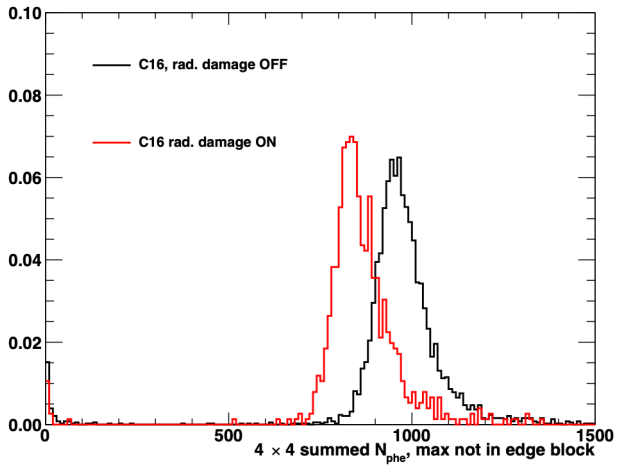

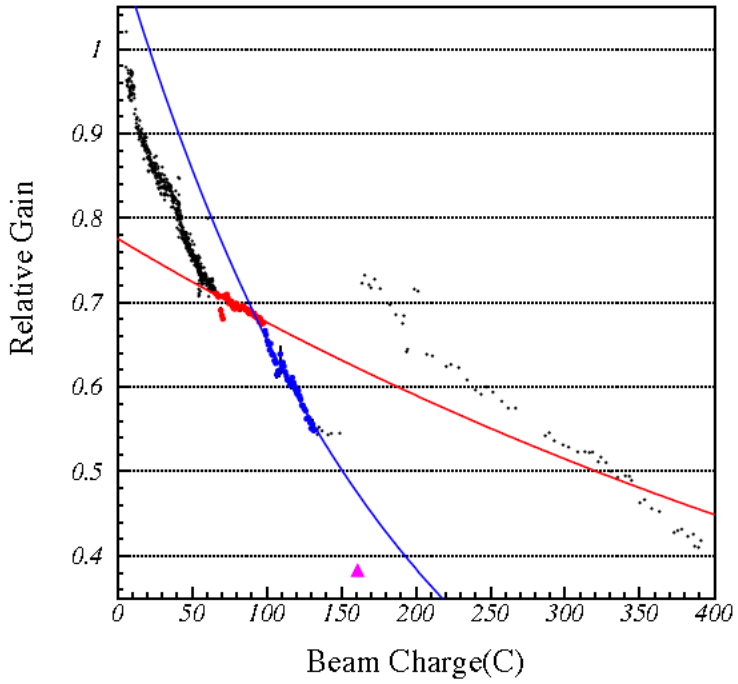

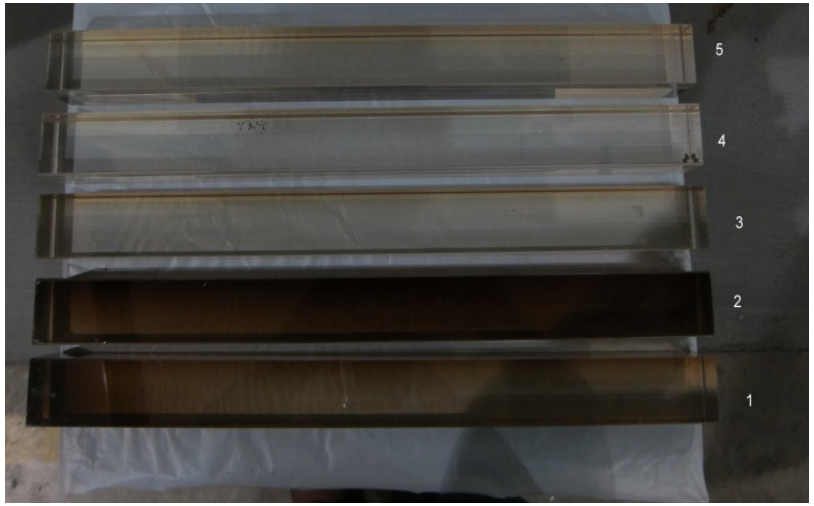

Figure 6 The lead glass blocks used to monitor the radiation dose after the C16 was placed at 10° and there was 20uA beam on the 15cm LH2 target. Block 1 was placed parallel to the C16 along the beamline side of the C16. Block 1 has damage at the front (left side of photo) and along the side. Block 2 was placed in front of the C16 and perpendicular to the front face. Blocks 3,4 and 5 were located at different locations on the spectrometer platform that was near 30°. These blocks show only moderate damage.

- Above, left: GEp-III BigCal, radiation-induced darkening of lead-glass, 2008
- Below, left: Benchmarking continuous thermal annealing prototype in simulation
- Above, center: Signal reduction due to radiation damage during GEp-III
- Above, right: Comparison of lead-glass blocks irradiated in Hall A, inside and outside the 250 deg. C oven

FPP Kin. 3 azimuthal distribution and asymmetry

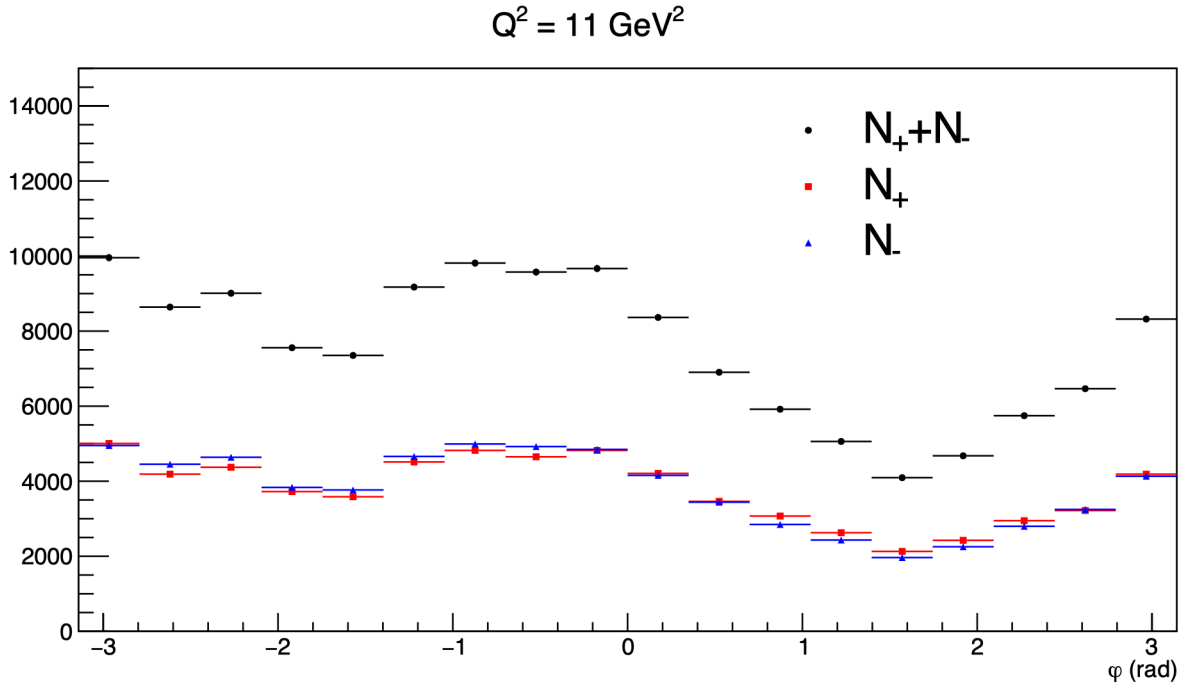

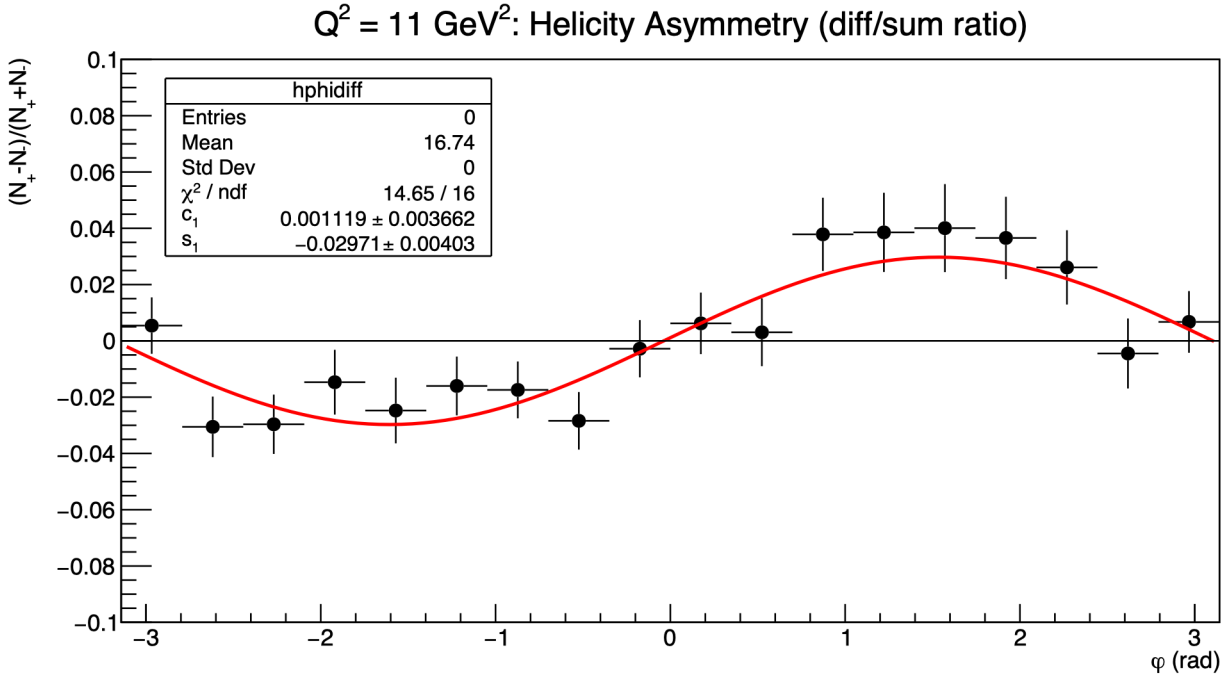

- I've aggregated many different Kin. 3 replays done over summer 2025 here.
- False asymmetry distribution is still quite ugly due to front/back misalignment and acceptance/efficiency nonuniformity
- Helicity asymmetry (diff/sum ratio) shows expected sinusoidal behavior, consistent sign/magnitude with expectation
- $(3 \pm 0.4)\%$ $\sin(\varphi)$ asymmetry indicates analyzing power is good, roughly in line with expectation
- $\cos(\varphi)$ asymmetry consistent with zero (also as expected given small P_T component)
- Lots of work to do but this result is super-encouraging

Generalized Parton Distributions and transverse densities:

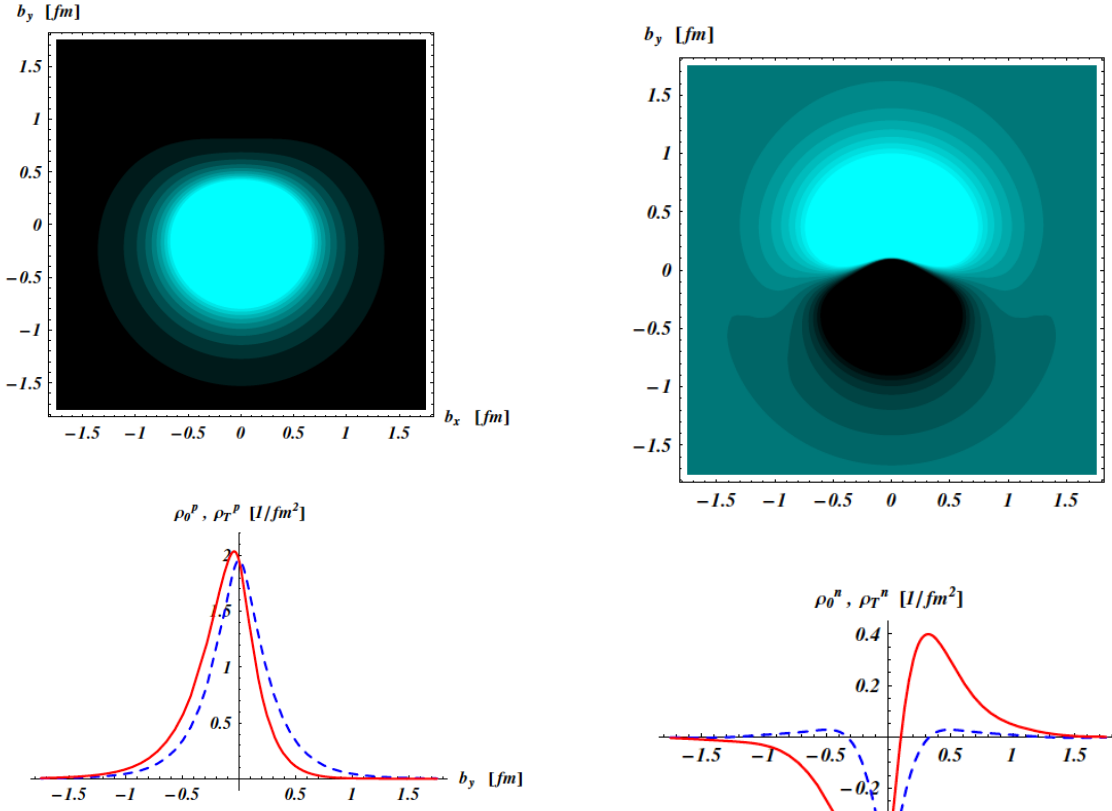

FIG. 1: Quark transverse charge densities in the *proton*. The upper panel shows the density in the transverse plane for a proton polarized along the x-axis. The light (dark) regions correspond with largest (smallest) values of the density. The lower panel compares the density along the y-axis for an unpolarized proton (dashed curve), and for a proton polarized along the x-axis (solid curve). For the proton e.m. FFs, we use the empirical parameterization of Arrington *et al.* [14].

FIG. 2: Same as Fig. 1 for the quark transverse charge densities in the *neutron*. For the neutron e.m. FFs, we use the empirical parameterization of Bradford *et al.* [15].

Proton (left) and neutron (right) 2D transverse charge densities from Carlson and Vanderhaeghen: Phys. Rev. Lett. 100, 032004 (2008)

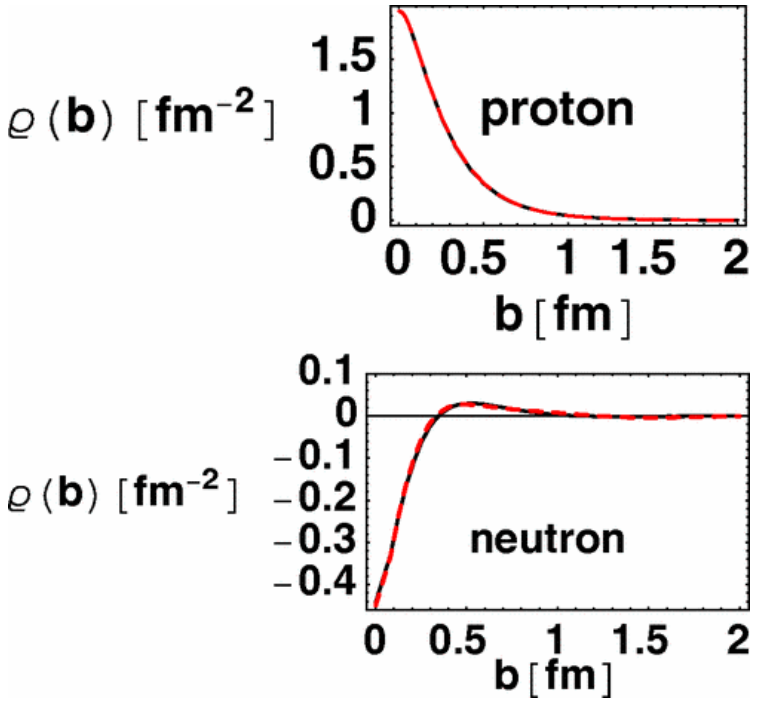

- G. Miller, *Phys.Rev.Lett.* 99 (2007) 112001
- G. Miller, *Ann. Rev. Nucl. Part. Sci.* 60 (2010) 1-25
- Model-independent sum rules relating FF to GPD moments lead to model-independent impact-parameter-space densities as 2D FT of FF in the infinite momentum frame